STUDIES ON NANOCRYSTALLINE PRUSSIAN BLUE AND ITS MIXED METAL ANALOGUE FOR ANALYTICAL APPLICATION

THESIS

SUBMITTED FOR THE AWARD OF THE DEGREE OF

Doctor of Philosophy
in
Chemistry

Submitted by

Digvijay Panday

Supervisor

Prof. P. C. Pandey

DEPARTMENT OF CHEMISTRY
INDIAN INSTITUTE OF TECHNOLOGY
(BANARAS HINDU UNIVERSITY)
VARANASI-221005, INDIA

Enrollment No. : 340519

2016

CHAPTER-

Five

In this chapter, the method for the synthesis of PBNPs mediated through PEI is further explored for the synthesis of nanocrystalline mixed metal analogues especially copper-iron hexacyanoferrates and nickel-iron hexacyanoferrates. As synthesized mixed metal hexacyanoferrates was used for the electrochemical detection of dopamine and hydrazine. As mixed metal analogues also shows the peroxidase mimetic behaviour so the both the nanoparticles were also used for detection of H_2O_2 as peroxidase mimetic activity.

Polyethylenimine mediated synthesis of copper-Iron and nickel-iron hexacyanoferrate nanoparticles and their analytical applications

1 PEI mediated synthesis of Cu-Fe HCFs and Ni-Fe HCFs nanoparticles and their analytical applications

1.1 Introduction

Transition metal hexacyanoferrates are the important class of coordination compounds. Among these, Prussian blue and its metal analogues have shown significant attention to the scientific community due to its unique physical, optical, magnetic, ion sensing, chemical and electrochemical properties. Mixed metal hexacyanoferrates have shown different properties depending upon the combination of transition metal ions like Ni-Fe, Co-Fe, Cu-Fe, Cu-Co, Ni-Pd, Mn-Fe, or Ni-Co [(Kulesza *et al.* 1999; Pandey and Pandey 2013d; Safavi *et al.* 2011; Yu *et al.* 2013)]. As far as electrochemical properties of mixed metal hexacyanoferrates are concerned, the mixed metal hexacyanoferrate shows unique and different electrochemical behaviour as a function of transition metal ions present into the crystal lattice of Prussian blue. The presence of other transition metal ions altered the properties and have been exploited in the electrochemical energy storage, electrochemical sensing of hydrazine, dopamine, and NADH and many more [(Cai *et al.* 1995a, b; Ghasemi *et al.* 2015; Pandey and Pandey 2013d; Salimi and Abdi 2004)].

Although many reports on the synthesis of Prussian are available in literature however the controlled nucleation of these materials have been one of the challenging tasks. In addition to that uncontrolled nucleation allows the formation of metal hexacyanoferrate which are not processable for practical applications. Normally the use of double precursor during Prussian blue formation leads uncontrolled nucleation whereas the use of singly precursor allow control over the nucleation process and may leads the formation of processable metal hexacyanoferrate [(Ding *et al.* 2009; Jia and Sun 2007; Ming *et al.* 2012; Pandey and Panday 2016b; Pandey and Pandey 2013c, 2014a; Wu *et al.* 2006)]. Recently, we have demonstrated controlled conversion of Prussian blue and it mixed metal analogues involving the participation of organic reducing agent that precisely control the nucleation process and lead the formation of stabilized Prussian blue

nanoparticles [(Pandey and Panday 2016a; Pandey and Panday 2016b; Pandey and Pandey 2013a, b, c, d, 2014a)]. The use of 3-aminopropyltrimethoxysilane (3-APTMS) and cyclohexanone allow controlled formation of Prussian blue nanoparticles (PBNPs) having electrochemistry with electron transfer rate constant to the order of 32.1 s^{-1} [(Pandey and Pandey 2013a, c)]. Similar process allows controlled synthesis of super peroxidase mimetic mixed metal hexacyanoferrate [(Pandey and Pandey 2013a, d)]. The use 3-APTMS introduced inherent disadvantage of alkoxide functionality that ultimately undergo the formation of –Si-O-Si- linkage through auto-hydrolysis and condensation of 3-APTMS as a function of time. To overcome this problem, another organic reagent tetrahydrofuran-hydroperoxide (THF-HP) justified the synthesis of stable, processable PBNPs [(Pandey and Pandey 2014a)]. THF-HP enables the conversion of potassium hexacyanoferrate into PBNPs at room temperature in 12 hours. THF-HP is also capable of reducing noble metal cations into respective nanoparticles in the presence of 3-APTMS [(Pandey and Pandey 2014b; Pandey *et al.* 2014b)] whereas $K_3[Fe(CN)_6]$ undergo controlled conversion into PBNPs even in absence of 3-APTMS. However, poor commercial availability of THF-HP directed us to investigate whether such conversion may be accompanied with easily available organic reducing agents like tetrahydrofuran and hydrogen peroxide [(Pandey and Panday 2016b)] and indeed interesting finding on the synthesis of Prussian blue and its Ni-FeHCF has been recorded [(Pandey and Panday 2016b)]. It was found that $K_3[Fe(CN)_6]$ undergo controlled conversion in to well disperse PBNPs in the presence of tetrahydrofuran (THF), hydrogen peroxide (H_2O_2) at 60 °C in 20 minutes. The same method efficiently enabled the synthesis of Ni-Fe hexacyanoferrate [(Pandey and Panday 2016a)]. Although such process allowed several advantages however, suffered from the following problems: (i) poor crystallinity of as made Prussian blue and its mixed metal analogues, (ii) limited to Ni-Fe hexacyanoferrate formation and was unable to precisely control the formation of Cu-Fe HCFs. These limitations may ultimately affect the electrocatalytic and versatile approach for making Prussian blue analogues. Accordingly, there is a need of another organic reducing agent that not

only precisely allow controlled formation of mixed metal analogues of all transition metal combination along with better crystallinity of as made nanomaterial which has been attempted in this investigation. The use of PEI has been demonstrated for the reduction of noble metal ions like gold into gold nanoparticles [(Mohammed *et al.* 2013; Sun *et al.* 2004, 2006; Wen *et al.* 2013)]. Recently, we have demonstrated that polyethylenimine (PEI) enable controlled and rapid synthesis of gold nanoparticles in the presence of formaldehyde [(Pandey *et al.* 2016)]. Accordingly, the use of PEI for controlled conversion of Prussian blue and its mixed metal analogue has been attempted. Indeed interesting finding on controlled synthesis of Cu-Fe HCFs and Ni-Fe HCFs has been recorded. The use of cationic polymer also allowed enhancing the crystalline behaviour of mixed metal hexacyanoferrate with good processability for use in both homogeneous and heterogeneous electrocatalysis. The findings based on; (i) PEI mediated synthesis of Cu-Fe HCFs and Ni-Fe HCFs nanoparticles from single precursor, (ii) Structural and elemental characterization of as synthesized mixed metal nanoparticles, (iii) electrochemical characterization of as synthesized mixed metal nanoparticles, (iv) homogeneous catalysis of hydrogen peroxide by as synthesized MHCs nanoparticles, (v) usability of these material in the electrocatalytic oxidation of dopamine, hydrazine and electrocatalytic reduction of H_2O_2 sensing; are reported in this chapter.

1.2 Experimental

1.2.1 Material and Methods

Potassium ferricyanide [$K_3[Fe(CN)_6]$], Potassium ferrocyanide [$K_4[Fe(CN)_6]$], hydrogen peroxide (H_2O_2), nickel sulphate ($NiSO_4$) and copper sulphate ($CuSO_4$) were purchased from Merck, India. Polyethylenimine (PEI) (Mol wt 60,000), Graphite powder (1-2 μm), nujol oil (density 0.838 g ml^{-1}), o-dianisidine, hydrazine hydrate and dopamine were procured from Sigma Aldrich Chemical Co. India. All reagents used were of analytical grade and used without further purification. Double distilled water was used in all the experiments performed (Alga water purification system).

1.2.2 Synthesis of Cu-Fe hexacyanoferrates and Cu-hexacyanoferrates

Synthesis of Cu-Fe HCFs involves mixing of single precursor potassium ferricyanide, PEI, $CuSO_4$ and HCl in an optimum concentration and allowing the reaction to proceed at 60 °C for 3 hours in a vacuum oven. In a typical procedure, 70 µl aqueous solution of $K_3[Fe(CN)_6]$ (50 mM) and 20 µl of PEI (0.1 g/ml) are mixed together under stirring condition over cyclomixture followed by addition of 5 µl hydrochloric acid solution (6.5 M). To this add 70 µl of aqueous solution of $CuSO_4$ solution (0.05 M) mixed vigorously over cyclomixture and keep it at 60 °C for 3 hours in an oven. A yellow colour solution was turned into blue colour indicating the synthesis of Cu-Fe HCFs. Cu-Fe HCFs was made through the varying the molar ratio of Cu:Fe and observed in the electrochemical behaviour of these materials. Copper hexacyanoferrate (CuHCFs) was synthesized in a single step by mixing 100 µl aqueous solution of $CuSO_4$ (0.01 M) with 100 µl aqueous solution of potassium ferricyanide (0.01 M) containing 0.01 M KCl under stirring. The use of potassium ferrocyanide ($K_4[Fe(CN)_6]$) in place $K_3[Fe(CN)_6]$ under similar condition also allowed the formation of similar nanomaterial.

1.2.3 Synthesis of Ni-Fe hexacyanoferrates and Ni-hexacyanoferrates

Synthesis of Ni-Fe HCFs involves the mixing of optimum concentration of single precursor $K_3[Fe(CN)_6]$, PEI, $NiSO_4$ and HCl and allowed the reaction mixture at 60 °C for 3 hours in oven. In a typical procedure, 70 µl aqueous solution of $K_3[Fe(CN)_6]$ and 20 µl aqueous solution of PEI (0.1 mg/ml) was mixed over cyclomixture followed by addition of 5 µl of hydrochloric acid (6.5 M). To this solution, add 25 µl of aqueous solution of $NiSO_4$ was mixed and allowed to reaction happen at 60 °C for 3 hours. As a resultant of this reaction, yellow colour solution turned into blue colour indicating the synthesis of Ni-Fe hexacyanoferrate. Ni-Fe hexacyanoferrates was also synthesized by varying the molar ratio of Ni:Fe and studied the effect of the same through cyclic voltammetry. Nickel hexacyanoferrate (NiHCFs) was synthesized in a single step by mixing 100 µl aqueous solution of nickel sulphate (0.01 M) with 100 µl aqueous solution of $K_3[Fe(CN)_6]$ (0.01 M) containing 0.01 M KCl under stirring.

The use of potassium ferrocyanide ($K_4[Fe(CN)_6]$) in place $K_3[Fe(CN)_6]$ under similar condition also allowed the formation of similar nanomaterial.

1.2.4 Structural characterization of mixed metal hexacyanoferrates

Formation of mixed metal hexacyanoferrates was confirmed by UV-Vis spectrophotometer, X-ray diffraction analysis (XRD), Scanning Electron Microscopy (SEM) and Transmission Electron Microscopy (TEM) coupled with energy dispersive spectroscopy analysis (EDS). Hitachi U-2900 spectrophotometer was used for all UV-Vis spectroscopy measurements. XRD analysis was done in thin film of mixed metal analogues which was prepared by dip coating of the respective solution onto the transparent glass slides and dried at 60 °C in a vacuum oven. XRD analysis was done on a Rigaku miniflex II diffractometer using nickel filtered CuKα (λ = 1.506 Å) radiation. The crystallite size was calculated using Debye–Scherrer formula [(Zheng *et al.* 2007)]. Dilute sample was dip coated onto the Indium Tin oxide coated glass which was dried at room temperature and used for the SEM analysis. TEM analysis was performed using a TECHNAI 200 Kv TEM (Fei, Electron Optics). A dilute solution of sample was dip casted and dried at room temperature on the carbon coated copper grid (Mesh size-400) obtained from Electron Microscopy Sciences, USA. The concentration of copper and nickel in the respective solution was determined by the Atomic Absorption Spectroscopy by Shimadzu Corporation.

1.2.5 Peroxidase mimetic activity of mixed metal hexacyanoferrates

Peroxidase mimetic activity of as synthesized mixed metal analogues was performed as described earlier [(Pandey and Panday 2016b)]. In a typical procedure, peroxidase mimetic activity was performed spectrophotometrically using Hitachi spectrophotometer by measuring the formation of the oxidized product of o-dianisidine (brown in colour) at 430 nm ($\varepsilon = 11.3\ mM^{-1}\ cm^{-2}$) which was formed in the presence of reduced form of o-dianisidine, hydrogen peroxide and mixed metal analogues which acts as a mimetic catalyst. Each reaction was performed in 2 ml, 0.1 M phosphate buffer (pH=7.0) containing 15 µl ml^{-1} mixed

metal analogues and 50 μM o-dianisidine and varying concentration of hydrogen peroxide (0 – 25 mM) at room temperature. The variation in the absorbance as a function of time was monitored at 430 nm (ε = 11.3 mM^{-1} cm^{-2}) and kinetic parameters were calculated as described elsewhere [(Pandey and Panday 2016b)].

1.2.6 Fabrication of modified graphite paste electrode

The electrochemical measurements were performed on mixed metal analogues modified graphite paste electrode. The electrode body was procured from Bioanalytical Systems, West Lafayette, In (MF 2010). The well of the electrode body was filled with active paste of composition in (w/w): Cu-Fe HCFs or Ni-Fe HCFs 2.5%, graphite powder (1-2 μm) 67.5% and nujol oil 30%. The mixture was mixed thoroughly in a blender and filled the electrode body and finally electrode surface was manually smoothed on a clean butter paper.

1.2.7 Electrochemical Measurements

All the electrochemical measurements were performed in a three electrode assembly system with a working volume of 3 ml solution on a workstation Model CHI660B, CH instruments Inc, TX. Modified graphite paste electrode, Ag|AgCl electrode (Orion, Beverly, MA, USA) and platinum plate electrode were functioned as working, reference and counter electrode respectively. Cyclic voltammetry was performed at various scan rates from 0.01 V s^{-1} to 0.3 V s^{-1} to analyze the scan rates (ν) dependence on peak current density (j) on the mixed metal analogues modified graphite paste electrode. All potential given throughout text are relative to the Ag|AgCl reference electrode. Electrochemical oxidation of dopamine, H_2O_2 and hydrazine was performed on 0.1 M phosphate buffer containing 0.5 M KCl and 0.1 M $NaNO_3$ solution respectively. Effect of pH on the electrochemical behaviour and the stability was performed by cyclic voltammetry in 0.1 M phthalate buffer (pH= 4), 0.1 M phosphate buffer (pH=7.0) and 0.1 M borate buffer (pH=9.0) containing 0.5 M KCl.

1.3 **Results**

1.3.1 PEI mediated synthesis of nanocrystalline mixed metal hexacyanoferrates

The method for PEI mediated synthesis of PBNPs has been described in chapter 4 and the same method for the synthesis of Cu-Fe HCFs and Ni-Fe HCFs has been successfully explored further. The active role of each component has been studied through UV-Vis spectroscopy and visual photography of respective solutions. Figure.5.1. shows the importance of each component during the conversion of $K_3[Fe(CN)_6]$ into mixed metal analogues depending on the respective transition metal.

The possibility of utilizing $K_4[Fe(CN)_6]$ in place of $K_3[Fe(CN)_6]$ was also explored by synthesizing Cu-Fe HCFs (1:1) and Ni-Fe HCFs (1:5) under identical condition of 60 °C for 3 hours. The synthesis of Cu-Fe HCFs (1:1) and Ni-Fe HCFs (1:5) made through $K_4[Fe(CN)_6]$ was confirmed by UV-Vis spectroscopy and cyclic voltammetry on respective graphite paste modified electrode in 0.1 M KNO_3 and compared with the Cu-Fe HCFs (1:1) and Ni-Fe HCFs (1:5) made through $K_3[Fe(CN)_6]$ and the result is shown in Figure.5.2. and Figure.5.3. which confirms that the Cu-Fe HCFs (1:1) and Ni-Fe HCFs (1:5) synthesized by $K_3[Fe(CN)_6]$ was better.

The temperature in the synthesis of mixed metal hexacyanoferrates was also studied by varying the temperature of the synthesis. Synthesis was carried out at room temperature, 60 °C and 90 °C for both Cu-Fe HCFs (1:1) and Ni-Fe HCFs (1:5) using optimized concentration of $K_3[Fe(CN)_6]$, PEI , HCl and other transition metal ions. The confirmation was done by UV-Vis spectroscopy and cyclic voltammetry of as synthesized mixed metal hexacyanoferrates using graphite paste electrode in 0.1 M KNO_3 as shown in Figure.5.4. and Figure.5.5. As can be seen, there is very less amount of synthesis of PB and mixed metal hexacyanoferrates at room temperature even keeping the reaction mixture for 4 days. As we increase the temperature, the reaction is getting faster. The synthesis of mixed metal hexacyanoferrates was done in 2 hours at 90 °C but the electrochemical behaviour was better when the synthesis was done at 60 °C in 3 hours.

It was also intended to study the role of PEI in the present method for the synthesis of mixed metal hexacyanoferrates. Synthesis of Cu-Fe HCFs (1:1) and Ni-Fe HCFs (1:5) was performed without involving the PEI at 60 °C in 24 hours. For this, synthesis of Cu-Fe HCFs (1:1) and Ni-Fe HCFs (1:5) was done by involving optimized concentration of $K_3[Fe(CN)_6]$, HCl and other transition metal ions and confirmed by UV-Vis spectroscopy and cyclic voltammetry. Figure.5.6. shows the UV-Vis spectroscopy and cyclic voltammetry performed on graphite paste electrode in 0.1 M KNO_3 for as synthesized mixed metal hexacyanoferrates. This justifies that there is less synthesis of mixed metal hexacyanoferrates in case of no PEI even keeping the reaction mixture for 24 hours.

1.3.2 Structural characterization

In the first instance, the formation of nanocrystalline mixed metal hexacyanoferrates was characterized by UV-Vis spectroscopy. Figure.5.1. shows UV-Vis spectroscopy of both the metal hexacyanoferrates as synthesized. Both hexacyanoferrate shows the strong absorption at 680 nm which is the characteristic peak of all the metal hexacyanoferrates. The absorptions at 680 nm can be assigned to the inter-metal charge transfer (CT) band from Fe^{2+} to Fe^{3+} in PBNPs [(Gotoh *et al.* 2007)].

As synthesized mixed metal hexacyanoferrates was further characterised by FT-IR analysis. Figure.5.7. (A) and (B) represents the FT-IR spectra of Cu-Fe HCFs (1:1) and Ni-Fe HCFs (1:5) respectively which shows the characteristic peaks available in the mixed metal hexacyanoferrates. Cu-Fe HCFs (1:1) and Ni-Fe HCFs (1:5) was further characterised by XRD analysis. Figure.5.8. shows the XRD diffractogram for the Cu-Fe HCFs (1:1) and Ni-Fe HCFs (1:5) mixed metal analogues respectively. This shows the common and characteristic peaks available in the mixed metal analogues. The crystallite size was calculated by Debye-Scherrer formula as described in the chapter.2 [(Zheng *et al.* 2007)]. The particle size of the mixed metal analogues has been further evaluated by SEM and TEM analysis as shown in Figure.5.9. for the Cu-Fe HCFs (1:1) and Ni-Fe HCFs (1:5) respectively. These figures confirm the nanosized of as synthesized mixed metal

analogues. Energy Dispersive spectroscopy (EDS) was done for the elemental analysis of as synthesized mixed metal analogues. Figure.5.10. shows the EDS spectra of as synthesized Cu-Fe HCFs (1:1) and Ni-Fe HCFs (1:5) respectively. This indicates the presence of the characteristic peaks assigned to the carbon, potassium, iron, and transition metal ions. The percentage atomic contents of these nanoparticles were also shown in the inset to the respective figure.

1.3.3 Electrochemical characterization

As synthesized mixed metal nanoparticles were further characterized by cyclic voltammetry on graphite paste electrode performed in 0.1 M KNO_3 as supporting electrolyte. It was found that the electrochemical behaviour gets affected by the varying concentration of transition metal to the iron present in the mixed metal analogues therefore the effect of transition metal was evaluated by varying concentration of transition metal ions in the respective mixed metal analogues.

1.3.3.1 -Electrochemical behaviour of mixed Cu-Fe hexacyanoferrates and Cu-hexacyanoferrates

The electrochemical behaviour of mixed Cu-Fe HCFs was studied through graphite paste modified electrode in 0.1 M KNO_3 solution and compared to that of PBNPs. The results based on the cyclic voltammetry for PBNPs, mixed Cu-Fe HCFs (different ratio) and Cu-hexacyanoferrates are as shown in Figure.5.11. As can be seen from the figure, there is a gradual change in the electrochemical behaviour of PBNPs modified electrode as a function of copper ion concentration. The result shown in Figure.5.11. (B) to (H) justify the significance of heterotransition metal atom in 3-dimentional network, since there are redox peak at - 0.2 V and 0.9 V *vs*. Ag|AgCl (characteristic peak of PBNPs modified electrode) and a redox peak at 0.7 V (characteristic peak of CuHCF) [Figure.5.11.(I)] [(Pandey and Pandey 2013b)]. The result shows that the mixed Cu-Fe HCFs which contains molar ratio of Cu to Fe i,e; 1:1 [Figure.5.11. (F)] tends to produce characteristic peak of CuHCFs and also of PBNPs. Figure.5.12. shows cyclic voltammogram of various as synthesized Cu-Fe HCFs in 0.1 M

KNO_3 at various scan rates between 0.01 V s^{-1} to 0.3 V s^{-1}. This shows that peak current increases as increase in the scan rate [Figure.5.13].

1.3.3.2 Electrochemical behaviour of mixed Ni-Fe hexacyanoferrates and Ni-hexacyanoferrates

The electrochemical behaviour of as synthesized Ni-Fe HCFs was studied by cyclic voltammetry (CV). Figure.5.14. shows the cyclic voltammetric behaviour of mixed Ni-Fe HCFs of varying Ni:Fe ratio modified electrode in 0.1 M KNO_3 as a supporting electrolyte. Figure.5.14. (B) to (F) shows the CV of Ni-Fe HCFs with varying molar ratio of Ni:Fe. Figure.5.14. (A) shows the CV of PBNPs made through same protocol as Ni-Fe HCFs. NiHCFs was also used for the comparative purpose to the PBNPs and Ni-Fe HCFs modified graphite paste electrode [Figure.5.14. (G)]. As can be seen from the Figure.5.14.(D) is the best composition of Ni-Fe HCFs since it contains both electrochemical behaviour of PBNPs as well as NiHCFs [(Pandey and Pandey 2013a)]. Figure.5.15. shows cyclic voltammogram of various as synthesized Ni-Fe HCFs in 0.1 M KNO_3 at various scan rates between 0.01 V s^{-1} to 0.3 V s^{-1}. This shows that peak current increases as increase in the scan rate. The plot of scan rate *vs.* peak current was done for the respective composition of Ni-Fe HCFs and shows that the peak current was increasing as increasing the scan rate for the as modified graphite electrode [Figure.5.16.].

The electrode behaviour of as synthesized Cu-Fe HCFs (1:1) and Ni-Fe HCFs was studied by cyclic voltammetry in different pH buffer on graphite paste modified electrode as shown in Figure.5.17.

1.3.4 Peroxidase mimetic activity of as synthesized Cu-Fe HCFs (1:1) and Ni-Fe HCFs (1:5)

As discussed in the previous chapters, mixed metal analogues also shows the peroxidase mimetic behaviour therefore it is intended to analyze the peroxidase mimetic activity of as synthesized Cu-Fe HCFs (1:1) and Ni-Fe HCFs (1:5). Time scan mode was used for the formation of oxidised product of o-

dianisidine which gives brown colour (absorbance maxima at 430 nm) in the presence of H_2O_2 and mixed metal analogues. The kinetic parameters of Cu-Fe HCFs (1:1) and Ni-Fe HCFs (1:5) for the reactions were evaluated by the initial rate method. Figure.5.18. (A) and Figure.5.18. (B) shows the absorbance changes in the varying concentration H_2O_2 and a constant concentration of o-dianisidine. Figure.5.18. (C) and Figure.5.18. (D) shows that as synthesized mixed metal analogues follows the Michaelis-Menton like behaviour. The Michaelis-Menton constant (K_m) for Cu-Fe HCFs and Ni-Fe HCFs was found to be 1.5 and 4.2 mM respectively.

1.3.5 Electrocatalytic analysis of dopamine, hydrazine and H_2O_2 over Cu-Fe HCFs (1:1) and Ni-Fe HCFs (1:5) modified electrode

As synthesized Cu-Fe HCFs (1:1) and Ni-Fe HCFs (1:5) was used for the electrocatalytic detection of dopamine, hydrazine and H_2O_2.

1.3.5.1 Electrochemical oxidation of dopamine over Cu-Fe HCFs (1:1) and Ni-Fe HCFs (1:5) modified electrode

The electrochemical oxidation of dopamine was examined over Cu-Fe HCFs (1:1) and Ni-Fe HCFs (1:5) modified graphite paste electrode. Figure.5.19. (A) and (B) shows the voltammogram of mixed Cu-Fe HCFs (1:1) and Ni-Fe HCFs (1:5) respectively on modified electrode in 0.1 M phosphate buffer (pH=7.0) containing 0.5 M KCl in the absence and presence of 2 mM and 5 mM dopamine. The electrocatalytic oxidation for dopamine was studied over Cu-Fe HCFs (1:1) and Ni-Fe HCFs (1:5) monitored by amperometric analysis as shown in Figure.5.19. (C) and (D) by adding varying concentration of dopamine in phosphate buffer (pH=7.0) at fixed potential of 0.2 V *vs*. Ag|AgCl. Inset to the Figure.5.19. (C) and (D) shows the calibration curve of amperometric analysis of dopamine sensing for Cu-Fe HCFs (1:1) and Ni-Fe HCFs (1:5) graphite paste electrode respectively.

1.3.5.2 Electrochemical oxidation of hydrazine over Ni-Fe HCFs (1:5) and Cu-Fe HCFs (1:1) modified electrode

The oxidation of hydrazine was performed on Ni-Fe HCFs (1:5) and Cu-Fe HCFs (1:1) modified graphite paste electrode in 0.1 M KNO_3 solution as an electrolyte. The cyclic voltammogram on Ni-Fe HCFs (1:5) and Cu-Fe HCFs (1:1) in the absence and presence of hydrazine is shown in Figure.5.20. (A) and (B) respectively. As can be seen from the figure, the oxidative current starts increasing at potential of 0.2 V *vs*. Ag|AgCl reference electrode. The finding was further justified by the experimental observation based on the amperometry. Figure.5.20. (C) and (D) show the typical amperometric response of Ni-Fe HCFs (1:5) and Cu-Fe HCFs (1:1) on successive additions of hydrazine in 0.1 M $NaNO_3$. Successive addition of hydrazine resulted in a significant increase in the oxidation current. Inset to the Figure.5.20. (C) and (D) show the calibration plot of Ni-Fe HCFs (1:5) and Cu-Fe HCFs (1:1) system respectively. The calibration plot for hydrazine determination is linear in the range of 0.5 μM to 5 mM.

1.3.5.3 Electrochemical reduction of H_2O_2 over Cu-Fe HCFs (1:1) and Ni-Fe HCFs (1:5) modified electrode

The electrocatalytic reduction of H_2O_2 was performed on Cu-Fe HCFs (1:1) and Ni-Fe HCFs (1:5) modified graphite paste electrode in 0.1 M phosphate buffer containing 0.5 M KCl. The cyclic voltammogram on Cu-Fe HCFs (1:1) and Ni-Fe HCFs (1:5) in the absence and presence of H_2O_2 is shown in Figure.5.21. (A) and (B) respectively. The finding was further justified by amperometric analysis. Figure.5.21. (C) and (D) show the typical amperometric response of Cu-Fe HCFs (1:1) and Ni-Fe HCFs (1:5) on successive additions of H_2O_2 in 0.1 M phosphate buffer containing 0.5 M KCl. Successive addition of H_2O_2 resulted in a significant increase in reduction current. Inset to the Figure.5.21. (C) and (D) shows the calibration plot of Cu-Fe HCFs (1:1) and Ni-Fe HCFs (1:5) system respectively. The calibration plot for H_2O_2 determination in linear in the range of 0.5 μM to 1 mM.

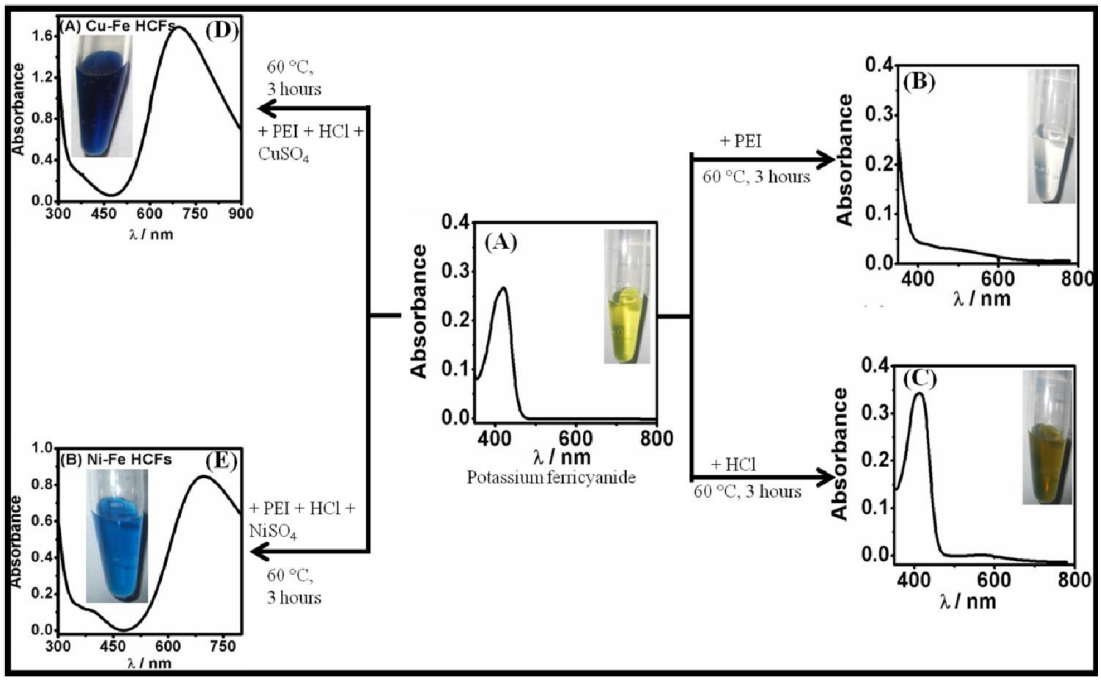

Figure.5.1. Schematic presentation of PEI mediated synthesis of Cu-Fe hexacyanoferrates and Ni-Fe hexacyanoferrates nanoparticles.

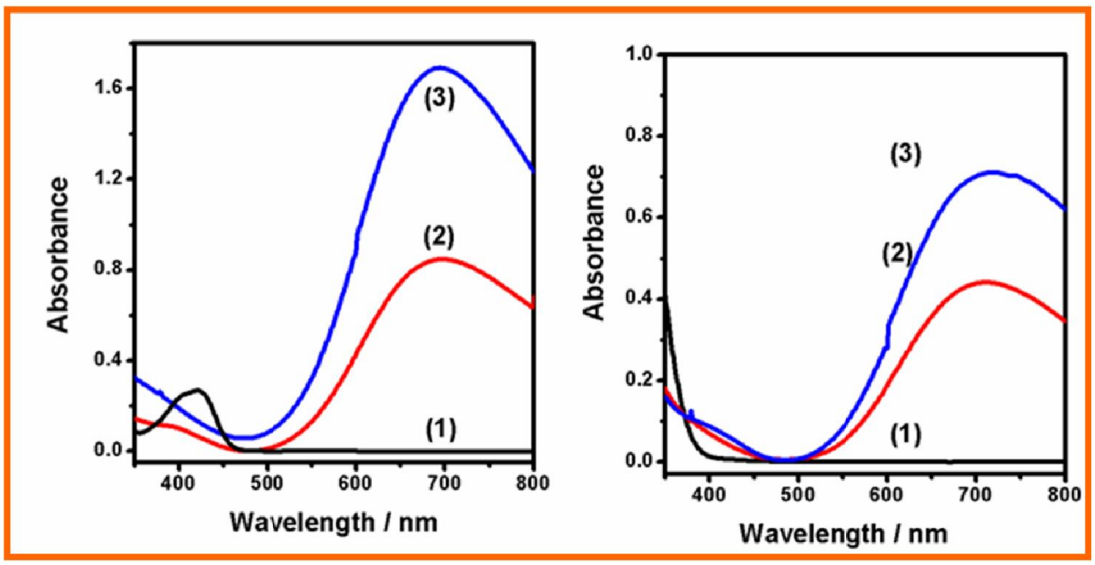

Figure.5. 2. UV-Vis spectroscopy of Cu-Fe HCFs (1:1) and Ni-Fe HCFs (1:5) made through $K_4[Fe(CN)_6]$ and $K_3[Fe(CN)_6]$ at 60 °C in 3 hours.

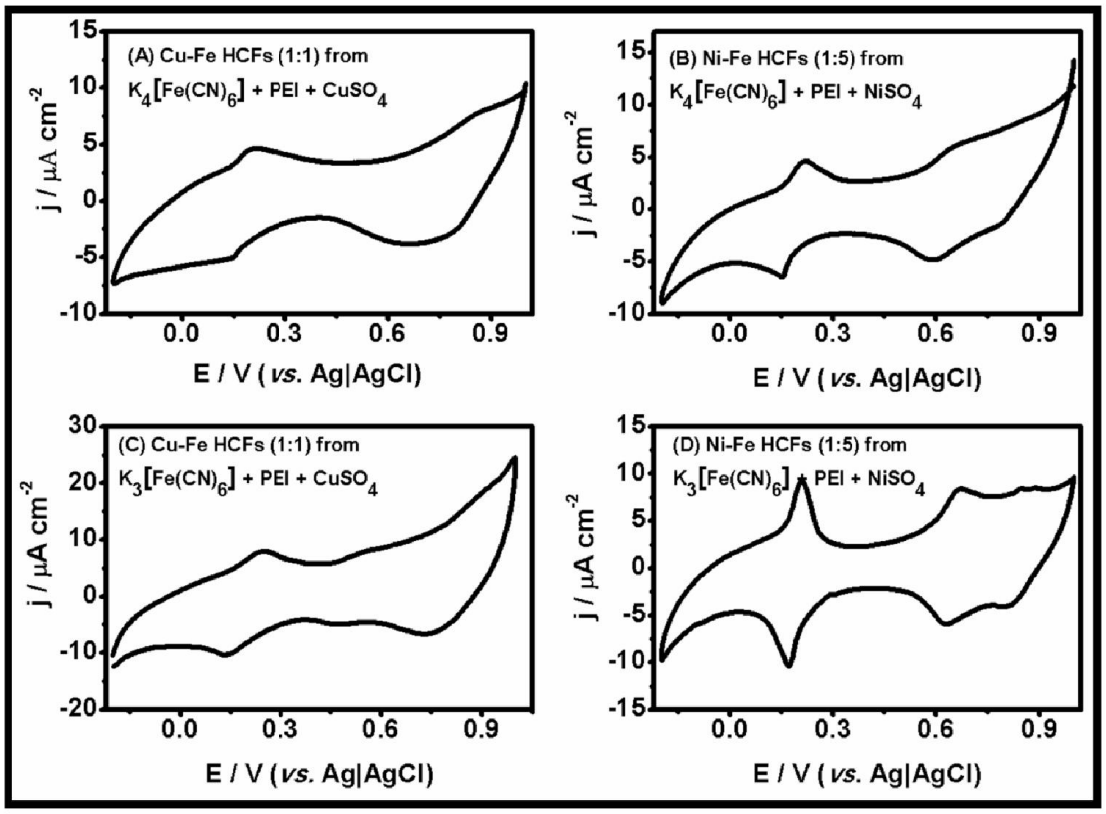

Figure.5. 3. Cyclic voltammogram of (A) Cu-Fe HCFs (1:1) (B) Ni-Fe HCFs (1:5) [made through $K_4Fe(CN)_6$ and PEI at 60 °C); and (C) Cu-Fe HCFs (1:1) (D) Ni-Fe HCFs (1:5) [made through $K_3Fe(CN)_6$ and PEI at 60 °C].

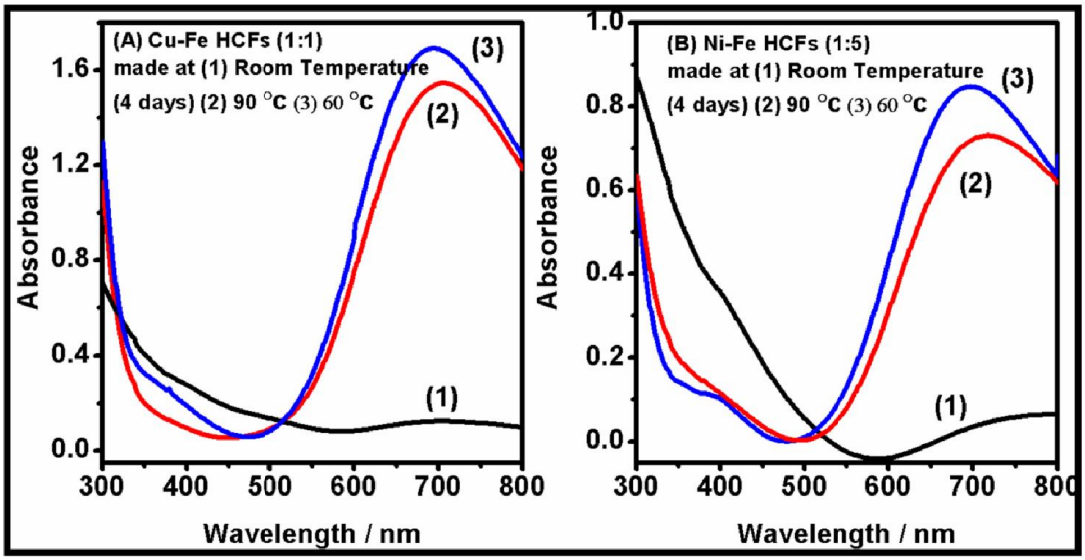

Figure.5. 4. UV-Vis spectroscopy of (A) Cu-Fe HCFs (1:1) (B) Ni-Fe HCFs (1:5) made at (1) room temperature (2) 90 °C and (3) 60 °C.

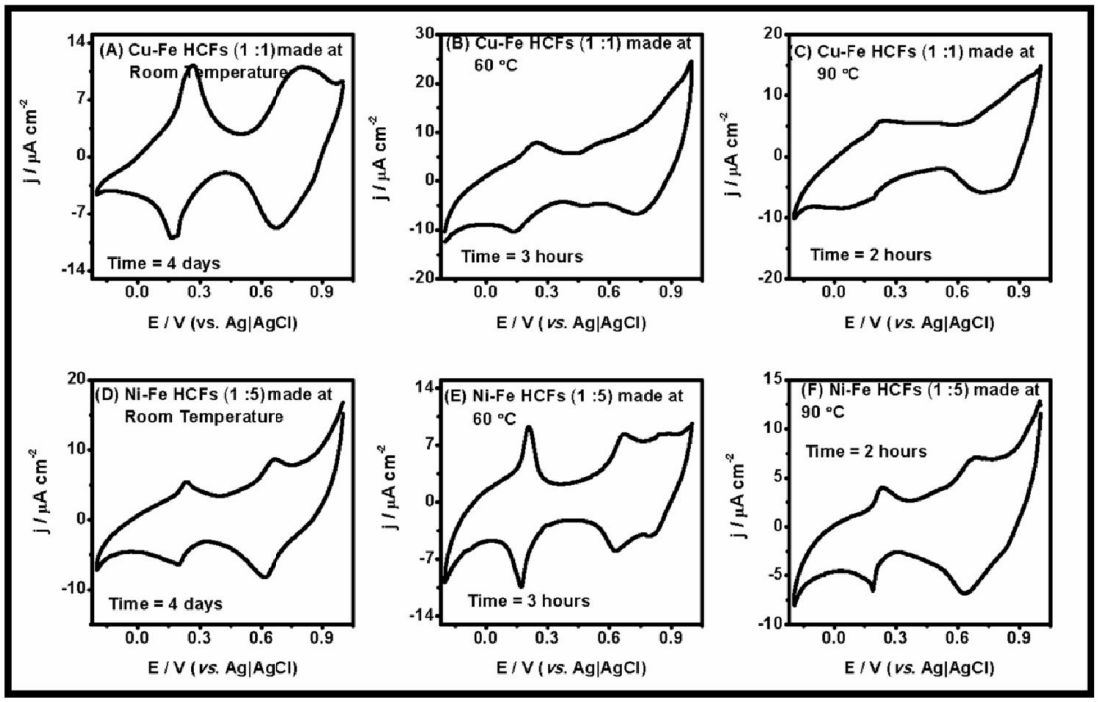

Figure.5. 5. Cyclic voltammetry of (A) to (C) for Cu-Fe HCFs (1:1) and (D) to (F) for Ni-Fe HCFs (1:5) [synthesized at room temperature, 60 °C and 90 °C] in 0.1 M KNO_3 as electrolyte.

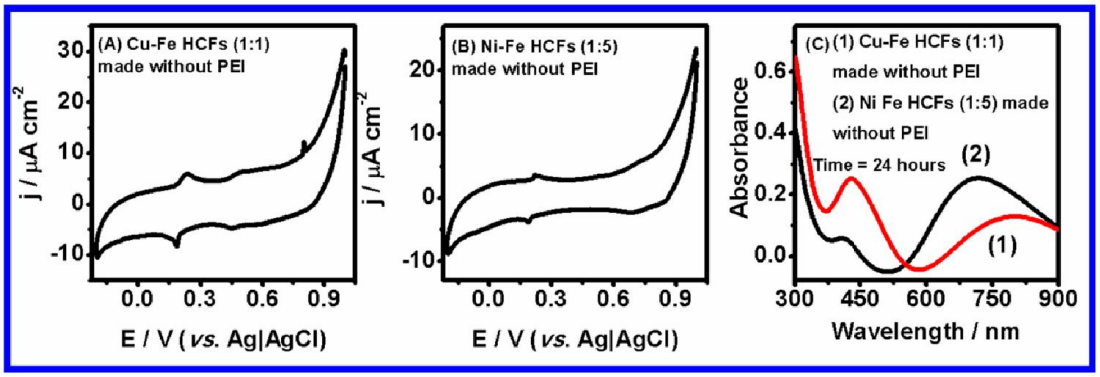

Figure.5. 6. Cyclic voltammogram of (A) Cu-Fe HCFs (1:1) and (B) Ni-Fe HCFs (1:5) made without PEI at scan rate of 0.01 V s^{-1} in 0.1 M KNO_3 as a electrolyte; UV-Vis spectroscopy (C) of the (1) Ni-Fe HCFs (1:5) and (2) Cu-Fe HCFs (1:1) synthesized without PEI in 24 hours.

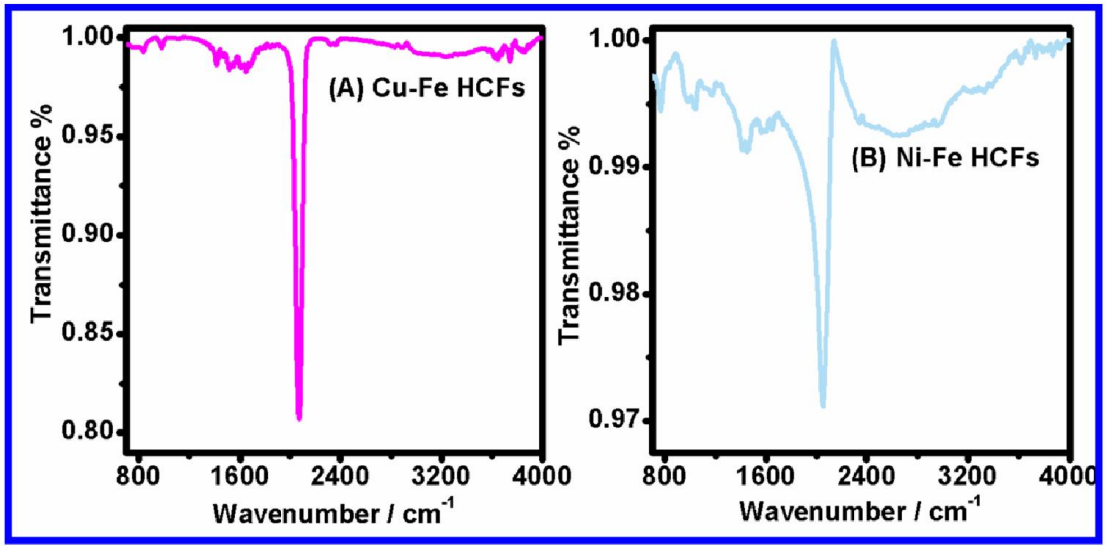

Figure.5. 7. FT-IR spectra of (A) Cu-Fe HCFs (1:1) and (B) Ni-Fe HCFs (1:5).

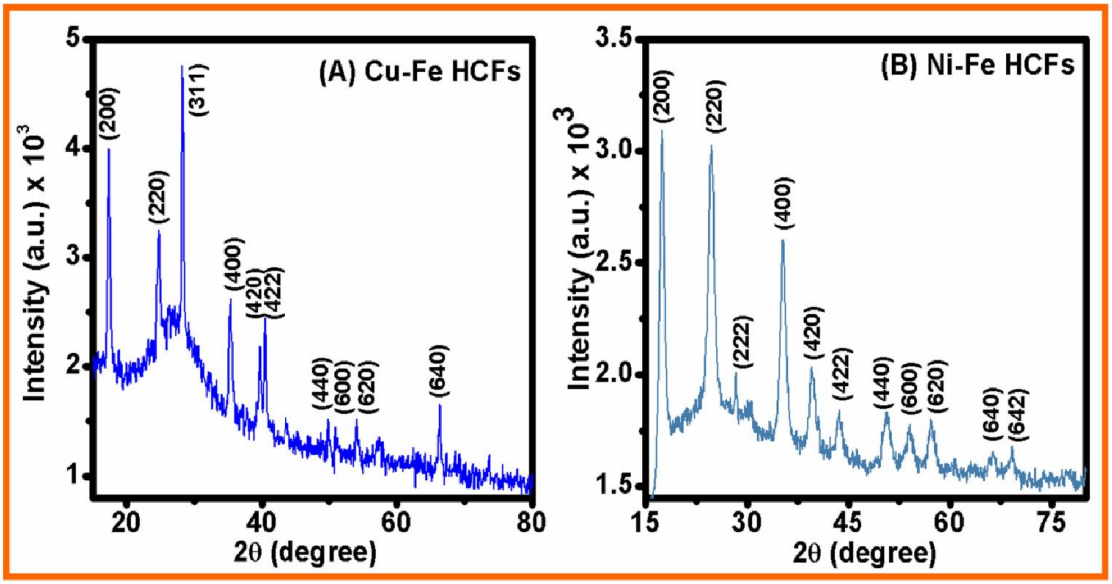

Figure.5. 8. XRD analysis of (A) Cu-Fe HCFs (1:1) and (B) Ni-Fe HCFs (1:5).

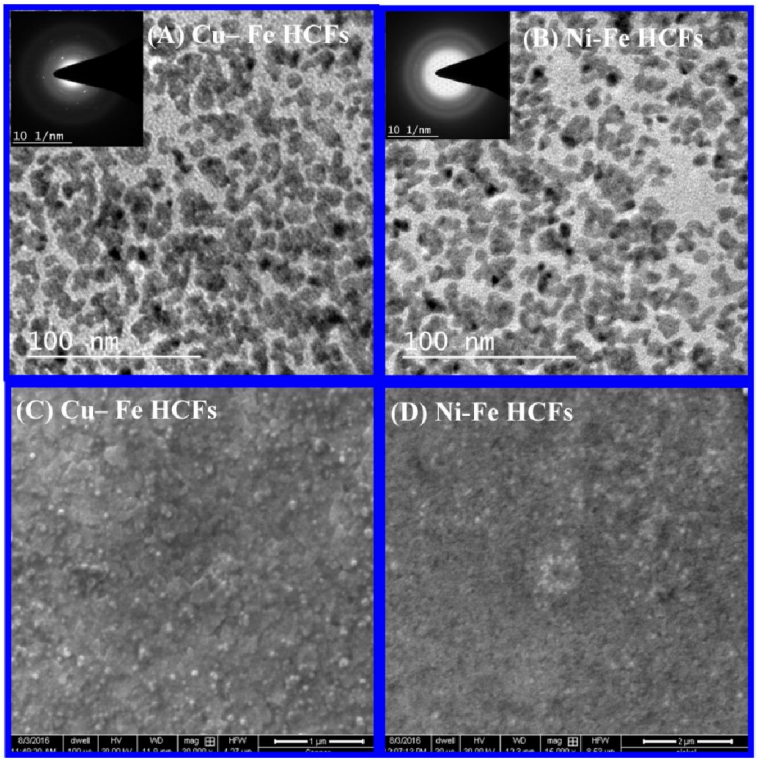

Figure.5. 9. TEM image of (A) Cu-Fe HCFs (1:1) and (B) Ni-Fe HCFs (1:5); inset to the each figure shows the SAED pattern of respective metal hexacyanoferrates; SEM image of (C) Cu-Fe HCFs (1:1) and (D) Ni-Fe HCFs (1:5).

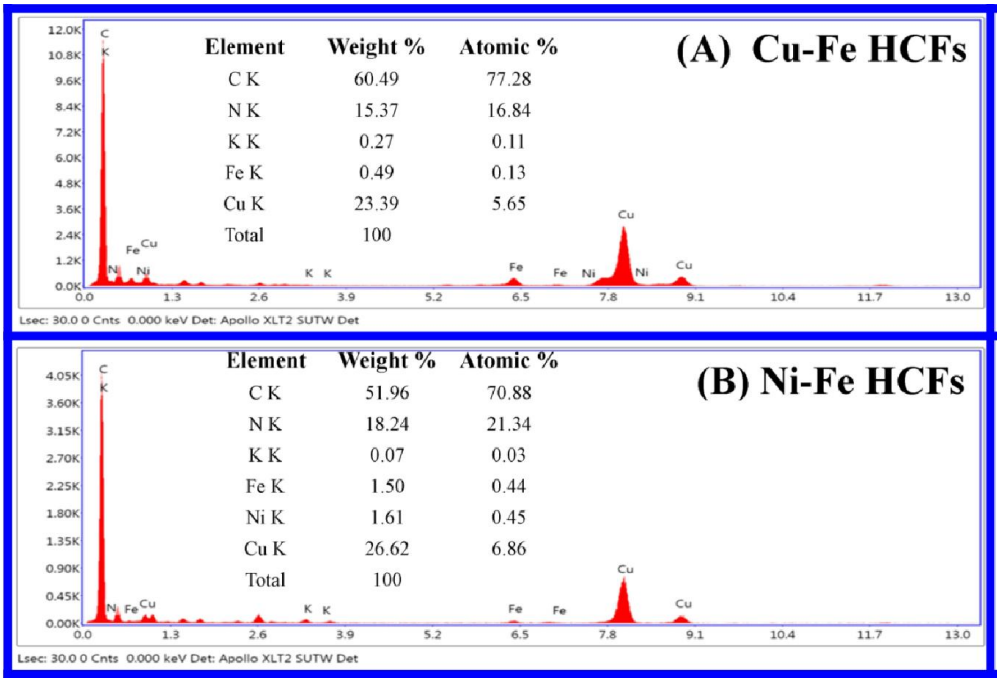

Figure.5. 10. EDS spectra of (A) Cu-Fe HCFs (1:1) and (B) Ni-Fe HCFs (1:5).

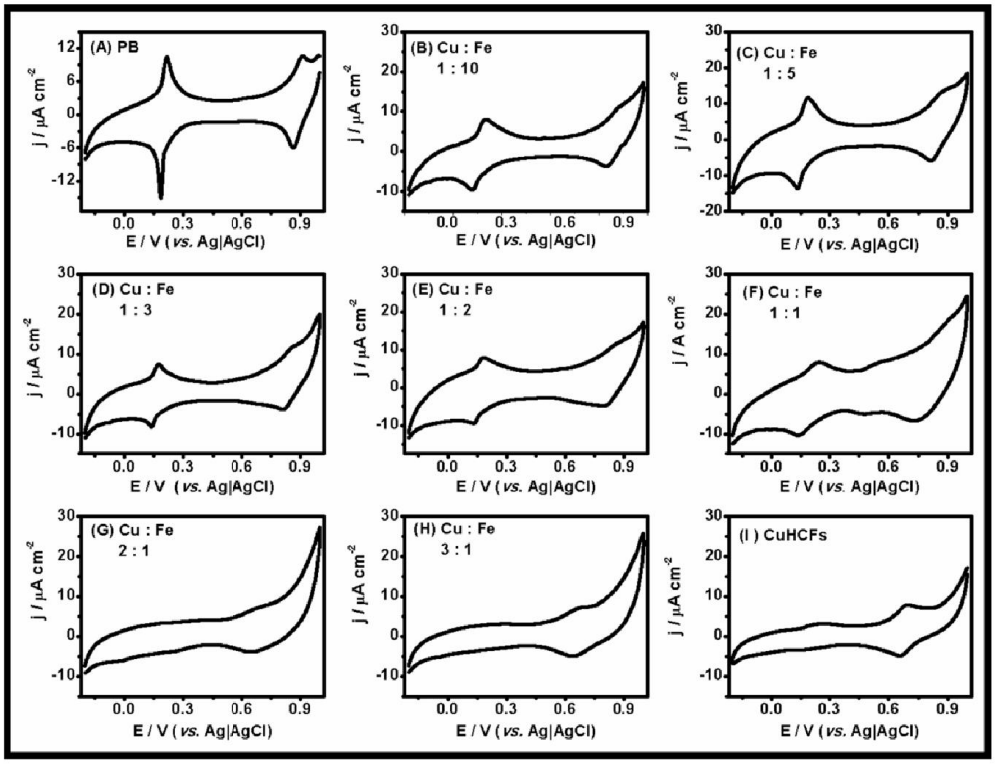

Figure.5. 11. Cyclic voltammetry response of Cu-Fe HCFs modified graphite paste electrode in 0.1 M KNO_3 at scan rate of 0.01 V s^{-1} made at different Cu:Fe molar ratio [A] PBNPs; [B] Cu:Fe (1:10); [C] Cu:Fe (1:5); [D] Cu:Fe (1:3); [E] Cu:Fe (1:2); [F] Cu:Fe (1:1); (G) Cu:Fe (2:1); [H] Cu:Fe (3:1); and [I] CuHCFs

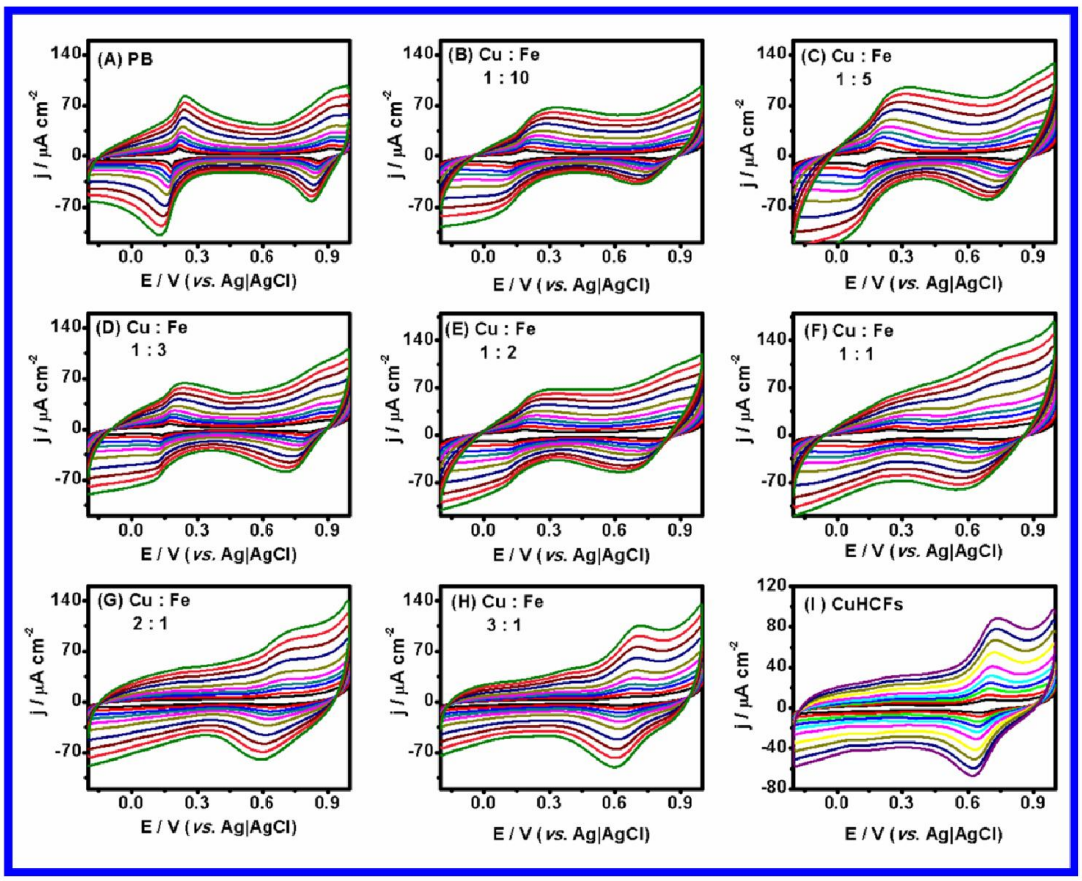

Figure.5. 12. Cyclic voltammetry response of Cu-Fe HCFs modified graphite paste electrode in 0.1 M KNO_3 at scan rate of 0.01, 0.02, 0.035, 0.05, 0.07, 0.10, 0.15, 0.20, 0.25, 0.30 V s^{-1} made at different Cu:Fe molar ratio [A] PBNPs; [B] Cu:Fe (1:10); [C] Cu:Fe (1:5); [D] Cu:Fe (1:3); [E] Cu:Fe (1:2); [F] Cu:Fe (1:1); (G) Cu:Fe (2:1); [H] Cu:Fe (3:1) and [I] CuHCFs.

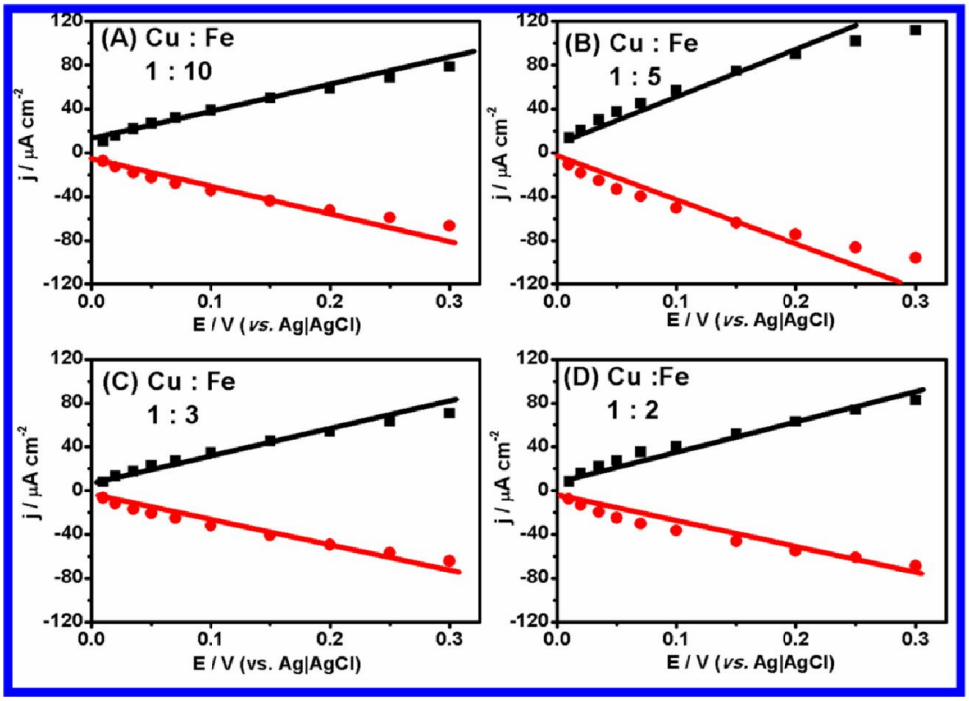

Figure.5. 13. The plots of peak current density *vs*. scan rate for Cu-Fe HCFs made at different molar ratio of Cu:Fe [A] 1:10 [B] 1:5 [C] 1:3 and [D] 1:2.

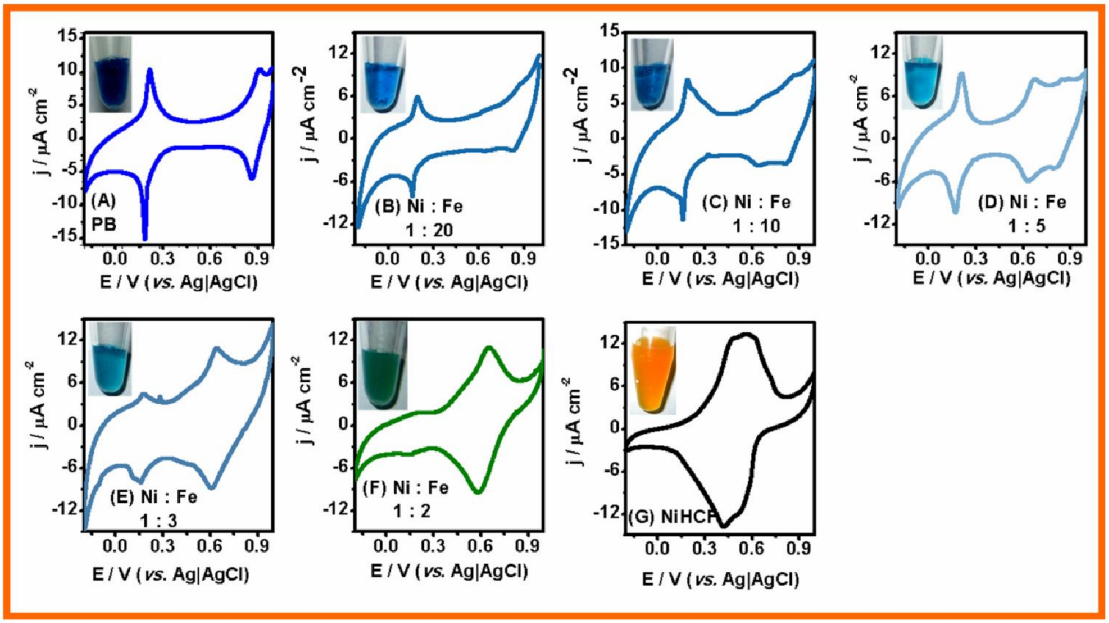

Figure.5. 14. Cyclic voltammetry response of Ni-Fe HCFs modified graphite paste electrode in 0.1 M KNO_3 at scan rate of 0.01 V s^{-1} made at different Ni:Fe molar ratio [A] only PBNPs; [B] Ni:Fe (1:20); [C] Ni:Fe (1:10); [D] Ni:Fe (1:5); [E] Ni:Fe (1:3); [F] Ni:Fe (1:2); [G] NiHCFs.

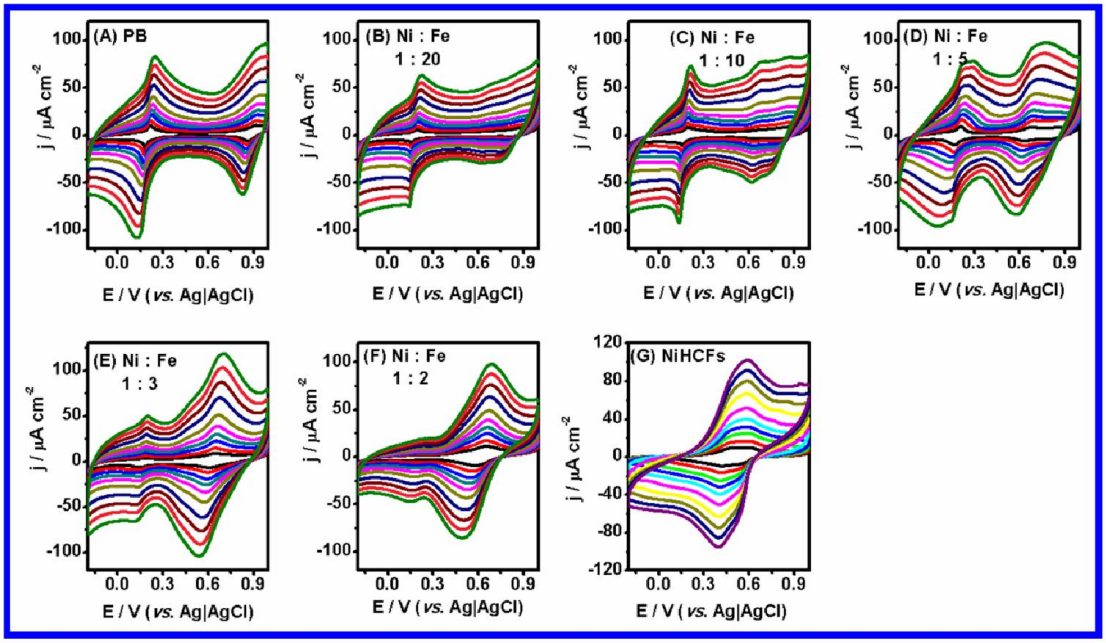

Figure.5. 15. Cyclic voltammetry response of Ni-Fe HCFs modified graphite paste electrode in 0.1 M KNO_3 at varying scan rate of 0.01, 0.02, 0.035, 0.05, 0.07, 0.10, 0.15, 0.20, 0.25, 0.30 V s^{-1} made at different Ni:Fe molar ratio [A] PBNPs; [B] Ni:Fe (1:20); [C] Ni:Fe (1:10); [D] Ni:Fe (1:5); [E] Ni:Fe (1:3); [F] Ni:Fe (1:2); and [G] NiHCFs.

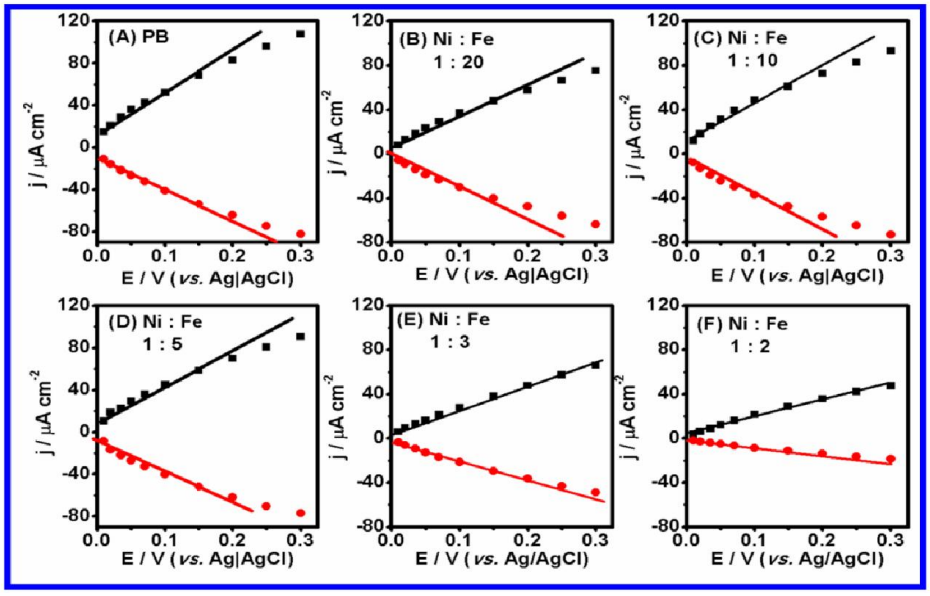

Figure.5. 16. The plots of peak current density *vs*. scan rate for Ni-Fe HCFs made at different molar ratio of Ni:Fe [A] PB [B] 1:20 [C] 1:20 [D] 1:10 [E] 1:5, [F] 1:3 and [1:2].

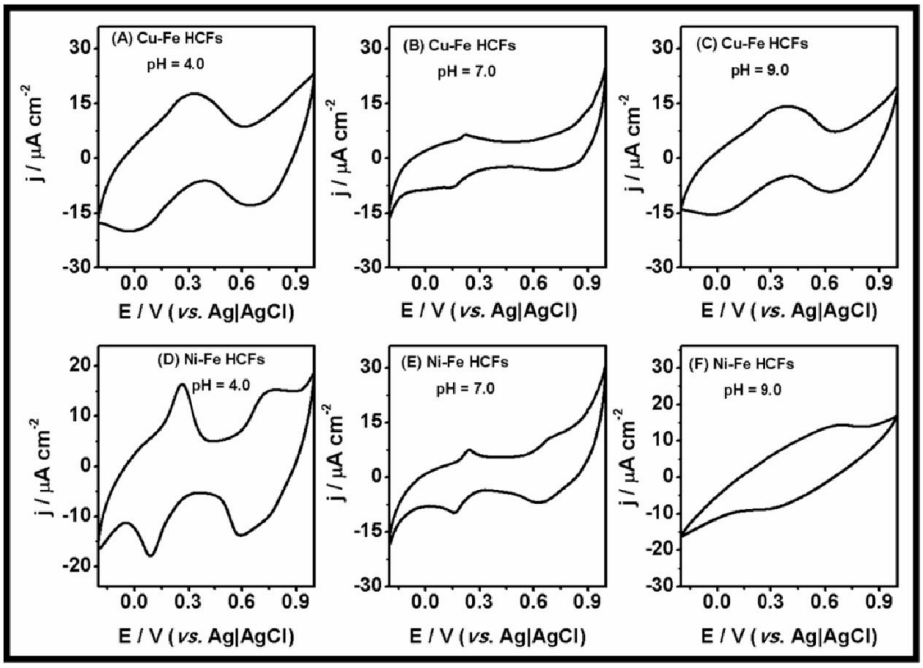

Figure.5. 17. Cyclic voltammetry of (A) to (C) for Cu-Fe HCFs (1:1) and (D) to (F) for Ni-Fe HCFs (1:5) under different pH=4.0 (phthalate buffer), pH=7.0 (phosphate buffer) and pH=9.0 (borate buffer) containing 0.5 M KCl.

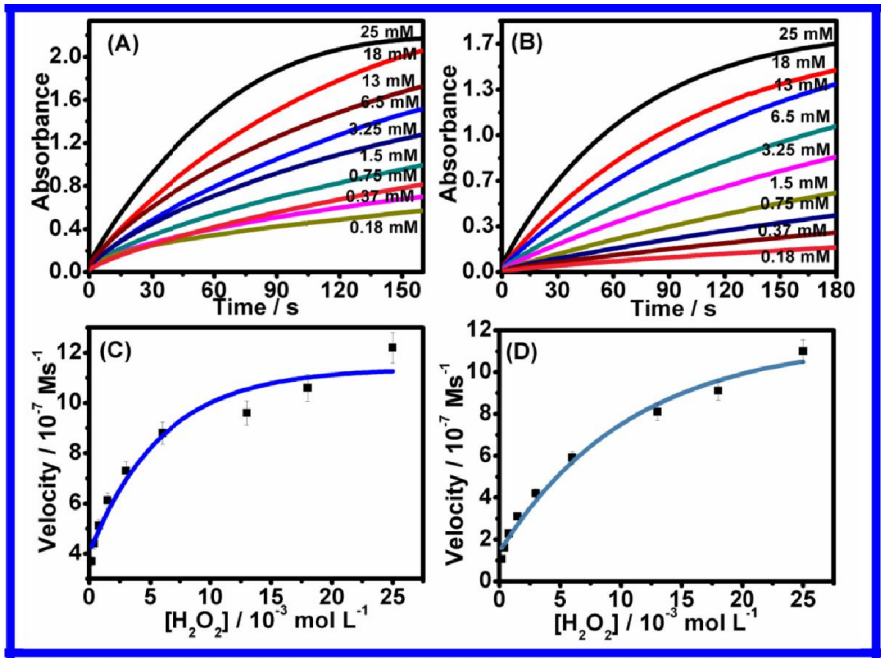

Figure.5. 18. Time dependent absorbance changes at 430 nm in the presence of different concentration (25, 18, 13, 6.5, 3.25, 1.5, 0.75, 0.75, 0.37 and 0.18 mM) of H_2O_2 and fixed concentration of o-dianisidine (50 μM) catalyzed by (A) Cu-Fe HCFs (1:1) and (B) Ni-Fe HCFs (1:5); and kinetic analysis of (C) Cu:Fe HCFs (1:1) and (D) Ni-Fe HCFs (1:5) with H_2O_2 as substrate.

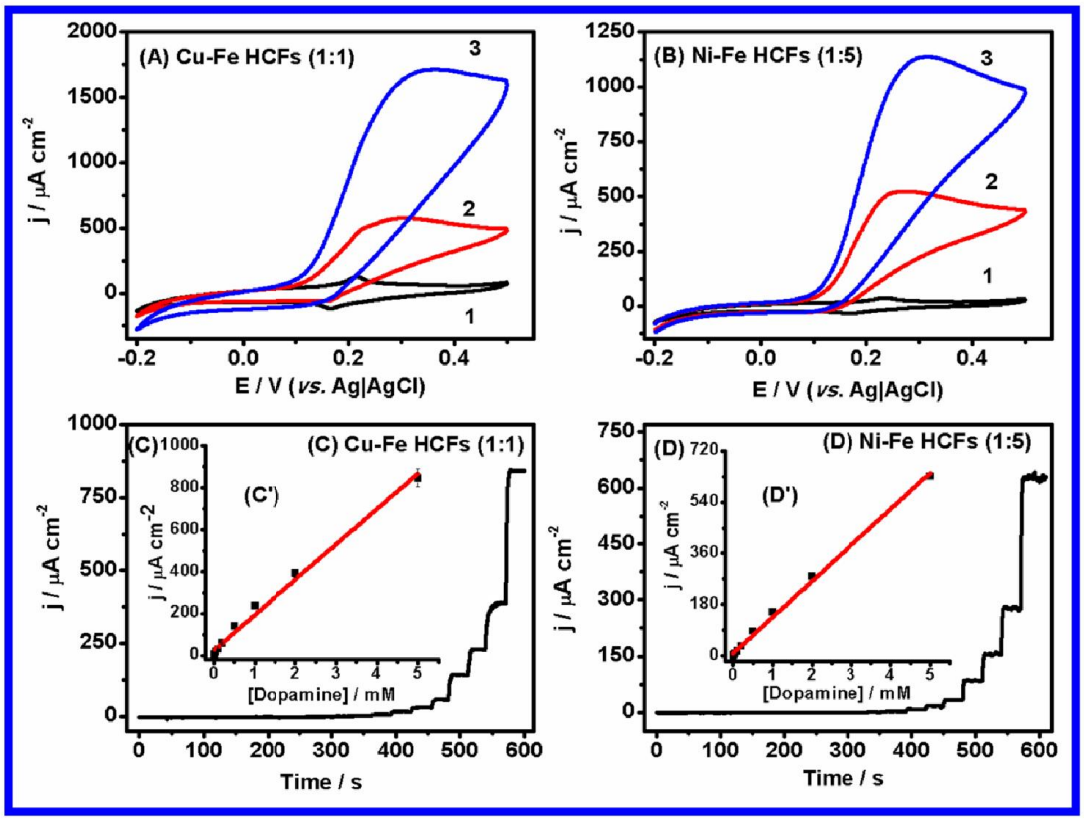

Figure.5. 19. Cyclic voltammogram of (A) Cu-Fe HCFs (1:1) and (B) Ni-Fe HCFs (1:5) in the absence (1) and presence of (2) 2 mM and (3) 5 mM dopamine recorded in 0.1 M phosphate buffer containing 0.5 M KCl, (pH=7.0) at scan rate of 0.01 V s-1; (B) amperometric response of (C) Cu-Fe HCFs (1:1) and (D) Ni-Fe HCFs (1:5) modified graphite paste electrode on the addition of varying concentration of dopamine between 0.01 μM to 5 mM; operating potential 0.2 V; 0.1 M phosphate buffer containing 0.5 M KCl was the supporting electrolyte; the inset (C') and (D') shown the calibration curve for dopamine analysis for the respective modified electrode.

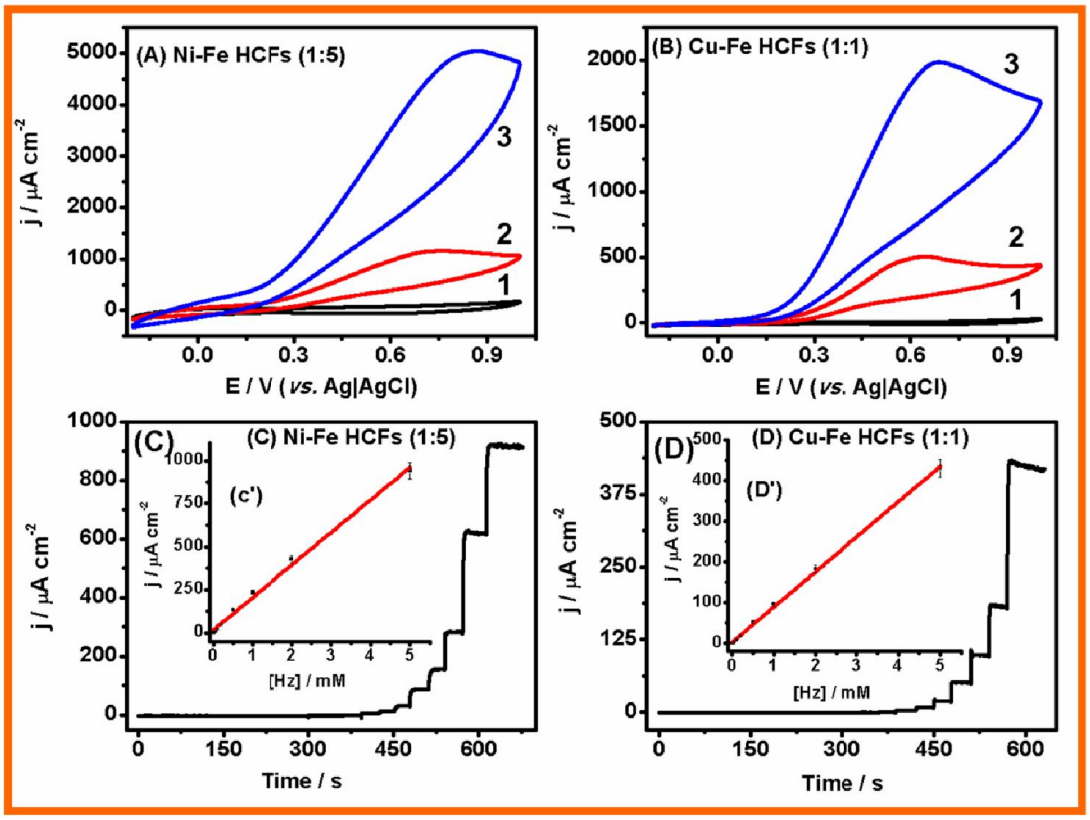

Figure.5. 20. Cyclic voltammogram of (A) Ni-Fe HCFs (1:5) (B) Cu-Fe HCFs (1:1) in the absence (1) and presence of (2) 1 mM and (3) 5 mM hydrazine recorded in 0.1M $NaNO_3$ scan rate of 0.01 V s-1; (B) amperometric response of (C) Ni-Fe HCFs (1:5) and (D) Cu-Fe HCFs (1:1) modified graphite paste electrode on the addition of varying concentration of hydrazine between 0.01 μM to 5 mM; operating potential 0.3 V; 0.1 M $NaNO_3$ was the supporting electrolyte; the inset (C') and (D') shown the calibration curve for hydrazine analysis for the respective modified electrode.

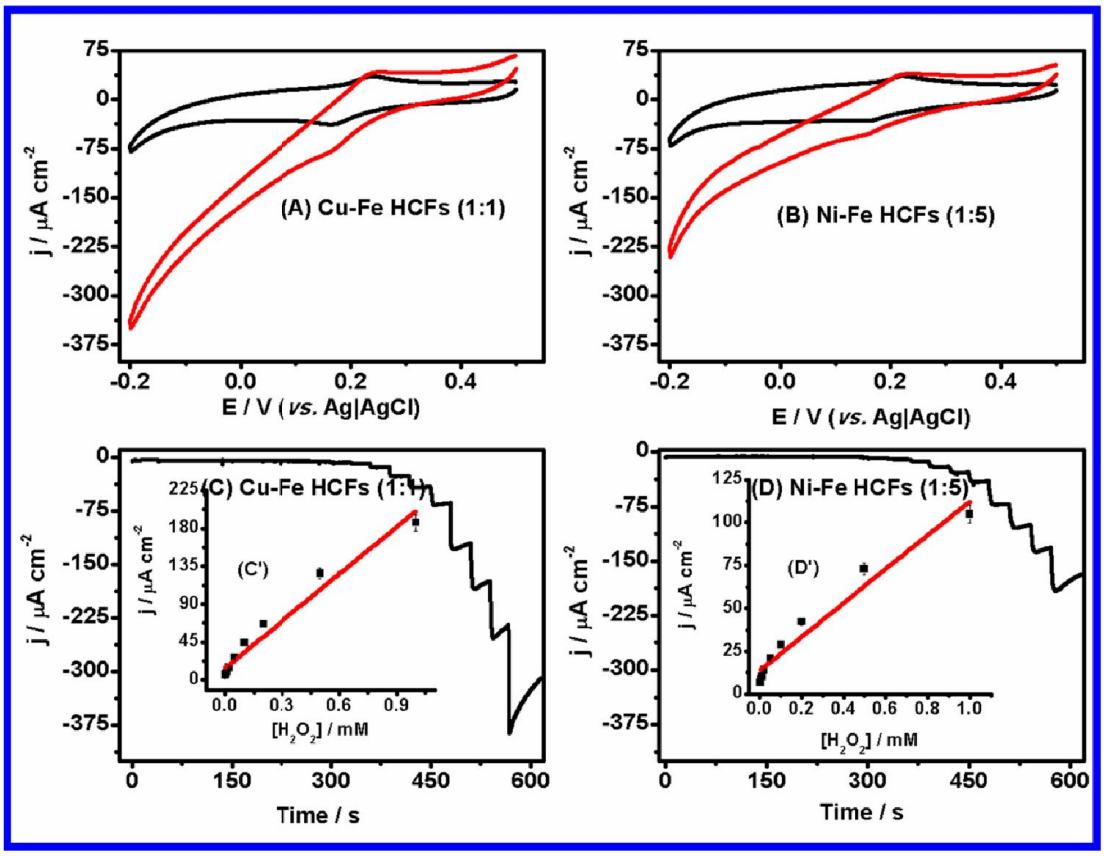

Figure.5. 21. Cyclic voltammogram of (A) Cu-Fe HCFs (1:1) and (B) Ni-Fe HCFs (1:5) in the absence (1) and presence of (2) 1 mM H_2O_2 recorded in 0.1 M phosphate buffer containing 0.5 M KCl, pH=7.0 at scan rate of 0.01 V s^{-1}; (B) amperometric response of (C) Cu-Fe HCFs (1:1) and (D) Ni-Fe HCFs (1:5) modified graphite paste electrode on the addition of varying concentrations of H_2O_2 between 0.01 μM to 5 mM; operating potential 0.0 V; 0.1 M phosphate buffer containing 0.5 M KCl was the supporting electrolyte; the inset (C') and (D') shown the calibration curve for H_2O_2 analysis for the respective modified electrode.

1.4 Discussion

1.4.1 PEI mediated synthesis of nanocrystalline Cu-Fe HCF and Ni-Fe HCFs

We have recently demonstrated the synthesis of Ni-Fe hexacyanoferrates nanoparticles involving the active participation of THF and H_2O_2. [(Pandey and Panday 2016a)] However, the same process does not allow the formation of Cu-Fe hexacyanoferrates. This could be due to the structural deformation happening by the insertion of Cu^{2+} in the 3 dimensional networks of PBNPs in the presence of THF and H_2O_2. In addition to that the crystalline behaviour of as made Prussian blue and its mixed metal analogues was significantly reduced due to the presence of high concentrations of organic moiety. Accordingly, the need of another suitable organic reducing agent overcoming such limitation is desirable that not only allows the controlled formation of mixed metal analogues of several combinations of transitions metal hetero ions but also improve the crystalline behaviour of the as made material. We have recently demonstrated the reducing ability of polycationic polymer, polyethylenimine (PEI) during the synthesis of gold nanoparticles that directed to investigate whether such reagent may be useful for efficient synthesis of Cu-Fe HCFs and Ni-Fe HCFs nanoparticles. It was found that single precursor $K_3[Fe(CN)_6]$, PEI, HCl and Cu^{2+} or Ni^{2+} can be effectively converted into Cu-Fe HCFs and Ni-Fe HCFs nanoparticles respectively at 60 °C in 3 hours having good stability and processability as shown in Figure.5.1. During the conversion process of $K_3[Fe(CN)_6]$ into mixed metal hexacyanoferrate, the yellow colour solution turned into blue colour solution having absorbance maxima at 680 nm. Figure.5.1.(A, B, C, D and E) depict that when all three components are present in an optimum concentration then only stable, well dispersed mixed metal hexacyanoferrates synthesized at 60 °C in 3 hours. Figure.5.1. justify the role of each component during the synthesis of mixed metal hexacyanoferrates. The finding as shown in Figure.5.1.(B) justify the conversion of white colour solution while mixing PEI to $K_3[Fe(CN)_6]$ at 60 °C for 3 hours in absence of HCl [inset to Figure.5.1.(B)] and confirm the conversion of $K_3[Fe(CN)_6]$ into $K_4[Fe(CN)_6]$ as evidenced from the disappearances of absorption maxima at 420 nm which is characteristic of $K_3[Fe(CN)_6$. Similarly when $K_3[Fe(CN)_6]$ is mixed

with HCl and allowed to stand at and keep it at 60 °C for 3 hours, the conversion deep yellow colour from light yellow colour [inset to Figure.5.1.(C)] with little increase in absorbance at 420 nm along with appearance of a new peak at 590 nm [Figure.1.(C)] indicating probable break down of $K_3[Fe(CN)_6]$. Finally when all the components ($K_3[Fe(CN)_6]$, PEI and HCl) are mixed together with $CuSO_4$/$NiSO_4$ and allowed to stand at 60 °C for 3 hours the formation of Cu-Fe HCFs [Figure.5.1(D)] and Ni-Fe HCFs [Figure.5.1.(E)] with good Prussian blue/metal hexacyanoferrate character as evidence from the absorption maxima recorded at 680 nm. The possibility of utilization of $K_4Fe(CN)_6$ in place of $K_3[Fe(CN)_6]$ was explored by synthesizing Cu-Fe HCFs (1:1) and Ni-Fe HCFs (1:5) at the similar condition of mixed metal hexacyanoferrates synthesis and performed the UV-Vis spectroscopy and cyclic voltammetry of as synthesized material over graphite paste electrode in 0.1 M KNO_3. As evidenced from the Figure.5.2 and Figure.5.3. Cu-Fe HCFs (1:1) and Ni:Fe HCFs (1:5) made from $K_3[Fe(CN)_6]$ had better absorbance maxima and better electrochemical behaviour in comparison to the material made through $K_4[Fe(CN)_6]$.

Next stage of the investigation is to understand the role of temperature on PEI mediated synthesis of Cu-Fe HCF/Ni-Fe HCF. Accordingly, the similar processes was allowed to take place at 25 °C and 90 °C respectively. The finding as shown in Figure.5.4. (A) (1) and Figure.5.4.(B) (1) reveals poor rate of Cu-Fe HCF/Ni-Fe HCF synthesis with considerable decrease in PB character as evidenced from absorption maxima recorded at 680 nm which was even observed after keeping the reaction mixture for 4 days at 25 °C. An increase in temperature from 60 °C to 90 °C caused little faster rate of conversion *i.e.* within 2 hours however the absorption maxima shows little red shift with decrease in PB character as shown in Figure.5.4. (A) (2) and Figure.5.4. (B) (2) as compared to that of recorded at 60 °C within 3 hours (Figure.5.4.(A) (3) and Figure.5.4.(B) (3). The UV-Vis spectroscopy result was also confirmed by cyclic voltammetric experiment performed in 0.1 M KNO_3 on graphite paste electrode as shown in Figure.5.5.

We also intended to understand the role of PEI during mixed metal hexacyanoferrate formation. The mixture of optimum concentrations $K_3[Fe(CN)_6$ and HCl was allowed to stand at 60 °C for 24 hours. The results as shown in Figure.5.6. justify appearance significant less in PB character with poor electrochemical behaviour.

The possible mechanism for the synthesis of Cu-Fe HCF/Ni-Fe HCF may involve the following steps: (i) the formation of some Fe^{3+} ions and some undissociated ferricyanide ions (ii) PEI may acts as a reducing agent and stabilizing agent which converts Fe^{3+} into Fe^{2+} ions (iii) undissociated ferricyanide ions, Fe^{2+} ions, and Ni^{2+} or Cu^{2+} ions leads to the synthesis of mixed metal hexacyanoferrates based on possible evidenced recorded in Figure.5.1.

1.4.2 Characterization of Cu-Fe HCFs (1:1) and Ni-Fe HCFs (1:5)

1.4.2.1 FT-IR analysis

Prussian blue character is evaluated from the absorbance maxima recorded at 680 nm as shown in Figure.5.1. FT-IR spectroscopy of as made nanomaterial (Cu-Fe HCFs and Ni-Fe HCFs) as shown in Figure.5.7.(A) and Figure.5.7.(B) reveals a strong absorption peak at 2075 cm^{-1} representing the characteristic peaks of PB and its mixed metal analogues which represents to the stretching vibration of –CN group for $Fe^{III}HCF^{II}$ [(Ghosh 1974; Pandey and Panday 2016b; Pyrasch *et al.* 2003a)]. Absorption bands near 3400 cm^{-1} and 1684 cm^{-2} are assigned to the O-H stretching mode and H-O-H bending mode respectively that can be assigned for the existence of interstitial forces of attraction in the sample [(Itaya *et al.* 1986; Pandey and Panday 2016a)]. The corresponding vibrations in the Ni-Fe HCFs are present at 2059 cm^{-1}, 3400 cm^{-1} and 1643 cm^{-1} which represents as described in the above part of Cu-Fe HCFs.

1.4.2.2 X-Ray diffraction analysis

As synthesized mixed metal hexacyanoferrate was also characterized by X-ray diffraction analysis. Figure.5.8. shows X-ray diffractogram of as synthesized Cu-Fe HCFs and Ni-Fe HCFs respectively. Figure.5.8. (A) shows the XRD pattern

of as synthesized Cu-Fe HCFs (1:1). There are few major peaks at c.a. 17.4°, 24.5°, 28.5°, 35.5°, 39.5°, 40.6° (2θ values) which can be assigned as (200), (220), (311), (400), (420), and (420). The crystallite size of as synthesized Cu-Fe HCFs are found to be 18.2 nm, 9.8 nm, 24.8 nm, 13.4 nm, 25.0 nm and 28.2 nm respectively. Figure.5.8. (B) shows the XRD pattern of as synthesized Ni-Fe HCFs. There are four major characteristic peaks available in Ni-Fe HCFs (1:1) which are at c.a. 17.5°, 24.7°, 35.4°, and 39.7° (2θ values). The crystallite sizes at the major peaks are 9.67 nm, 7.7 nm, 26.8 nm and 8.2 nm respectively. Some other peaks are also present at c.a. 30.5°, 43.7°, 50.7°, 54.5°, 57.4°, 66.3° and 69.2° which can be assigned as (200), (220), (400), (420), (222), (422), (440), (600), (620), (640), (642) and (822) respectively (JCPDS file no- 73-0687).

1.4.2.3 Transmission Electron Microscopy (TEM) analysis and scanning Electron Microscopy (SEM) of mixed metal analogues

Transmission Electron Microscopy (TEM) was done to evaluate the nanogeometry of as synthesized mixed metal analogues (Cu-Fe HCFs and Ni-Fe HCFs). Figure.5.9. (A) and (B) shows TEM images of Cu-Fe HCFs (1:1) and Ni-Fe HCFs (1:5) respectively and justify that the PEI mediated synthesis of Cu-Fe HCFs (1:1) and Ni-Fe HCFs (1:5) are nanoparticles with almost circular in nature. The particle sizes are found in between of 5 nm to 20 nm. Inset to the respective Figure.5.9. (A) and (B) shows the SAED pattern of the respective metal hexacyanoferrate which reveals the polycrystallinity of the as synthesized metal hexacyanoferrates. As compared to the crystallite size obtained from XRD analysis is closely related to the particle size obtained from the TEM analysis for as synthesized mixed metal hexacyanoferrates. Figure.5.9. (C) and (D) shows the SEM characterization of as synthesized Cu-Fe HCFs (1:1) and Ni-Fe HCFs (1:5) respectively which also confirms the nanoparticle behaviour of as synthesized mixed metal hexacyanoferrates.

1.4.2.4 EDS analysis of as synthesized mixed metal analogues

Elemental analysis of as synthesized mixed metal analogues was done by Energy Dispersive Spectroscopy (EDS) analysis. EDS analysis of Cu- Fe HCFs

(1:1) and Ni-Fe HCFs (1:5) are shown in Figure.5.10. (A) and (B) respectively and reveals the presence of all the essential elements available in the respective mixed metal hexacyanoferrates.

1.4.3 Electrochemical behaviour of mixed metal analogue

1.4.3.1 Electrochemistry of Cu-Fe hexacyanoferrates

Electrochemical behaviour of Cu-Fe HCFs nanoparticles was evaluated in 0.1 M KNO_3 solution by cyclic voltammetry on graphite paste modified electrode as shown in Figure.5.11. along with the similar findings on PBNPs modified electrode [(Figure.5.11.(A)]. Figure.5.11.(A) shows the voltammograms of PBNPs modified electrode revealing redox activity at - 0.2 V and ~ 0.9 V due to the redox processes of the outer sphere $Fe^{2+/3+}$ and the inner sphere $[Fe(CN)6]^{4-/3-}$ couples of PB respectively [(Ricci and Palleschi 2005)]. CuHCFs is showing a set of redox couple as shown in Figure.5.11..(I) with a formal potential of approximately 0.6 V. This redox process is due to the Cu^{II}/Fe^{II} to Cu^{II}/Fe^{III} transition and is equivalent to the last redox couple in the PB system [(Siperko and Kuwana 1983)]. Figure.5.11.(B-H) shows the electrochemical behaviour of as synthesized Cu-Fe HCFs with varying molar ratio of Cu-Fe. As can be seen in the Figure.5.11.(A) there are well defined characteristic reversible peak of Prussian blue, one is at -0.2 V *vs.* Ag|AgCl and another is at ~ 0.9 V *vs.* Ag|AgCl which is the characteristic of the oxidation of Prussian white and the reduction of Prussian blue whereas the second redox couple corresponds to the oxidation of PB and the reduction of Berlin green as reported earlier [(Ricci and Palleschi 2005)]. As can be observed from the different composition of Cu-Fe HCFs [(Figure.5.11.(B) to (H)], an increase in Cu-content, the electrochemical behaviour of Prussian blue alters that justify the turning toward individual behaviour of CuHCF [Figure.5.11.(I)] [(Baioni *et al.* 2007a; Wessells *et al.* 2011a)]. The results clearly show that mixed metal analogue with the molar ratio of Cu:Fe (1:1) contains the characteristic voltammetric peaks of CuHCFs and also of PBNPs and designated as Cu-Fe HCFs (1:1). Other composition with the less molar ratio of Cu:Fe contains the PB character predominantly with the broadening in the cyclic

voltammetry. The cyclic voltammograms at different scan rate from 0.01 V s^{-1} to 0.3 V s^{-1} of as synthesized Cu-Fe HCFs are shown in Figure.5.12. The dependence of peak current on the scan rate of cyclic voltammetry was recorded at different scan rate from 0.01 V s^{-1} to 0.3 V s^{-1} and found that on increasing scan rate, the peak current increases which is shown in Figure.5.13.

1.4.3.2 Electrochemistry of as synthesized Ni-Fe hexacyanoferrates

Electrochemical behaviour of as synthesized Ni-Fe HCFs was evaluated by cyclic voltammetry as a function of Ni:Fe molar ratio in Ni-Fe HCFs in 0.1 M KNO_3 solution (Figure.5.14) along with similar results on PBNPs modified graphite paste electrode. Figure.5.14.(B-F) shows the cyclic voltammetric responses recorded for Ni-Fe HCFs at variable Ni:Fe ratio whereas Figure.5.14.(A) shows the voltammograms of PBNPs modified graphite paste electrode revealing redox activity at - 0.2 V and ~ 0.9 V due to the redox processes of the outer sphere $Fe^{2+/3+}$ and the inner sphere $[Fe(CN)6]^{4-/3-}$ couples of PB respectively [(Ricci and Palleschi 2005)]. On the other hand the redox property of NiHCFs as shown in Figure.5.14.(G) shows similar activity at 0.65 V [(Prabakar and Narayanan 2008)]. There are two well defined characteristic redox peaks of Prussian blue as shown in Figure.5.14.(A), the first one is at -0.2 V and another one at ~ 0.9 V *vs.* Ag|AgCl [(Ricci and Palleschi 2005)]. While increasing the concentration of Ni^{2+} in Ni-Fe HCFs (Ni:Fe = 1:10), the PB character starts decreasing and a new peak at 0.46 V *vs*. Ag|AgCl starts appearing along with the PB characteristic peaks [Figure.5.14.(C)]. On further increasing the molar ratio of Ni: Fe (1:5), there is two more peaks (at ~ 0.46 V and ~ 0.6 V *vs*. Ag|AgCl) along with characteristic PB peaks are available. At molar ratio (Ni:Fe = 1:3), again PB character decreases and NiHCFs character [Figure.5.14.(G)] starts dominating. At molar ratio (Ni:Fe = 1:2), the PB character is almost diminished showing the redox peaks at only ~ 0.6 V. These findings reveal that the effect of transition metal ions on the cyclic voltammetry on the Prussian blue and its Ni-Fe HCFs and also justify the presence of other transition metal ion in the 3-dimentional crystal lattice of metal hexacyanoferrates. Since in the Ni-Fe HCFs with the molar ratio

Ni:Fe (1:5) [designated as Ni-Fe HCFs (1:5)] contains well defined PB character [Figure.5.14.(A)] as well as NiHCFs [Figure.5.14.(G)] [(Pandey and Pandey 2013a)] character that is why we choose this composition for all the study related to the as synthesized Ni-Fe HCFs [Figure.5.14.(D)]. The dependence of electrochemical behaviour on the scan rate of all the compositions like PB, Ni-Fe HCFs (1:20), (1:10), (1:5), (1:3) and (1:2) between 0.01 V s^{-1} to 0.3 V *vs.* Ag|AgCl in 0.1 M KNO_3 has been recorded and shown in Figure.5.15. Peak current is low at slow scan rate while it gets increasing on increasing scan rate as shown in Figure.5.16.

The stability of Cu-Fe HCFs (1:1) / Ni- Fe HCFs (1:5) modified electrode was evaluated at different pH by cyclic voltammetry recorded in Phthalate buffer (pH=4.0), Phosphate buffer (pH=7.0) and borate buffer (pH=9.0) containing 0.5 M KCl. Both Cu-Fe HCFs (1:1) and Ni-Fe HCFs (1:5) modified electrode show good electrochemical behaviour at pH=7.0 while at pH=9.0 both metal hexacyanoferrates modified electrode shows sluggish electrochemical behaviour. At pH 4, Ni-Fe HCF (1:5) shows relatively better redox activity whereas Cu-Fe HCF (1:1) shows sluggish redox behaviour under similar condition [Figure.5.17.].

1.4.4 Peroxidase mimetic activity of Cu-Fe HCFs (1:1) and Ni-Fe HCFs (1:5)

Prussian blue nanoparticles and its mixed metal analogues have shown a potential material for the homogeneous detection of hydrogen peroxide [(Dutta *et al.* 2012a; Pandey and Panday 2016b; Zhang *et al.* 2014)]. Prussian blue nanoparticles and its mixed metal analogue can converts reduced form of o-dianisidine to the oxidized form of o-dianisidine which gives absorbance maxima at 430 nm in UV-Vis spectroscopy [(Dutta *et al.* 2012a; Pandey and Panday 2016b; Pandey and Pandey 2013c, d)]. Therefore, it is required to estimate the peroxidase mimetic activity of as synthesized mixed metal analogues. O-dianisidine catalyzed peroxidase mimetic reaction can be represented as:

$$H_2O_2 + \text{O-dianisidine}_{(\text{reduced})} \xrightarrow{\text{Cu-Fe HCFs / Ni-Fe HCFs}} \text{O-dianisidine}_{(\text{oxidised})} + H_2O$$

Where o-dianisidine (ox.), o-dianisidine (red.) can be expressed for oxidized and reduced form of organic dye o-dianisidine. The peroxidase like activity was measured by steady state kinetic experiments which was carried out by varying the H_2O_2 concentration in a 2 ml phosphate buffer (pH=7.0) while keeping o-dianisidine concentration (50 μM) constant in each reaction (Figure.5.18.). Figure.5.18. (A) and (C) show the peroxidase mimetic activity of as synthesized Cu-Fe HCFs (1:1) and Ni-Fe HCFs (1:5) respectively by varying concentration of H_2O_2. Curve in Figure.5.18. (B) and (D) represents that as synthesized Cu-Fe HCFs (1:1) and Ni-Fe HCFs (1:5) show the Michaelis-Menton kinetics. The Michaelis-Menton constant (K_m) for as synthesized Cu-Fe HCFs (1:1) and Ni-Fe HCFs (1:5) are found to be 1.5 mM and 4.2 mM respectively justifying their use in the practical application.

1.4.5 Electrocatalytic oxidation of dopamine, hydrazine and hydrogen peroxide over Cu-Fe HCFs (1:1) and Ni-Fe HCFs (1:5)

Typical applications of as made mixed metal hexacyanoferrate has been examined in the detection of biologically important analyte like dopamine, hydrazine and H_2O_2. The electrochemical application of these nanomaterials was examined over graphite paste electrode.

1.4.5.1 Electrocatalytic oxidation of dopamine over Cu-Fe HCFs (1:1) and Ni-Fe HCFs (1:5) modified electrode

Cu-Fe HCFs (1:1) and Ni-Fe HCFs (1:5) modified graphite paste electrodes were used for the electrocatalytic oxidation of dopamine. Electrocatalytic oxidation of dopamine was performed by cyclic voltammetric in absence (1) and presence (2) and (3) of 2 mM and 5mM dopamine as shown in Figure.5.15. (A) and Figure.5.19. (B) for Cu-Fe HCFs (1:1) and Ni-Fe HCFs (1:5) respectively. There is an increase in anodic current at 0.1 V *vs.* Ag|AgCl in the presence of dopamine justifying the electrocatalytic oxidation of dopamine over Cu-Fe HCFs (1:1) and Ni-Fe HCFs (1:5) modified graphite paste electrode. Electrocatalytic oxidation of dopamine was quantified by amperometry. Since dopamine undergoes direct oxidation above 0.3 V *vs*. Ag|AgCl accordingly the amperometric

sensing of the same is recorded at 0.2 V *vs*. Ag|AgCl to avoid the contribution due to direct oxidation of dopamine. The amperometric response of dopamine sensing was performed by addition of increasing concentrations of dopamine (0.01, 0.02, 0.05, 0.1, 0.2, 0.5, 1, 2, 5, 10, 20, 50, 150, 300, 700, 1000, 2000 and 5000 μM respectively in 0.1 M phosphate buffer, pH=7.0 at 0.2 V *vs.* Ag|AgCl. The amperometric response of dopamine analysis recorded at 0.2 V *vs.* Ag|AgCl is shown in Figure.5.19. (C) and Figure.5.19. (D) for Cu-Fe HCFs (1:1) and Ni-Fe HCFs (1:5) respectively. The sensitivity of dopamine sensing was found to be 192.4 μA mM^{-1} cm^{-2} and 129.0 μA mM^{-1} cm^{-2} for Cu-Fe HCFs (1:1) and Ni-Fe HCFs (1:5) modified electrode respectively. The dependence of anodic current on the concentration of dopamine was linear between 0.5 μM to 5 mM for both the electrodes. The lowest detection limit was found to be 100 nM and 0.5 μM for Cu-Fe HCFs (1:1) and Ni-Fe HCFs (1:5) modified electrode respectively [Inset to the Figure.5.19. (C) and Figure.5.19. (D)].

1.4.5.2 Electrocatalytic oxidation of hydrazine over Ni-Fe HCFs (1:5) and Cu-Fe HCFs (1:1) modified electrode

As synthesized Ni-Fe HCFs (1:5) and Cu-Fe HCFs (1:1) modified graphite paste electrodes were explored for the detection of hydrazine in 0.1 M $NaNO_3$. Figure.5.20. (A) and Figure.5.20. (B) shows the cyclic voltammograms in the absence (1) and presence (2) and (3) of 1 mM and 5 mM hydrazine in 0.1 M $NaNO_3$ over Ni-Fe HCFs (1:5) and Cu-Fe HCFs (1:1) modified graphite paste electrode respectively. The electro-oxidation of hydrazine was recorded close to 0.3 V *vs.* Ag|AgCl reveals at the surface of Ni-Fe HCFs (1:5) and Cu-Fe HCFs (1:1) modified electrodes. Hydrazine undergoes direct oxidation above 0.4 V *vs*. Ag|AgCl accordingly the amperometric sensing of the same is recorded at 0.3 V *vs*. Ag|AgCl to avoid the contribution due to direct oxidation. The amperometric response of hydrazine sensing was performed by addition of increasing concentration of hydrazine (0.01, 0.02, 0.05, 0.1, 0.2, 0.5, 1, 2, 5, 10, 20, 50, 150, 300, 700, 1000, 2000 and 5000 μM respectively in 0.1 M 0.1 M $NaNO_3$ at 0.3 V *vs.* Ag|AgCl. Figure.5.20 (C) and Figure.5.20 (D). shows the amperometric

response for hydrazine oxidation at 0.3 V *vs*. Ag|AgCl under stirring for Ni-Fe HCFs (1:5) and Cu-Fe HCFs (1:1) modified electrodes. The sensitivity of electroanalysis was found to the order of 221.9 μA mM^{-1} cm^{-2} and 97.4 μA mM^{-1} cm^{-2} with the lowest detection limit of 50 nM and 0.2 μM for Ni-Fe HCFs (1:5) and Cu-Fe HCFs (1:1) modified graphite paste electrode respectively. The dependence of anodic current on the concentration of hydrazine was linear between 0.5 μM to 5 mM.

1.4.5.3 Electrocatalytic reduction of H_2O_2 over Cu-Fe HCFs (1:1) and Ni-Fe HCFs (1:5) modified electrode

As synthesized Cu-Fe HCFs (1:1) and Ni-Fe HCFs (1:5) possesses the Prussian blue character therefore it is intended to do the electrocatalytic reduction of H_2O_2 over Cu-Fe HCFs (1:1) and Ni-Fe (1:5) modified graphite paste electrodes. Electrocatalytic reduction of H_2O_2 was performed over these modified electrode in 0.1 M phosphate buffer (pH=7.0) containing 0.5 M KCl. Figure.5.21. (A) and Figure.5.21. (B) shows the cyclic voltammograms of in the absence (1) and presence (2) of 1 mM H_2O_2 in 0.1 M phosphate buffer containing 0.5 M KCl over Cu-Fe HCFs (1:1) and Ni-Fe HCFs (1:5) modified graphite paste electrodes. The amperometric response of H_2O_2 sensing was performed by addition of increasing concentration of H_2O_2 (0.01, 0.02, 0.05, 0.1, 0.2, 0.5, 1, 2, 5, 10, 20, 50, 150, 300, 700, 1000, 2000 and 5000 μM) in 0.1 M phosphate buffer, (pH 7=0) at 0.0 V *vs.* Ag|AgCl. The electrocatalytic reduction of H_2O_2 was measured by amperometric analysis over these modified electrodes at fixed potential of 0.0 V *vs.* Ag|AgCl. The sensitivity of electroanalysis was found to the order of 203.2 μA mM^{-1} cm^{-2} and 112.9 μA mM^{-1} cm^{-2} with the lowest detection limit of 0.2 μM and 2 μM for Cu-Fe HCFs (1:1) and Ni-Fe HCFs (1:5) modified graphite paste electrode respectively. The dependence of anodic current on the concentration of H_2O_2 was linear between 0.5 μM to 1 mM for both Cu-Fe HCFs (1:1) and Ni-Fe HCFs (1:5) modified electrode [Inset to the Figure.5.21. (C) and Figure.5.21. (D)].

1.4.6 Stability and Reproducibility

Stability of the present systems was evaluated by repetitive experiments on cyclic voltammetry for 100 continuous cycles at 10 mV s^{-1}. The peak current was found to be decreases by 4% after 100 cycles justifying better stability of the modified electrode.. The reproducibility of these modified electrodes were examined by cyclic voltammetry in the reaction system containing 2 mM dopamine in case of Cu-Fe HCFs electrode whereas 1 mM hydrazine in case of Ni-Fe HCFs electrode for 20 repetitive cycles at 10 mV s^{-1}. It was found that the oxidation peak potential of dopamine and hydrazine was not changed and the anodic peak current was decreased by less than 3.9 %. The relative standard deviation (RSD) of the current response to 2 mM dopamine at 0.2 V was found to be 3.2 % for 12 successive measurements in case of Cu-Fe HCFs electrode surface. The relative standard deviation (RSD) during hydrazine (1 mM) sensing at 0.3 V was found to be 2.8 % for 12 successive measurements in case of Ni-Fe HCFs electrode surface.

Summary

The thesis entitled "Studies on nanocrystalline Prussian blue and its mixed metal analogue for analytical application" has been divided into following five chapters:

1. General Introduction.
2. Tetrahydrofuran and hydrogen peroxide mediated synthesis of nanocrystalline Prussian blue nanoparticles and its analytical applications.
3. Tetrahydrofuran and hydrogen peroxide mediated synthesis of nanocrystalline Nickel-iron hexacyanoferrates nanoparticles and its analytical applications.
4. Polyethylenimine mediated Synthesis of nanocrystalline Prussian blue nanoparticles and cooperative self assembly of gold nanoparticles on polycationic surface and their analytical applications.
5. Polyethylenimine mediated synthesis of nanocrystalline mixed metal analogues and their analytical applications.

Chapter 1 describes an overview of metal hexacyanoferrates (MHCFs) in special reference to Prussian blue. An extensive survey on the structure, synthesis of Prussian blue nanoparticles (PBNPs) and its mixed metal analogues was reported followed by their use in the field of medical, environmental, energy storage devices *etc*. The utilization of PBNPs and its mixed metal analogues in the development of electrochemical sensor was critically reviewed. Later, definition of the problem, objective of the present programme and the work plan is reported.

Chapter 2 describes the tetrahydrofuran (THF) and hydrogen peroxide (H_2O_2) mediated synthesis of nanocrystalline Prussian blue nanoparticles (PBNPs) and their characterization through various techniques like AFM, FT-IR, XRD, TEM and through electrochemical. We found that potassium ferricyanide $K_3[Fe(CN)_6]$ in the presence of THF and H_2O_2 at 60 °C gets converted into stable nanocrystalline PBNPs with the crystallite size of 14.0 nm which shows good electrochemical behaviour. As synthesized PBNPs was used for the electrochemical reduction of H_2O_2. The as synthesized PBNPs was also explored its peroxidase mimetic activity in the presence of o-dianisidine. The Michaelis–Menten constant (K_m) and the maximal reaction velocity (V_{max}) for H_2O_2 analysis

was found to be 0.49 mM and 6.03 10^{-7} M s^{-1} justifying the use of nanomaterial as perfect peroxidase replacement.

Chapter 3 describes THF and H_2O_2 mediated synthesis of nanocrystalline Nickel-iron hexacyanoferrates (Ni-Fe HCFs). It was observed that in the presence of THF, H_2O_2, $NiSO_4$ and $K_3[Fe(CN)_6]$ gets converted into Ni-Fe HCFs at 60 °C in 30 minutes. As synthesized Ni-Fe HCFs was characterized by FT-IR, XRD, SEM, TEM and EDS. The crystallite size was found to be 11 nm and the particle size was 31 nm. As synthesized Ni-Fe HCFs showed differential redox activity depending upon the molar ratio of Ni:Fe. As synthesized Ni-Fe HCFs was found to water soluble therefore it could be used for both homogeneous and heterogeneous catalysis. So, Ni-Fe HCFs was efficiently used for the electrocatalytic oxidation of hydrazine and homogeneous detection of H_2O_2. Ni-Fe HCFs show excellent peroxidase mimetic activity with the Michaelis–Menten constant (K_m) and V_{max} in the order of 1.5 mM and 3.06 × 10^{-7} M s^{-1} respectively for H_2O_2 mediated oxidation of o-dianisidine thus representing novel material for both homogeneous and heterogeneous catalysis.

Chapter 4 describes polyethylenimine (PEI) mediated synthesis of nanocrystalline PBNPs and their assembly to the gold nanoparticles (AuNPs). It was observed that in the presence of PEI, HCl and $K_3[Fe(CN)_6]$ converts into PBNPs at 60 °C in 3 hours. As synthesized PBNPs was water dispersible and stable. It was also found that by mixing gold chloride salt into the as synthesized PBNPs leads to the synthesis of AuNPs assembled PBNPs within 5 minutes at 60 °C. Both PBNPs and AuNPs assembled PBNPs was characterized by XRD, TEM analysis and cyclic voltammograms. The crystallite size of PBNPs was found to be 42 nm with the particle size of 5 – 25 nm. These materials were used for the electrocatalytic reduction and oxidation of H_2O_2 and homogeneous reduction of H_2O_2 as peroxidase mimetic materials. It was found that electrocatalytic efficiency of PBNPs was further increased on the incorporation of AuNPs.

Chapter 5 describes the PEI mediated synthesis of nanocrystalline mixed metal analogues like copper-iron (Cu-Fe HCFs) and nickel-iron hexacyanoferrates (Ni-Fe HCFs) at 60 °C in 3 hours. As synthesized mixed metal analogues was characterized by FT-IR, XRD, TEM, EDS and cyclic voltammetry. We observed

that the cyclic voltammograms of as synthesized mixed metal hexacyanoferrates depends upon the molar ratio of iron to respective transition metal. Therefore, it could be possible the tuning of redox potential of PBNPs justified the controlled incorporation of hetero-transition metal ions in the 3-dimentional cubic lattice. As synthesized mixed metal analogues were further explored for the possibility of replacement of peroxidase enzyme as peroxidase mimetic materials. Cu-Fe HCFs (1:1) and Ni-Fe HCFs (1:5) have excellent peroxidase mimetic activity with Michaelis–Menten constant (K_m) to the order of 1.5 mM and 4.2 mM respectively. Mixed metal analogues were used for the electrocatalytic oxidation of dopamine, hydrazine and H_2O_2 over Cu-Fe HCFs (1:1) and Ni-Fe HCFs (1:5) respectively.

Future Projection

This Ph.D. work covers the challenges associated with the synthesis of processable Prussian blue nanoparticles (PBNPs) and its mixed metal analogues having potential applications for many biological analytes. Moreover, the applicability of the present work involves single precursor based synthesis of PBNPs and its mixed metal analogues which have been utilized for the electrochemical sensing of hydrogen peroxide, hydrazine and dopamine. Applicability of these mixed metal nanoparticles as peroxidase mimetic reveals the perfect material for the replacement of peroxidase enzyme in biological reactions. However, the properties related to the magnetic, optical and secondary cell of such PB based nanomaterials have not been worked. The utilization of these materials in ferromagnetism, charging-discharging and optical behaviour of such nanomaterials would be helpful for the development of practical devices. In additions to these, the nanocomposite materials with as synthesized PBNPs and mixed metal analogues could improve the sensitivity and selectivity and have the possibility in the development of electrochemical sensor / biosensor for variety of analytes.

References

Abbaspour, A., Ghaffarinejad, A., 2008. Electrocatalytic oxidation of l-cysteine with a stable copper–cobalt hexacyanoferrate electrochemically modified carbon paste electrode. Electrochim. Acta 53(22), 6643-6650.

Abbaspour, A., Kamyabi, M.A., 2005a. Electrocatalytic oxidation of hydrazine on a carbon paste electrode modified by hybrid hexacyanoferrates of copper and cobalt films. J. Electroanal. Chem. 576(1), 73-83.

Abbaspour, A., Kamyabi, M.A., 2005b. Electrochemical formation of Prussian blue films with a single ferricyanide solution on gold electrode. J. Electroanal. Chem. 584(2), 117-123.

Adekunle, A.S., Farah, A.M., Pillay, J., Ozoemena, K.I., Mamba, B.B., Agboola, B.O., 2012. Electrocatalytic properties of prussian blue nanoparticles supported on poly (m-aminobenzenesulphonic acid)-functionalised single-walled carbon nanotubes towards the detection of dopamine. Colloids Surf. B. Biointerfaces 95, 186-194.

Adekunle, A.S., Mamba, B.B., Agboola, B.O., Ozoemena, K.I., 2011. Nitrite electrochemical sensor based on prussian blue/single-walled carbon nanotubes modified pyrolytic graphite electrode.

Agnihotri, S., Mukherji, S., Mukherji, S., 2014. Size-controlled silver nanoparticles synthesized over the range 5-100 nm using the same protocol and their antibacterial efficacy. RSC Adv 4(8), 3974-3983.

Ahmadalinezhad, A., Kafi, A., Chen, A., 2009. Glucose biosensing based on the highly efficient immobilization of glucose oxidase on a Prussian blue modified nanostructured Au surface. Electrochem. Commun. 11(10), 2048-2051.

Alamo, L.S.T., Tangkuaram, T., Satienperakul, S., 2010. Determination of sulfite by pervaporation-flow injection with amperometric detection using copper hexacyanoferrate-carbon nanotube modified carbon paste electrode. Talanta 81(4), 1793-1799.

André, R., Natálio, F., Humanes, M., Leppin, J., Heinze, K., Wever, R., Schröder, H.C., Müller, W.E., Tremel, W., 2011. V2O5 Nanowires with an Intrinsic Peroxidase-Like Activity. Adv. Funct. Mater. 21(3), 501-509.

Ang, J.Q., Nguyen, B.T.T., Toh, C.-S., 2011. A dual K+–Na+ selective Prussian blue nanotubes sensor. Sensors and Actuators B: Chemical 157(2), 417-423.

Asati, A., Santra, S., Kaittanis, C., Nath, S., Perez, J.M., 2009. Oxidase-like activity of polymer-coated cerium oxide nanoparticles. Angew. Chem. Int. Ed. Engl. 48(13), 2308-2312.

Ashrit, P.V., Benaissa, K., Bader, G., Girouard, F.E., Truong, V.-V., 1993. Lithiation studies on some transition metal oxides for an all-solid thin film electrochromic system. Solid State Ionics 59(1), 47-57.

Ayers, J.B., Waggoner, W.H., 1971. Synthesis and properties of two series of heavy metal hexacyanoferrates. J. Inorg. Nucl. Chem. 33(3), 721-733.

Baioni, A.P., Vidotti, M., Fiorito, P.A., Ponzio, E., Córdoba de Torresi, S.I., 2007a. Synthesis and characterization of copper hexacyanoferrate nanoparticles for building up long-term stability electrochromic electrodes. Langmuir 23(12), 6796-6800.

Baioni, A.P., Vidotti, M., Fiorito, P.A., Ponzio, E.A., Córdoba de Torresi, S.I., 2007b. Synthesis and Characterization of Copper Hexacyanoferrate Nanoparticles for Building Up Long-Term Stability Electrochromic Electrodes. Langmuir 23(12), 6796-6800.

Bao, S., Qin, W., Wu, Q., Liang, G., Zhu, F., Wu, Q., 2013. Synthesis and characterization of ultrathin metal coordination Prussian blue nanoribbons. Dalton Transactions 42(15), 5242-5246.

Barus, C., Gros, P., Comtat, M., Daunes-Marion, S., Tarroux, R., 2007. Electrochemical behaviour of N-acetyl-l-cysteine on gold electrode—A tentative reaction mechanism. Electrochim. Acta 52(28), 7978-7985.

Berrettoni, M., Giorgetti, M., Zamponi, S., Conti, P., Ranganathan, D., Zanotto, A., Saladino, M.L., Caponetti, E., 2010. Synthesis and Characterization of Nanostructured Cobalt Hexacyanoferrate. The Journal of Physical Chemistry C 114(14), 6401-6407.

Bharathi, S., Phani, K., Joseph, J., Pitchumani, S., Jeyakumar, D., Rao, G.P., Rangarajan, S., 1992. Zeolite matrix effects on the electrochemistry of metal hexacyanoferrates. J. Electroanal. Chem. 334(1), 145-153.

Bo, Y., Wang, W., Qi, J., Huang, S., 2011. A DNA biosensor based on graphene paste electrode modified with Prussian blue and chitosan. Analyst 136(9), 1946-1951.

Bocarsly, A.B., Sinha, S., 1982. Chemically-derivatized nickel surfaces: Synthesis of a new class of stable electrode interfaces. J Electroanal Chem Interfacial Electrochem 137(1), 157-162.

Boxhoorn, G., Moolhuysen, J., Coolegem, J.G.F., van Santen, R.A., 1985. Cyanometallates: an underestimated class of molecular sieves. J. Chem. Soc., Chem. Commun.(19), 1305-1307.

Boyer, A., Kalcher, K., Pietsch, R., 1990. Voltammetric behavior of perborate on prussian-blue-modified carbon paste electrodes. Electroanalysis 2(2), 155-161.

Bozorth, R., Williams, H., Walsh, D.E., 1956. Magnetic properties of some orthoferrites and cyanides at low temperatures. Physical Review 103(3), 572.

Breslow, R., Overman, L.E., 1970. " Artificial enzyme" combining a metal catalytic group and a hydrophobic binding cavity. J. Am. Chem. Soc. 92(4), 1075-1077.

Burke, L.D., Lyons, M.E., Murphy, O.J., 1982. Formation of hydrous oxide films on cobalt under potential cycling conditions. J Electroanal Chem Interfacial Electrochem 132, 247-261.

Burke, L.D., Murphy, O.J., 1980a. The electrochemical behaviour of RuO2-based mixed-oxide anodes in base. J Electroanal Chem Interfacial Electrochem 109(1), 199-212.

Burke, L.D., Murphy, O.J., 1980b. Electrochromic behaviour of oxide films grown on cobalt and manganese in base. J Electroanal Chem Interfacial Electrochem 109(1), 373-377.

Burke, L.D., O'Sullivan, E.J.M., 1978. Enhanced oxide growth at a rhodium surface in base under potential cycling conditions. J Electroanal Chem Interfacial Electrochem 93(1), 11-18.

Burke, L.D., Whelan, D.P., 1984. A voltammetric investigation of the charge storage reactions of hydrous iridium oxide layers. J Electroanal Chem Interfacial Electrochem 162(1), 121-141.

Buser, H.J., Ludi, A., Petter, W., Schwarzenbach, D., 1972. Single-crystal study of Prussian Blue: Fe4[Fe(CN)6]2, 14H2O. J. Chem. Soc., Chem. Commun.(23), 1299-1299.

Buser, H.J., Schwarzenbach, D., Petter, W., Ludi, A., 1977. The crystal structure of Prussian Blue: Fe4[Fe(CN)6]3.xH2O. Inorg. Chem. 16(11), 2704-2710.

Cai, C.-X., Ju, H.-X., Chen, H.-Y., 1995a. Catalytic oxidation of reduced nicotinamide adenine dinucleotide at a microband gold electrode modified with nickel hexacyanoferrate. Anal. Chim. Acta 310(1), 145-151.

Cai, C.-X., Ju, H.-X., Chen, H.-Y., 1995b. Cobalt hexacyanoferrate modified microband gold electrode and its electrocatalytic activity for oxidation of NADH. J. Electroanal. Chem. 397(1), 185-190.

Cai, C.-X., Xue, K.-H., Xu, S.-M., 2000. Electrocatalytic activity of a cobalt hexacyanoferrate modified glassy carbon electrode toward ascorbic acid oxidation. J. Electroanal. Chem. 486(2), 111-118.

Campus, F., Bonhôte, P., Grätzel, M., Heinen, S., Walder, L., 1999. Electrochromic devices based on surface-modified nanocrystalline TiO2 thin-film electrodes. Sol. Energy Mater. Sol. Cells 56(3–4), 281-297.

Cao, L., Liu, Y., Zhang, B., Lu, L., 2010. In situ Controllable Growth of Prussian Blue Nanocubes on Reduced Graphene Oxide: Facile Synthesis and Their Application as Enhanced Nanoelectrocatalyst for H2O2 Reduction. ACS Applied Materials & Interfaces 2(8), 2339-2346.

Carpenter, M.K., Conell, R.S., Simko, S.J., 1990. Electrochemistry and electrochromism of vanadium hexacyanoferrate. Inorg. Chem. 29(4), 845-850.

Castro, S.S., Balbo, V.R., Barbeira, P.J., Stradiotto, N.R., 2001. Flow injection amperometric detection of ascorbic acid using a Prussian Blue film-modified electrode. Talanta 55(2), 249-254.

Chandra Das, G., Bhuyan, D., Sen Sarma, N., Kumar Medhi, O., 2014. Synthesis and properties of Prussian blue nanoparticles prepared by using Cetyl Pyridinium Chloride as protecting agent. International Journal of Nano Dimension 6(2), 129-133.

Che, X., Yuan, R., Chai, Y., Li, J., Song, Z., Li, W., Zhong, X., 2011. A glucose biosensor based on chitosan–Prussian blue–multiwall carbon nanotubes–hollow PtCo nanochains formed by one-step electrodeposition. Colloids Surf. B. Biointerfaces 84(2), 454-461.

Chen, H., Li, Y., Zhang, F., Zhang, G., Fan, X., 2011. Graphene supported Au-Pd bimetallic nanoparticles with core-shell structures and superior peroxidase-like activities. J. Mater. Chem. 21(44), 17658-17661.

Chen, L.C., Tseng, K.S., Ho, K.C., 2006. General kinetic model for amperometric sensors based on prussian blue mediator and its analogs: Application to cysteine detection. Electroanalysis 18(13-14), 1313-1321.

Chen, W., Chen, J., Feng, Y.-B., Hong, L., Chen, Q.-Y., Wu, L.-F., Lin, X.-H., Xia, X.-H., 2012a. Peroxidase-like activity of water-soluble cupric oxide nanoparticles and its analytical application for detection of hydrogen peroxide and glucose. Analyst 137(7), 1706-1712.

Chen, W., Tang, J., Cheng, H.-J., Xia, X.-H., 2009. A simple method for fabrication of sole composition nickel hexacyanoferrate modified electrode and its application. Talanta 80(2), 539-543.

Chen, X., Chen, Z., Tian, R., Yan, W., Yao, C., 2012b. Glucose biosensor based on three dimensional ordered macroporous self-doped polyaniline/Prussian blue bicomponent film. Anal. Chim. Acta 723, 94-100.

Chi, Q., Dong, S., 1995. Amperometric biosensors based on the immobilization of oxidases in a Prussian blue film by electrochemical codeposition. Anal. Chim. Acta 310(3), 429-436.

Chiu, J.-Y., Yu, C.-M., Yen, M.-J., Chen, L.-C., 2009. Glucose sensing electrodes based on a poly (3, 4-ethylenedioxythiophene)/Prussian blue bilayer and multi-walled carbon nanotubes. Biosens. Bioelectron. 24(7), 2015-2020.

Christensen, P.A., Harriman, A., Neta, P., Richoux, M.-C., 1985. Photo-oxidation of water using Prussian Blue as catalyst. Journal of the Chemical Society, Faraday Transactions 1: Physical Chemistry in Condensed Phases 81(10), 2461-2466.

Chu, H.-W., Thangamuthu, R., Chen, S.-M., 2007. Zinc Oxide/Zinc Hexacyanoferrate Hybrid Film-Modified Electrodes for Guanine Detection. Electroanalysis 19(18), 1944-1951.

Coon, D.R., Amos, L.J., Bocarsly, A.B., Fitzgerald Bocarsly, P.A., 1998. Analytical applications of cooperative interactions associated with charge transfer in cyanometalate electrodes: Analysis of sodium and potassium in human whole blood. Anal. Chem. 70(15), 3137-3145.

Cui, L., Zhu, J., Meng, X., Yin, H., Pan, X., Ai, S., 2012. Controlled chitosan coated Prussian blue nanoparticles with the mixture of graphene nanosheets and carbon nanoshperes as a redox mediator for the electrochemical oxidation of nitrite. Sensors and Actuators B: Chemical 161(1), 641-647.

Cui, R., Han, Z., Zhu, J.J., 2011. Helical carbon nanotubes: intrinsic peroxidase catalytic activity and its application for biocatalysis and biosensing. Chemistry–A European Journal 17(34), 9377-9384.

Cui, X., Hong, L., Lin, X., 2002. Electrochemical preparation, characterization and application of electrodes modified with hybrid hexacyanoferrates of copper and cobalt. J. Electroanal. Chem. 526(1–2), 115-124.

Davidson, D., Welo, L.A., 1928. The Nature of Prussian Blue. The Journal of Physical Chemistry 32(8), 1191-1196.

de la Escosura, A., Verwegen, M., Sikkema, F.D., Comellas-Aragones, M., Kirilyuk, A., Rasing, T., Nolte, R.J.M., Cornelissen, J.J.L.M., 2008. Viral capsids as templates for the production of monodisperse Prussian blue nanoparticles. Chem. Commun.(13), 1542-1544.

de Tacconi, N.R., Rajeshwar, K., Lezna, R.O., 2003. Metal Hexacyanoferrates: Electrosynthesis, in Situ Characterization, and Applications. Chem. Mater. 15(16), 3046-3062.

DeLongchamp, D.M., Hammond, P.T., 2004a. High-contrast electrochromism and controllable dissolution of assembled Prussian blue/polymer nanocomposites. Adv. Funct. Mater. 14(3), 224-232.

DeLongchamp, D.M., Hammond, P.T., 2004b. Multiple-Color Electrochromism from Layer-by-Layer-Assembled Polyaniline/Prussian Blue Nanocomposite Thin Films. Chem. Mater. 16(23), 4799-4805.

Devadas, B., Cheemalapati, S., Chen, S.-M., Rajkumar, M., 2014a. Investigation of morphologies and characterization of rare earth metal samarium hexacyanoferrate and its composite with surfactant intercalated graphene oxide for sensor applications. RSC Adv 4(86), 45895-45902.

Devadas, B., Madhu, R., Chen, S.-M., Yeh, H.-T., 2014b. Controlled electrochemical synthesis of new rare earth metal lutetium hexacyanoferrate on

reduced graphene oxide and its application as a salicylic acid sensor. Journal of Materials Chemistry B 2(43), 7515-7523.

Di Paola, A., Di Quarto, F., Sunseri, C., 1978. Electrochromism in Anodically Formed Tungsten Oxide Films. J. Electrochem. Soc. 125(8), 1344-1347.

Ding, Y., Hu, Y.-L., Gu, G., Xia, X.-H., 2009. Controllable Synthesis and Formation Mechanism Investigation of Prussian Blue Nanocrystals by Using the Polysaccharide Hydrolysis Method. The Journal of Physical Chemistry C 113(33), 14838-14843.

Domínguez-Vera, J.M., Colacio, E., 2003. Nanoparticles of Prussian Blue Ferritin: A New Route for Obtaining Nanomaterials. Inorg. Chem. 42(22), 6983-6985.

Dong, S., Che, G., 1991. Electrocatalytic oxidation of ascorbic acid at a prussian blue film modified microdisk electrode. J Electroanal Chem Interfacial Electrochem 315(1), 191-199.

Dong, S., Jin, Z., 1989. Electrochemistry of indium hexacyanoferrate film modified electrodes. Electrochim. Acta 34(7), 963-968.

Dostal, A., Meyer, B., Scholz, F., Schroeder, U., Bond, A.M., Marken, F., Shaw, S.J., 1995. Electrochemical study of microcrystalline solid Prussian blue particles mechanically attached to graphite and gold electrodes: electrochemically induced lattice reconstruction. The Journal of Physical Chemistry 99(7), 2096-2103.

Du, D., Wang, M., Qin, Y., Lin, Y., 2010. One-step electrochemical deposition of Prussian Blue-multiwalled carbon nanotube nanocomposite thin-film: preparation, characterization and evaluation for H2O2 sensing. J. Mater. Chem. 20(8), 1532-1537.

Dunford, H.B., Hasinoff, B.B., 1970. Kinetics of the oxidation of ferrocyanide by horseradish peroxidase compounds I and II. Biochemistry (Mosc). 9(25), 4930-4939.

Düssel, H., Dostal, A., Scholz, F., 1996. Hexacyanoferrate-based composite ion-sensitive electrodes for voltammetry. Fresenius J. Anal. Chem. 355(1), 21-28.

Dutta, A.K., Maji, S.K., Srivastava, D.N., Mondal, A., Biswas, P., Paul, P., Adhikary, B., 2012a. Peroxidase-like activity and amperometric sensing of hydrogen peroxide by Fe2O3 and Prussian Blue-modified Fe2O3 nanoparticles. J. Mol. Catal. A: Chem. 360, 71-77.

Dutta, A.K., Maji, S.K., Srivastava, D.N., Mondal, A., Biswas, P., Paul, P., Adhikary, B., 2012b. Peroxidase-like activity and amperometric sensing of hydrogen peroxide by Fe 2 O 3 and Prussian Blue-modified Fe 2 O 3 nanoparticles. Journal of Molecular Catalysis A: Chemical 360, 71-77.

Eftekhari, A., 2003. A high-voltage solid-state secondary cell based on chromium hexacyanometallates. J. Power Sources 117(1), 249-254.

Eftekhari, A., 2004a. Fabrication of all-solid-state thin-film secondary cells using hexacyanometallate-based electrode materials. J. Power Sources 132(1), 291-295.

Eftekhari, A., 2004b. Potassium secondary cell based on Prussian blue cathode. J. Power Sources 126(1), 221-228.

Ellis, D., Eckhoff, M., Neff, V., 1981. Electrochromism in the mixed-valence hexacyanides. 1. Voltammetric and spectral studies of the oxidation and reduction of thin films of Prussian blue. The Journal of Physical Chemistry 85(9), 1225-1231.

Entley, W.R., Girolami, G.S., 1995. High-temperature molecular magnets based on cyanovanadate building blocks: spontaneous magnetization at 230 k. Science 268(5209), 397-400.

Evgen'ev, M., Garmonov, S.Y., Evgen'eva, I., Ugrichich-Trebinskii, V., 1998. Selective flow-injection determination of hydrazine. J. Anal. Chem. 53(3), 240-245.

Fan, J., Yin, J.-J., Ning, B., Wu, X., Hu, Y., Ferrari, M., Anderson, G.J., Wei, J., Zhao, Y., Nie, G., 2011. Direct evidence for catalase and peroxidase activities of ferritin–platinum nanoparticles. Biomaterials 32(6), 1611-1618.

Fang, B., Shen, R., Zhang, W., Wang, G., Zhang, C., 2009. Electrocatalytic oxidation of hydrazine at a chromium hexacyanoferrate/single-walled carbon nanotube modified glassy carbon electrode. Microchimica Acta 165(1-2), 231-236.

Fang, B., Wei, Y., Li, M., Wang, G., Zhang, W., 2007. Study on electrochemical behavior of tryptophan at a glassy carbon electrode modified with multi-walled carbon nanotubes embedded cerium hexacyanoferrate. Talanta 72(4), 1302-1306.

Farah, A.M., Shooto, N.D., Thema, F.T., Modise, J.S., Dikio, E.D., 2012. Fabrication of Prussian blue/multi-walled carbon nanotubes modified glassy carbon electrode for electrochemical detection of hydrogen peroxide. International Journal of Electrochemical Science 7(5), 4302-4313.

Feng, L.-D., Gu, M.-M., Yang, Y.-L., Liang, G.-X., Zhang, J.-R., Zhu, J.-J., 2009. Electrochemical Synthesis for Flowerlike and Fusiform Christmas-Tree-like Cerium Hexacyanoferrate(II). The Journal of Physical Chemistry C 113(20), 8743-8749.

Ferlay, S., Mallah, T., Ouahes, R., Veillet, P., Verdaguer, M., 1995. A room-temperature organometallic magnet based on Prussian blue. Nature 378(6558), 701-703.

Ferlay, S., Mallah, T., Ouahes, R., Veillet, P., Verdaguer, M., 1999. A chromium-vanadyl ferrimagnetic molecule-based magnet: Structure, magnetism, and orbital interpretation. Inorg. Chem. 38(2), 229-234.

Fiorito, P.A., de Torresi, S.I.C., 2005. Hybrid nickel hexacyanoferrate/polypyrrole composite as mediator for hydrogen peroxide detection and its application in oxidase-based biosensors. J. Electroanal. Chem. 581(1), 31-37.

Fiorito, P.A., Gonçales, V.R., Ponzio, E.A., de Torresi, S.I.C., 2005. Synthesis, characterization and immobilization of Prussian blue nanoparticles. A potential tool for biosensing devices. Chem. Commun.(3), 366-368.

Folch, B., Larionova, J., Guari, Y., Molvinger, K., Luna, C., Sangregorio, C., Innocenti, C., Caneschi, A., Guerin, C., 2010. Synthesis and studies of water-soluble Prussian Blue-type nanoparticles into chitosan beads. PCCP 12(39), 12760-12770.

Fornasieri, G., Bleuzen, A., 2008. Controlled synthesis of photomagnetic nanoparticles of a Prussian blue analogue in a silica xerogel. Angew. Chem. Int. Ed. 47(40), 7750-7752.

Fu, G., Yue, X., Dai, Z., 2011. Glucose biosensor based on covalent immobilization of enzyme in sol–gel composite film combined with Prussian blue/carbon nanotubes hybrid. Biosens. Bioelectron. 26(9), 3973-3976.

Gao, L., Zhuang, J., Nie, L., Zhang, J., Zhang, Y., Gu, N., Wang, T., Feng, J., Yang, D., Perrett, S., Yan, X., 2007. Intrinsic peroxidase-like activity of ferromagnetic nanoparticles. Nat Nano 2(9), 577-583.

Gao, Z., Wang, G., Li, P., Zhao, Z., 1991. Electrochemical and spectroscopic studies of cobalt-hexacyanoferrate film modified electrodes. Electrochim. Acta 36(1), 147-152.

García-Jareño, J.J., Sanmatías, A., Navarro-Laboulais, J., Vicente, F., 1998. The role of potassium and hydrogen ions in the Prussian Blue ⇄ Everitt's Salt process. Electrochim. Acta 44(2–3), 395-405.

García, T., Casero, E., Lorenzo, E., Pariente, F., 2005. Electrochemical sensor for sulfite determination based on iron hexacyanoferrate film modified electrodes. Sensors and Actuators B: Chemical 106(2), 803-809.

Garde, R., Villain, F., Verdaguer, M., 2002. Molecule-based room-temperature magnets: Catalytic role of V (III) in the synthesis of vanadium-chromium Prussian blue analogues. J. Am. Chem. Soc. 124(35), 10531-10538.

Garjonyte, R., Malinauskas, A., 2000a. Amperometric glucose biosensors based on Prussian Blue–and polyaniline–glucose oxidase modified electrodes. Biosens. Bioelectron. 15(9), 445-451.

Garjonyte, R., Malinauskas, A., 2000b. Glucose biosensor based on glucose oxidase immobilized in electropolymerized polypyrrole and poly (o-phenylenediamine) films on a Prussian Blue-modified electrode. Sensors and Actuators B: Chemical 63(1), 122-128.

Garrod, S., Bollard, M.E., Nicholls, A.W., Connor, S.C., Connelly, J., Nicholson, J.K., Holmes, E., 2005. Integrated metabonomic analysis of the multiorgan effects of hydrazine toxicity in the rat. Chem. Res. Toxicol. 18(2), 115-122.

Ghaffarinejad, A., Sadeghi, N., Kazemi, H., Khajehzadeh, A., Amiri, M., Noori, A., 2012. Effect of metal hexacyanoferrate films on hydrogen evolution reaction. J. Electroanal. Chem. 685, 103-108.

Ghasemi, S., Hosseini, S.R., Asen, P., 2015. Preparation of graphene/nickel-iron hexacyanoferrate coordination polymer nanocomposite for electrochemical energy storage. Electrochim. Acta 160, 337-346.

Gholivand, M.B., Azadbakht, A., 2011. A novel hydrazine electrochemical sensor based on a zirconium hexacyanoferrate film-bimetallic Au–Pt inorganic–organic hybrid nanocomposite onto glassy carbon-modified electrode. Electrochim. Acta 56(27), 10044-10054.

Gholivand, M.B., Khodadadian, M., Omidi, M., 2013. Amperometric sensor based on a graphene/copper hexacyanoferrate nano-composite for highly sensitive electrocatalytic determination of captopril. Materials Science and Engineering: C 33(2), 774-781.

Ghosh, S.N., 1974. Infrared spectra of the Prussian blue analogs. J. Inorg. Nucl. Chem. 36(11), 2465-2466.

Giménez-Romero, D., Agrisuelas, J., García-Jareño, J.J., Gregori, J., Gabrielli, C., Perrot, H., Vicente, F., 2007. Electromechanical Phase Transition in Hexacyanometallate Nanostructure (Prussian Blue). J. Am. Chem. Soc. 129(22), 7121-7126.

Gong, H., Sun, M., Fan, R., Qian, L., 2012. One-step preparation of a composite consisting of graphene oxide, Prussian blue and chitosan for electrochemical sensing of hydrogen peroxide. Microchimica Acta 180(3), 295-301.

Gotoh, A., Uchida, H., Ishizaki, M., Satoh, T., Kaga, S., Okamoto, S., Ohta, M., Sakamoto, M., Kawamoto, T., Tanaka, H., 2007. Simple synthesis of three primary colour nanoparticle inks of Prussian blue and its analogues. Nanotechnology 18(34), 345609.

Grabner, E., Kalwellis-Mohn, S., 1987. Hexacyanoferrate layers as electrodes for secondary cells. J. Appl. Electrochem. 17(3), 653-656.

Guadagnini, L., Giorgetti, M., Tarterini, F., Tonelli, D., 2010. Electrocatalytic performances of pure and mixed hexacyanoferrates of Cu and Pd for the reduction of hydrogen peroxide. Electroanalysis 22(15), 1695-1701.

Gurban, A.-M., Noguer, T., Bala, C., Rotariu, L., 2008. Improvement of NADH detection using Prussian blue modified screen-printed electrodes and different strategies of immobilisation. Sensors and Actuators B: Chemical 128(2), 536-544.

Hansen, L.D., Litchman, W.M., Daub, G.H., 1969. Turnbull's blue and Prussian blue: KFe(III)[Fe(II)(CN)6]. J. Chem. Educ. 46(1), 46.

Hartmann, M., Grabner, E., Bergveld, P., 1991. Prussian Blue-coated interdigitated array electrodes for possible analytical application. Anal. Chim. Acta 242, 249-257.

Hatlevik, Ø., Buschmann, W.E., Zhang, J., Manson, J.L., Miller, J.S., 1999. Enhancement of the magnetic ordering temperature and air stability of a mixed valent vanadium hexacyanochromate (III) magnet to 99 C (372 K). Adv. Mater. 11(11), 914-918.

He, W., Liu, Y., Yuan, J., Yin, J.-J., Wu, X., Hu, X., Zhang, K., Liu, J., Chen, C., Ji, Y., 2011. Au@ Pt nanostructures as oxidase and peroxidase mimetics for use in immunoassays. Biomaterials 32(4), 1139-1147.

Heli, H., Majdi, S., Sattarahmady, N., 2010. Ultrasensitive sensing of N-acetyl-l-cysteine using an electrocatalytic transducer of nanoparticles of iron (III) oxide core–cobalt hexacyanoferrate shell. Sensors and Actuators B: Chemical 145(1), 185-193.

Herren, F., Fischer, P., Ludi, A., Haelg, W., 1980. Neutron diffraction study of Prussian Blue, Fe4[Fe(CN)6]3.xH2O. Location of water molecules and long-range magnetic order. Inorg. Chem. 19(4), 956-959.

Ho, K.-C., Lin, C.-L., 2001. A novel potassium ion sensing based on Prussian blue thin films. Sensors and Actuators B: Chemical 76(1), 512-518.

Ho, K.C., Rukavina, T.G., Greenberg, C.B., 1994. Tungsten Oxide-Prussian Blue Electrochromic System Based on a Proton-Conducting Polymer Electrolyte. J. Electrochem. Soc. 141(8), 2061-2067.

Holmes, S.M., Girolami, G.S., 1999. Sol−Gel Synthesis of KVII[CrIII(CN)6]·2H2O: A Crystalline Molecule-Based Magnet with a Magnetic Ordering Temperature above 100 °C. J. Am. Chem. Soc. 121(23), 5593-5594.

Honda, K., Ochiai, J., Hayashi, H., 1986. Polymerization of transition metal complexes in solid polymer electrolytes. J. Chem. Soc., Chem. Commun.(2), 168-170.

Hornok, V., Dékány, I., 2007. Synthesis and stabilization of Prussian blue nanoparticles and application for sensors. J. Colloid Interface Sci. 309(1), 176-182.

Hosseinzadeh, R., Sabzi, R.E., Ghasemlu, K., 2009. Effect of cetyltrimethyl ammonium bromide (CTAB) in determination of dopamine and ascorbic acid using carbon paste electrode modified with tin hexacyanoferrate. Colloids Surf. B. Biointerfaces 68(2), 213-217.

Hou, W., Wang, E., 1992. Flow-injection amperometric detection of hydrazine by electrocalytic oxidation at a Prussian Blue film-modified electrode. Anal. Chim. Acta 257(2), 275-280.

Hu, I.F., Kuwana, T., 1986. Oxidative mechanism of ascorbic acid at glassy carbon electrodes. Anal. Chem. 58(14), 3235-3239.

Hu, M., Furukawa, S., Ohtani, R., Sukegawa, H., Nemoto, Y., Reboul, J., Kitagawa, S., Yamauchi, Y., 2012a. Synthesis of Prussian Blue Nanoparticles with a Hollow Interior by Controlled Chemical Etching. Angew. Chem. 124(4), 1008-1012.

Hu, M., Torad, N.L., Yamauchi, Y., 2012b. Preparation of Various Prussian Blue Analogue Hollow Nanocubes with Single Crystalline Shells. Eur. J. Inorg. Chem. 2012(30), 4795-4799.

Hu, Y.-L., Yuan, J.-H., Chen, W., Wang, K., Xia, X.-H., 2005. Photochemical synthesis of Prussian blue film from an acidic ferricyanide solution and application. Electrochem. Commun. 7(12), 1252-1256.

Humphrey, B.D., Sinha, S., Bocarsly, A.B., 1987. Mechanisms of charge transfer at the chemically derivatized interface: the Ni/[NiII(CN)FeII/III(CN)5]2-/1- system as an electrocatalyst. The Journal of Physical Chemistry 91(3), 586-593.

Hurditch, R., 1975. Electrochromism in hydrated tungsten-oxide films. Electron. Lett, pp. 142-144. Institution of Engineering and Technology.

Imanishi, N., Morikawa, T., Kondo, J., Takeda, Y., Yamamoto, O., Kinugasa, N., Yamagishi, T., 1999. Lithium intercalation behavior into iron cyanide complex as positive electrode of lithium secondary battery. J. Power Sources 79(2), 215-219.

Ishizaki, M., Gotoh, A., Abe, M., Sakamoto, M., Tanaka, H., Kawamoto, T., Kurihara, M., 2010. Systematic Bathochromic Shift of Charge-transfer Bands of Mixed-metal Prussian-blue Nanoparticles Depending on Their Composition Ratios of Fe and Ni. Chem. Lett. 39(7), 762-763.

Ishizaki, M., Sajima, Y., Tsuruta, S., Gotoh, A., Sakamoto, M., Kawamoto, T., Tanaka, H., Kurihara, M., 2009. Preparation of Yellow Core–Blue Shell Coordination Polymer Nanoparticles Using Active Surface Coordination Sites on a Prussian-blue Analog. Chem. Lett. 38(11), 1058-1059.

Itaya, K., Akahoshi, H., Toshima, S., 1982a. Electrochemistry of Prussian Blue Modified Electrodes: An Electrochemical Preparation Method. J. Electrochem. Soc. 129(7), 1498-1500.

Itaya, K., Ataka, T., Toshima, S., 1982b. Electrochemical preparation of a Prussian blue analog: iron-ruthenium cyanide. J. Am. Chem. Soc. 104(13), 3751-3752.

Itaya, K., Ataka, T., Toshima, S., 1982c. Spectroelectrochemistry and electrochemical preparation method of Prussian blue modified electrodes. J. Am. Chem. Soc. 104(18), 4767-4772.

Itaya, K., Shibayama, K., Akahoshi, H., Toshima, S., 1982d. Prussian-blue-modified electrodes: An application for a stable electrochromic display device. J. Appl. Phys. 53(1), 804-805.

Itaya, K., Uchida, I., Neff, V.D., 1986. Electrochemistry of polynuclear transition metal cyanides: Prussian blue and its analogues. Acc. Chem. Res. 19(6), 162-168.

Ito, A., Suenaga, M., Ono, K., 1968a. Mössbauer study of soluble Prussian blue, insoluble Prussian blue, and Turnbull's blue. The Journal of Chemical Physics 48(8), 3597-3599.

Ito, A., Suenaga, M., Ôno, K., 1968b. Mössbauer Study of Soluble Prussian Blue, Insoluble Prussian Blue, and Turnbull's Blue. The Journal of Chemical Physics 48(8), 3597-3599.

Ivama, V.M., Serrano, S.H., 2003. Rhodium-Prussian Blue modified carbon paste electrode (Rh-PBMCPE) for amperometric detection of hydrogen peroxide. Journal of the Brazilian Chemical Society 14(4), 551-555.

Iveković, D., Milardović, S., Grabarić, B., 2004. Palladium hexacyanoferrate hydrogel as a novel and simple enzyme immobilization matrix for amperometric biosensors. Biosens. Bioelectron. 20(4), 872-878.

Jaffari, S., Pickup, J., 1996a. Novel hexacyanoferrate (III)-modified carbon electrodes: application in miniaturized biosensors with potential for in vivo glucose sensing. Biosens. Bioelectron. 11(11), 1167-1175.

Jaffari, S.A., Pickup, J.C., 1996b. Novel hexacyanoferrate (III)-modified carbon electrodes: application in miniaturized biosensors with potential for in vivo glucose sensing. Biosens. Bioelectron. 11(11), 1167-1175.

Jaffari, S.A., Turner, A.P., 1997. Novel hexacyanoferrate (III) modified graphite disc electrodes and their application in enzyme electrodes—Part I. Biosens. Bioelectron. 12(1), 1-9.

Jain, A.K., Singh, R.P., Bala, C., 1982. Solid Membranes of Copper Hriacyanoferrats (III) as Thallium (I) Sensitive Electrode. Anal. Lett. 15(19), 1557-1563.

Jayalakshmi, M., Scholz, F., 2000a. Charge–discharge characteristics of a solid-state Prussian blue secondary cell. J. Power Sources 87(1), 212-217.

Jayalakshmi, M., Scholz, F., 2000b. Performance characteristics of zinc hexacyanoferrate/Prussian blue and copper hexacyanoferrate/Prussian blue solid state secondary cells. J. Power Sources 91(2), 217-223.

Jayasri, D., Narayanan, S.S., 2007. Amperometric determination of hydrazine at manganese hexacyanoferrate modified graphite–wax composite electrode. J. Hazard. Mater. 144(1), 348-354.

Jayasri, D., Sriman Narayanan, S., 2007. Manganese(II) hexacyanoferrate based renewable amperometric sensor for the determination of butylated hydroxyanisole in food products. Food Chem. 101(2), 607-614.

Jeykumari, D.S., Ramaprabhu, S., Narayanan, S.S., 2007. A thionine functionalized multiwalled carbon nanotube modified electrode for the determination of hydrogen peroxide. Carbon 45(6), 1340-1353.

Jia, Z., 2011a. Synthesis of Prussian Blue nanocrystals with metal complexes as precursors: Quantitative calculations of species distribution and its effects on particles size. Colloids Surf. Physicochem. Eng. Aspects 389(1), 144-148.

Jia, Z., 2011b. Synthesis of Prussian Blue nanocrystals with metal complexes as precursors: Quantitative calculations of species distribution and its effects on particles size. Colloids Surf. Physicochem. Eng. Aspects 389(1–3), 144-148.

Jia, Z., Sun, G., 2007. Preparation of prussian blue nanoparticles with single precursor. Colloids Surf. Physicochem. Eng. Aspects 302(1–3), 326-329.

Jiang, H., Chen, Z., Cao, H., Huang, Y., 2012. Peroxidase-like activity of chitosan stabilized silver nanoparticles for visual and colorimetric detection of glucose. Analyst 137(23), 5560-5564.

Jiang, Y., Zhang, X., Shan, C., Hua, S., Zhang, Q., Bai, X., Dan, L., Niu, L., 2011. Functionalization of graphene with electrodeposited Prussian blue towards amperometric sensing application. Talanta 85(1), 76-81.

Jin, E., Bian, X., Lu, X., Wang, C., 2012. Fabrication of multiwalled carbon nanotubes/polypyrrole/Prussian blue ternary composite nanofibers and their application for enzymeless hydrogen peroxide detection. Journal of Materials Science 47(10), 4326-4331.

Jing, L., Liang, X., Deng, Z., Feng, S., Li, X., Huang, M., Li, C., Dai, Z., 2014. Prussian blue coated gold nanoparticles for simultaneous photoacoustic/CT bimodal imaging and photothermal ablation of cancer. Biomaterials 35(22), 5814-5821.

Johansson, A., Widenkvist, E., Lu, J., Boman, M., Jansson, U., 2005. Fabrication of High-Aspect-Ratio Prussian Blue Nanotubes Using a Porous Alumina Template. Nano Lett. 5(8), 1603-1606.

Josephy, P.D., Eling, T., Mason, R.P., 1982. The horseradish peroxidase-catalyzed oxidation of 3, 5, 3', 5'-tetramethylbenzidine. Free radical and charge-transfer complex intermediates. J. Biol. Chem. 257(7), 3669-3675.

Juszczyk, S., Johansson, C., Hanson, M., Ratuszna, A., Malecki, G., 1994. Ferromagnetism of the Me 3 (Fe(CN) 6) 2 .H 2 O compounds, where Me=Ni and Co. J. Phys.: Condens. Matter 6(29), 5697.

Kaneko, M., 1986. Polynuclear-metal-complex battery. Journal of Polymer Science Part C: Polymer Letters 24(9), 435-437.

Kaneko, M., Hara, S., Yamada, A., 1985. A photoresponsive graphite electrode coated with Prussian blue. J Electroanal Chem Interfacial Electrochem 194(1), 165-168.

Kaneko, M., Hou, X.-H., Yamada, A., 1986. Specific quenching of the photoexcited state of tris (2, 2′-bipyridine) ruthenium (II) by colloidal prussian blue. Journal of the Chemical Society, Faraday Transactions 1: Physical Chemistry in Condensed Phases 82(5), 1637-1642.

Kaneko, M., Okada, T., 1988. A secondary battery composed of multilayer Prussian Blue and its reaction characteristics. J Electroanal Chem Interfacial Electrochem 255(1), 45-52.

Karyakin, A.A., 2001. Prussian Blue and Its Analogues: Electrochemistry and Analytical Applications. Electroanalysis 13(10), 813-819.

Karyakin, A.A., Gitelmacher, O.V., Karyakina, E.E., 1994. A high-sensitive glucose amperometric biosensor based on Prussian Blue modified electrodes. Anal. Lett. 27(15), 2861-2869.

Karyakin, A.A., Gitelmacher, O.V., Karyakina, E.E., 1995. Prussian Blue-Based First-Generation Biosensor. A Sensitive Amperometric Electrode for Glucose. Anal. Chem. 67(14), 2419-2423.

Karyakin, A.A., Karyakina, E.E., 1999a. Prussian Blue-based `artificial peroxidase' as a transducer for hydrogen peroxide detection. Application to biosensors. Sensors and Actuators B: Chemical 57(1), 268-273.

Karyakin, A.A., Karyakina, E.E., 1999b. Prussian Blue-basedartificial peroxidase'as a transducer for hydrogen peroxide detection. Application to biosensors. Sensors and Actuators B: Chemical 57(1), 268-273.

Karyakin, A.A., Karyakina, E.E., Gorton, L., 1996. Prussian-Blue-based amperometric biosensors in flow-injection analysis. Talanta 43(9), 1597-1606.

Karyakin, A.A., Karyakina, E.E., Gorton, L., 1999. On the mechanism of H2O2 reduction at Prussian Blue modified electrodes. Electrochem. Commun. 1(2), 78-82.

Karyakin, A.A., Karyakina, E.E., Gorton, L., 2000. Amperometric biosensor for glutamate using Prussian blue-based “artificial peroxidase” as a transducer for hydrogen peroxide. Anal. Chem. 72(7), 1720-1723.

Karyakin, A.A., Puganova, E.A., Budashov, I.A., Kurochkin, I.N., Karyakina, E.E., Levchenko, V.A., Matveyenko, V.N., Varfolomeyev, S.D., 2004. Prussian Blue based nanoelectrode arrays for H2O2 detection. Anal. Chem. 76(2), 474-478.

Kaye, S.S., Long, J.R., 2005. Hydrogen Storage in the Dehydrated Prussian Blue Analogues M3[Co(CN)6]2 (M = Mn, Fe, Co, Ni, Cu, Zn). J. Am. Chem. Soc. 127(18), 6506-6507.

Keggin, J., Miles, F., 1936. Structures and formulae of the Prussian blues and related compounds. Nature 137(7), 577-578.

Keiichi, K., Katsumi, Y., Yoshio, I., 1983. Characteristics of Electro-Optic Device Using Conducting Polymers, Polythiophene and Polypyrrole Films. Japanese Journal of Applied Physics 22(7A), L412.

Koncki, R., 2002. Chemical Sensors and Biosensors Based on Prussian Blues. Crit. Rev. Anal. Chem. 32(1), 79-96.

Koncki, R., Lenarczuk, T., Radomska, A., Glab, S., 2001a. Optical biosensors based on Prussian Blue films. Analyst 126(7), 1080-1085.

Koncki, R., Lenarczuk, T., Radomska, A., Głąb, S., 2001b. Optical biosensors based on Prussian Blue films. Analyst 126(7), 1080-1085.

Koncki, R., Wolfbeis, O.S., 1998a. Composite films of Prussian Blue and N-substituted polypyrroles: fabrication and application to optical determination of pH. Anal. Chem. 70(13), 2544-2550.

Koncki, R., Wolfbeis, O.S., 1998b. Optical chemical sensing based on thin films of Prussian blue. Sensors and Actuators B: Chemical 51(1), 355-358.

Korsvik, C., Patil, S., Seal, S., Self, W.T., 2007. Superoxide dismutase mimetic properties exhibited by vacancy engineered ceria nanoparticles. Chem. Commun.(10), 1056-1058.

Krishnan, V., Xidis, A.L., Neff, V., 1990. Prussian blue solid-state films and membranes as potassium ion-selective electrodes. Anal. Chim. Acta 239, 7-12.

Kukulka-Walkiewicz, J., Stroka, J., Malik, M.A., Kulesza, P.J., Galus, Z., 2001. Films of mixed nickel (II) and thallium (I) hexacyanoferrates (III, II): voltammetric preparation and characterization. Electrochim. Acta 46(26), 4057-4063.

Kulesza, P.J., Malik, M.A., Schmidt, R., Smolinska, A., Miecznikowski, K., Zamponi, S., Czerwinski, A., Berrettoni, M., Marassi, R., 2000. Electrochemical preparation and characterization of electrodes modified with mixed hexacyanoferrates of nickel and palladium. J. Electroanal. Chem. 487(1), 57-65.

Kulesza, P.J., Malik, M.A., Skorek, J., Miecznikowski, K., Zamponi, S., Berrettoni, M., Giorgetti, M., Marassi, R., 1999. Hybrid metal cyanometallates

electrochemical charging and spectrochemical identity of heteronuclear nickel/cobalt hexacyanoferrate. J. Electrochem. Soc. 146(10), 3757-3761.

Kulesza, P.J., Malik, M.A., Zamponi, S., Berrettoni, M., Marassi, R., 1995a. Electrolyte-cation-dependent coloring, electrochromism and thermochromism of cobalt (II) hexacyanoferrate (III, II) films. J. Electroanal. Chem. 397(1), 287-292.

Kulesza, P.J., Malik, M.A., Zamponi, S., Berrettoni, M., Marassi, R., 1995b. Electrolyte-cation-dependent coloring, electrochromism and thermochromism of cobalt(II) hexacyanoferrate(III, II) films. J. Electroanal. Chem. 397(1–2), 287-292.

Kulesza, P.J., Miecznikowski, K., Chojak, M., Malik, M.A., Zamponi, S., Marassi, R., 2001. Electrochromic features of hybrid films composed of polyaniline and metal hexacyanoferrate. Electrochim. Acta 46(28), 4371-4378.

Kumar, A.V.N., Harish, S., Joseph, J., Phani, K.L., 2011. Nix–Fe (1− x) Fe (CN) 6 hybrid thin films electrodeposited on glassy carbon: Effect of tuning of redox potentials on the electrocatalysis of hydrogen peroxide. J. Electroanal. Chem. 659(2), 128-133.

Kumar, S.S., Joseph, J., Phani, K.L., 2007. Novel Method for Deposition of Gold−Prussian Blue Nanocomposite Films Induced by Electrochemically Formed Gold Nanoparticles: Characterization and Application to Electrocatalysis. Chem. Mater. 19(19), 4722-4730.

Kumar, S.S., Pillai, K.C., 2009. A kinetic study of the electrocatalytic oxidation of reduced glutathione at Prussian blue film-modified electrode using rotating-disc electrode voltammetry. Electrochim. Acta 54(28), 7374-7381.

Lawaczeck, R., Menzel, M., Pietsch, H., 2004. Superparamagnetic iron oxide particles: contrast media for magnetic resonance imaging. Appl. Organomet. Chem. 18(10), 506-513.

Lee, B., 2003. Review of the present status of optical fiber sensors. Optical Fiber Technology 9(2), 57-79.

Lee, H.-W., Wang, R.Y., Pasta, M., Lee, S.W., Liu, N., Cui, Y., 2014. Manganese hexacyanomanganate open framework as a high-capacity positive electrode material for sodium-ion batteries. Nature communications 5.

Lee, H., Kim, Y.-I., Park, J.-K., Choi, J.W., 2012. Sodium zinc hexacyanoferrate with a well-defined open framework as a positive electrode for sodium ion batteries. Chem. Commun. 48(67), 8416-8418.

Lenarczuk, T., Głąb, S., Koncki, R., 2001a. Application of Prussian blue-based optical sensor in pharmaceutical analysis. J. Pharm. Biomed. Anal. 26(1), 163-169.

Lenarczuk, T., Wencel, D., Głąb, S., Koncki, R., 2001b. Prussian blue-based optical glucose biosensor in flow-injection analysis. Anal. Chim. Acta 447(1), 23-32.

Leventis, N., Chung, Y.C., 1992a. New complementary electrochromic system based on poly(pyrrole)-Prussian blue composite, a benzylviologen polymer, and poly(vinylpyrrolidone)/potassium sulfate aqueous electrolyte. Chem. Mater. 4(6), 1415-1422.

Leventis, N., Chung, Y.C., 1992b. Poly(3-methylthiophene)-Prussian Blue: a new composite electrochromic material. J. Mater. Chem. 2(3), 289-293.

Lezna, R.O., Romagnoli, R., de Tacconi, N.R., Rajeshwar, K., 2003. Spectroelectrochemistry of palladium hexacyanoferrate films on platinum substrates. J. Electroanal. Chem. 544, 101-106.

Li, F., Dong, S., 1987. The electrocatalytic oxidation of ascorbic acid on prussian blue film modified electrodes. Electrochim. Acta 32(10), 1511-1513.

Li, J., Peng, T., Peng, Y., 2003. A Cholesterol Biosensor Based on Entrapment of Cholesterol Oxidase in a Silicic Sol-Gel Matrix at a Prussian Blue Modified Electrode. Electroanalysis 15(12), 1031-1037.

Li, J., Qiu, J.D., Xu, J.J., Chen, H.Y., Xia, X.H., 2007. The Synergistic Effect of Prussian-Blue-Grafted Carbon Nanotube/Poly (4-vinylpyridine) Composites for Amperometric Sensing. Adv. Funct. Mater. 17(9), 1574-1580.

Li, J., Yu, Q., Peng, T., 2005. Electrocatalytic oxidation of hydrogen peroxide and cysteine at a glassy carbon electrode modified with platinum nanoparticle-deposited carbon nanotubes. Anal. Sci. 21(4), 377-381.

Li, M., Zhao, G., Yue, Z., Huang, S., 2009. Sensor for traces of hydrogen peroxide using an electrode modified by multiwalled carbon nanotubes, a gold-chitosan colloid, and Prussian blue. Microchimica Acta 167(3-4), 167-172.

Li, T., Si, Z., Hu, L., Qi, H., Yang, M., 2012. Prussian Blue-functionalized ceria nanoparticles as label for ultrasensitive detection of tumor necrosis factor-α. Sensors and Actuators B: Chemical 171, 1060-1065.

Li, Z., Zhang, J., Mu, T., Du, J., Liu, Z., Han, B., Chen, J., 2004. Preparation of polyvinylpyrrolidone-protected Prussian blue nanocomposites in microemulsion. Colloids Surf. Physicochem. Eng. Aspects 243(1–3), 63-66.

Lien, C.-W., Huang, C.-C., Chang, H.-T., 2012. Peroxidase-mimic bismuth–gold nanoparticles for determining the activity of thrombin and drug screening. Chem. Commun. 48(64), 7952-7954.

Lin, C.-F., Hsu, C.-Y., Lo, H.-C., Lin, C.-L., Chen, L.-C., Ho, K.-C., 2011a. A complementary electrochromic system based on a Prussian blue thin film and a heptyl viologen solution. Sol. Energy Mater. Sol. Cells 95(11), 3074-3080.

Lin, J., Zhou, D.M., Hocevar, S.B., McAdams, E.T., Ogorevc, B., Zhang, X., 2005. Nickel hexacyanoferrate modified screen-printed carbon electrode for sensitive detection of ascorbic acid and hydrogen peroxide. Front. Biosci. 10, 483-491.

Lin, M., Tseng, T., 1998. Chromium (III) hexacyanoferrate (II)-based chemical sensor for the cathodic determination of hydrogen peroxide. Analyst 123(1), 159-163.

Lin, M., Yang, J., Cho, M., Lee, Y., 2011b. Hydrogen peroxide detection using a polypyrrole/Prussian blue nanowire modified electrode. Macromolecular Research 19(7), 673-678.

Lin, M.S., Jan, B.I., 1997. Determination of hydrogen peroxide by utilizing a cobalt (II) hexacyanoferrate-modified glassy carbon electrode as a chemical sensor. Electroanalysis 9(4), 340-344.

Lin, M.S., Shih, W.C., 1999. Chromium hexacyanoferrate based glucose biosensor. Anal. Chim. Acta 381(2–3), 183-189.

Liu, S.-Q., Chen, H.-Y., 2002. Spectroscopic and voltammetric studies on a lanthanum hexacyanoferrate modified electrode. J. Electroanal. Chem. 528(1–2), 190-195.

Liu, S.-Q., Li, H., Sun, W.-H., Wang, X.-M., Chen, Z.-G., Xu, J.-J., Ju, H.-X., Chen, H.-Y., 2011. Photoinducedly electrochemical preparation of Prussian blue film and electrochemical modification of the film with cetyltrimethylammonium cation. Electrochim. Acta 56(11), 4007-4014.

Liu, X.-W., Yao, Z.-J., Wang, Y.-F., Wei, X.-W., 2010a. Graphene oxide sheet–prussian blue nanocomposites: Green synthesis and their extraordinary electrochemical properties. Colloids Surf. B. Biointerfaces 81(2), 508-512.

Liu, Y., Chu, Z., Jin, W., 2009. A sensitivity-controlled hydrogen peroxide sensor based on self-assembled Prussian Blue modified electrode. Electrochem. Commun. 11(2), 484-487.

Liu, Y., Xu, L., 2007. Electrochemical sensor for tryptophan determination based on copper-cobalt hexacyanoferrate film modified graphite electrode. Sensors 7(10), 2446-2457.

Liu, Y., Yang, Z., Zhong, Y., Yu, J., 2010b. Construction of europium hexacyanoferrate film and its electrocatalytic activity to tyrosine determination. Appl. Surf. Sci. 256(10), 3148-3154.

Lu, D., Cagan, A., Munoz, R.A., Tangkuaram, T., Wang, J., 2006. Highly sensitive electrochemical detection of trace liquid peroxide explosives at a Prussian-blue 'artificial-peroxidase'modified electrode. Analyst 131(12), 1279-1281.

Ludi, A., 1981. Prussian blue, an inorganic evergreen. J. Chem. Educ. 58(12), 1013.

Ludi, A., Güdel, H., 1973. Structural chemistry of polynuclear transition metal cyanides. Inorg. Chem., pp. 1-21. Springer Berlin Heidelberg.

Lupu, S., Lete, C., Marin, M., Totir, N., Balaure, P.C., 2009. Electrochemical sensors based on platinum electrodes modified with hybrid inorganic–organic coatings for determination of 4-nitrophenol and dopamine. Electrochim. Acta 54(7), 1932-1938.

Ma, M., Zhang, Y., Gu, N., 2011. Peroxidase-like catalytic activity of cubic Pt nanocrystals. Colloids Surf. Physicochem. Eng. Aspects 373(1), 6-10.

Maer, K., Beasley, M.L., Collins, R.L., Milligan, W.O., 1968. Structure of the titanium-iron cyanide complexes. J. Am. Chem. Soc. 90(12), 3201-3208.

Majidi, M.R., Asadpour-Zeynali, K., Hafezi, B., 2010. Sensing L-cysteine in urine using a pencil graphite electrode modified with a copper hexacyanoferrate nanostructure. Microchimica Acta 169(3-4), 283-288.

Mao, Y., Bao, Y., Wang, W., Li, Z., Li, F., Niu, L., 2011. Layer-by-layer assembled multilayer of graphene/Prussian blue toward simultaneous electrochemical and SPR detection of H 2 O 2. Talanta 85(4), 2106-2112.

Martínez-García, R., Knobel, M., Balmaseda, J., Yee-Madeira, H., Reguera, E., 2007. Mixed valence states in cobalt iron cyanide. J. Phys. Chem. Solids 68(2), 290-298.

Marvaud, V., Decroix, C., Scuiller, A., Guyard-Duhayon, C., Vaissermann, J., Gonnet, F., Verdaguer, M., 2003. Hexacyanometalate molecular chemistry: heptanuclear heterobimetallic complexes; control of the ground spin state. Chemistry–A European Journal 9(8), 1677-1691.

McCormac, T., Cassidy, J., Cameron, D., 1996. Electrochemical deposition of Prussian blue films across interdigital array electrodes and their use in gas sensing. Electroanalysis 8(2), 195-198.

McHale, R., Ghasdian, N., Liu, Y., Wang, H., Miao, Y., Wang, X., 2010. Synthesis of Prussian Blue Coordination Polymer Nanocubes via Confinement of the Polymerization Field Using Miniemulsion Periphery Polymerization (MEPP). Macromol. Rapid Commun. 31(9-10), 856-860.

Meeussen, J.C.L., Keizer, M.G., Van Riemsdijk, W.H., De Haan, F.A.M., 1992. Dissolution behavior of iron cyanide (Prussian blue) in contaminated soils. Environ. Sci. Technol. 26(9), 1832-1838.

Miao, Y., Liu, J., 2016. Assembly and electroanalytical performance of Prussian blue/polypyrrole composite nanoparticles synthesized by the reverse micelle method. Science and Technology of Advanced Materials.

Ming, H., Torad, N.L.K., Chiang, Y.-D., Wu, K.C.W., Yamauchi, Y., 2012. Size- and shape-controlled synthesis of Prussian Blue nanoparticles by a polyvinylpyrrolidone-assisted crystallization process. CrystEngComm 14(10), 3387-3396.

Mohammed, F.S., Cole, S.R., Kitchens, C.L., 2013. Synthesis and enhanced colloidal stability of cationic gold nanoparticles using polyethyleneimine and carbon dioxide. ACS Sustainable Chemistry & Engineering 1(7), 826-832.

Moscone, D., D'ottavi, D., Compagnone, D., Palleschi, G., Amine, A., 2001. Construction and analytical characterization of Prussian blue-based carbon paste electrodes and their assembly as oxidase enzyme sensors. Anal. Chem. 73(11), 2529-2535.

Muñoz, E.C., Córdova, R.A., Henríquez, R.G., Schrebler, R.S., Cisternas, R., Marotti, R.E., 2011a. Electrochemical synthesis and nucleation and growth mechanism of Prussian blue films on p-Si(100) electrodes. J. Solid State Electrochem. 16(1), 93-100.

Muñoz, E.C., Henríquez, R.G., Córdova, R.A., Schrebler, R.S., Cisternas, R., Ballesteros, L., Marotti, R.E., Dalchiele, E.A., 2011b. Photoelectrochemical and optical characterization of Prussian blue onto p-Si(100). J. Solid State Electrochem. 16(1), 165-171.

Muthirulan, P., Velmurugan, R., 2011. Direct electrochemistry and electrocatalysis of reduced glutathione on CNFs–PDDA/PB nanocomposite film modified ITO electrode for biosensors. Colloids Surf. B. Biointerfaces 83(2), 347-354.

Nangia, Y., Kumar, B., Kaushal, J., Suri, C.R., 2012. Palladium@ gold bimetallic nanostructures as peroxidase mimic for development of sensitive fluoroimmunoassay. Anal. Chim. Acta 751, 140-145.

Narayanan, S.S., Scholz, F., 1999. A comparative study of the electrocatalytic activities of some metal hexacyanoferrates for the oxidation of hydrazine. Electroanalysis 11(7), 465-469.

Navarro-Laboulais, J., Vilaplana, J., López, J., García-Jareño, J.J., Benito, D., Vicente, F., 2000. Prussian blue films deposited on graphite+epoxy composite electrodes: electrochemical detection of the second percolation threshold. J. Electroanal. Chem. 484(1), 33-40.

Neff, V.D., 1978. Electrochemical Oxidation and Reduction of Thin Films of Prussian Blue. J. Electrochem. Soc. 125(6), 886-887.

Neff, V.D., 1985. Some performance characteristics of a Prussian blue battery. J. Electrochem. Soc.;(United States) 132.

Nguyen, B.T.T., Ang, J.Q., Toh, C.-S., 2009. Sensitive detection of potassium ion using Prussian blue nanotube sensor. Electrochem. Commun. 11(10), 1861-1864.

Nie, P., Shen, L., Luo, H., Ding, B., Xu, G., Wang, J., Zhang, X., 2014. Prussian blue analogues: a new class of anode materials for lithium ion batteries. Journal of Materials Chemistry A 2(16), 5852-5857.

Nossol, E., Zarbin, A.J.G., 2013. Electrochromic properties of carbon nanotubes/Prussian blue nanocomposite films. Sol. Energy Mater. Sol. Cells 109, 40-46.

Ohzuku, T., Sawai, K., Hirai, T., 1985. On a Homogeneous Electrochemical Reaction of Prussian Blue/Everitt's Salt System: A Model of System. J. Electrochem. Soc. 132(12), 2828-2834.

Paixão, T.R., Bertotti, M., 2008a. Ruthenium oxide hexacyanoferrate modified electrode for hydrogen peroxide detection. Electroanalysis 20(15), 1671-1677.

Paixão, T.R.L.C., Bertotti, M., 2008b. Ruthenium Oxide Hexacyanoferrate Modified Electrode for Hydrogen Peroxide Detection. Electroanalysis 20(15), 1671-1677.

Pan, D., Chen, J., Nie, L., Tao, W., Yao, S., 2004. Amperometric glucose biosensor based on immobilization of glucose oxidase in electropolymerized o-aminophenol film at Prussian blue-modified platinum electrode. Electrochim. Acta 49(5), 795-801.

Pan, Q., Huang, K., Ni, S., Yang, F., He, D., 2009. Synthesis of two-dimensional micron-size single-crystalline Prussian blue nanosheets by hydrothermal methods assisted by glucose. Mater. Res. Bull. 44(2), 388-392.

Pandey, P.C., Chauhan, D.S., 2012. 3-Glycidoxypropyltrimethoxysilane mediated in situ synthesis of noble metal nanoparticles: Application to hydrogen peroxide sensing. Analyst 137(2), 376-385.

Pandey, P.C., Panday, D., 2016a. Novel synthesis of nickel-iron hexacyanoferrate nanoparticles and its application in electrochemical sensing. J. Electroanal. Chem. 763, 63-70.

Pandey, P.C., Panday, D., 2016b. Tetrahydrofuran and hydrogen peroxide mediated conversion of potassium hexacyanoferrate into Prussian blue nanoparticles: Application to hydrogen peroxide sensing. Electrochim. Acta 190, 758-765.

Pandey, P.C., Pandey, A.K., 2012a. Electrochemical Behavior of Hydrogen Peroxide at Nanocomposite of Prussian Blue with Palladium of Variable Nanogeometery Modified Electrode. J. Electrochem. Soc. 159(11), G128-G136.

Pandey, P.C., Pandey, A.K., 2012b. Size-dependence enhancement in electrocatalytic activity of NiHCF-gold nanocomposite: potential application in electrochemical sensing. Analyst 137(14), 3306-3313.

Pandey, P.C., Pandey, A.K., 2013a. Cyclohexanone and 3-aminopropyltrimethoxysilane mediated controlled synthesis of mixed nickel-iron hexacyanoferrate nanosol for selective sensing of glutathione and hydrogen peroxide. Analyst 138(3), 952-959.

Pandey, P.C., Pandey, A.K., 2013b. Electrochemical sensing of dopamine and pyrogallol on mixed analogue of Prussian blue nanoparticles modified electrodes Role of transition metal on the electrocatalysis and peroxidase mimetic activity. Electrochim. Acta 109, 536-545.

Pandey, P.C., Pandey, A.K., 2013c. Novel synthesis of Prussian blue nanoparticles and nanocomposite sol: Electro-analytical application in hydrogen peroxide sensing. Electrochim. Acta 87, 1-8.

Pandey, P.C., Pandey, A.K., 2013d. Novel synthesis of super peroxidase mimetic polycrystalline mixed metal hexacyanoferrates nanoparticles dispersion. Analyst 138(8), 2295-2301.

Pandey, P.C., Pandey, A.K., 2014a. Tetrahydrofuran hydroperoxide mediated synthesis of Prussian blue nanoparticles: a study of their electrocatalytic activity and intrinsic peroxidase-like behavior. Electrochim. Acta 125, 465-472.

Pandey, P.C., Pandey, A.K., Chauhan, D.S., 2012. Nanocomposite of Prussian blue based sensor for L-cysteine: Synergetic effect of nanostructured gold and palladium on electrocatalysis. Electrochim. Acta 74, 23-31.

Pandey, P.C., Pandey, G., 2014b. Tunable functionality and nanogeometry in tetrahydrofuran hydroperoxide and 3-aminopropyl-trimethoxysilane mediated synthesis of gold nanoparticles; functional application in glutathione sensing. Journal of Materials Chemistry B 2(21), 3383-3390.

Pandey, P.C., Pandey, G., Narayan, R.J., 2016. Controlled synthesis of polyethylenimine coated gold nanoparticles: Application in glutathione sensing and nucleotide delivery. Journal of Biomedical Materials Research Part B: Applied Biomaterials.

Pandey, P.C., Prakash, A., Pandey, A.K., 2014a. Studies on electrochemical and peroxidase mimetic behavior of Prussian blue nanoparticles in presence of Pd-WO3-SiO2 Nanocomposite, bioelectro-catalytic sensing of H2O2. Electrochim. Acta 127, 132-138.

Pandey, P.C., Singh, R., Pandey, A.K., 2014b. Tetrahydrofuran hydroperoxide and 3-Aminopropyltrimethoxysilane mediated controlled synthesis of Pd, Pd-Au, Au-Pd nanoparticles: Role of Palladium nanoparticles on the redox electrochemistry of ferrocene monocarboxylic acid. Electrochim. Acta 138, 163-173.

Pandey, P.C., Upadhyay, B.C., 2005. Studies on differential sensing of dopamine at the surface of chemically sensitized ormosil-modified electrodes. Talanta 67(5), 997-1006.

Pandey, P.C., Upadhyay, B.C., Upadhyay, A.K., 2004. Differential selectivity in electrochemical oxidation of ascorbic acid and hydrogen peroxide at the surface of functionalized ormosil-modified electrodes. Anal. Chim. Acta 523(2), 219-223.

Pandey, P.C., Upadhyay, S., Sharma, S., 2003. Functionalized ormosils-based biosensor - Probing a horseradish peroxidase-catalyzed reaction. J. Electrochem. Soc. 150(4), H85-H92.

Pandey, P.C., Upadhyay, S., Tiwari, I., Tripathi, V.S., 2001. An ormosil-based peroxide biosensor - a comparative study on direct electron transport from horseradish peroxidase. Sens, Actuators B-Chem. 72(3), 224-232.

Pandey, P.C., Upadhyay, S., Upadhyay, B., 1997. Peroxide biosensors and mediated electrochemical regeneration of redox enzymes. Anal. Biochem. 252(1), 136-142.

Patra, S., Roy, E., Karfa, P., Kumar, S., Madhuri, R., Sharma, P.K., 2015. Dual-responsive polymer coated superparamagnetic nanoparticle for targeted drug delivery and hyperthermia treatment. ACS applied materials & interfaces 7(17), 9235-9246.

Piermarini, S., Migliorelli, D., Volpe, G., Massoud, R., Pierantozzi, A., Cortese, C., Palleschi, G., 2013. Uricase biosensor based on a screen-printed electrode modified with Prussian blue for detection of uric acid in human blood serum. Sensors and Actuators B: Chemical 179, 170-174.

Pournaghi-Azar, M., Ahour, F., 2008. Palladized aluminum electrode covered by Prussian blue film as an effective transducer for electrocatalytic oxidation and hydrodynamic amperometry of N-acetyl-cysteine and glutathione. J. Electroanal. Chem. 622(1), 22-28.

Pournaghi-Azar, M., Dastangoo, H., 2002. Electrochemical characteristics of an aluminum electrode modified by a palladium hexacyanoferrate film, synthesized by a simple electroless procedure. J. Electroanal. Chem. 523(1), 26-33.

Prabakar, S.R., Narayanan, S.S., 2008. Amperometric determination of hydrazine using a surface modified nickel hexacyanoferrate graphite electrode fabricated following a new approach. J. Electroanal. Chem. 617(2), 111-120.

Prabhu, P., Babu, R.S., Narayanan, S.S., 2011. Electrocatalytic oxidation of L-tryptophan using copper hexacyanoferrate film modified gold nanoparticle graphite-wax electrode. Colloids Surf. B. Biointerfaces 87(1), 103-108.

Pyrasch, M., Toutianoush, A., Jin, W., Schnepf, J., Tieke, B., 2003a. Self-Assembled Film of Prussian Blue and Analogues: Optical and Electrochemical Properties and Application as Ion-Sieving Membranes. ChemInform 34(12), no-no.

Pyrasch, M., Toutianoush, A., Jin, W., Schnepf, J., Tieke, B., 2003b. Self-assembled Films of Prussian Blue and Analogues: Optical and Electrochemical Properties and Application as Ion-Sieving Membranes. Chem. Mater. 15(1), 245-254.

Qian, L., Zheng, R., Zheng, L., 2013. Fabrication of Prussian blue nanocubes through reducing a single-source precursor with graphene oxide and their electrocatalytic activity for H2O2. J. Nanopart. Res. 15(7), 1-9.

Qin, K., Xingguo, C., Jinli, Y., Desheng, X., 2005. Preparation of poly(N-vinyl-2-pyrrolidone)-stabilized transition metal (Fe, Co, Ni and Cu) hexacyanoferrate nanoparticles. Nanotechnology 16(1), 164.

Qiu, J.-D., Peng, H.-Z., Liang, R.-P., Li, J., Xia, X.-H., 2007. Synthesis, Characterization, and Immobilization of Prussian Blue-Modified Au Nanoparticles: Application to Electrocatalytic Reduction of H2O2. Langmuir 23(4), 2133-2137.

Qu, L., Yang, S., Li, G., Yang, R., Li, J., Yu, L., 2011. Preparation of yttrium hexacyanoferrate/carbon nanotube/Nafion nanocomposite film-modified electrode: Application to the electrocatalytic oxidation of l-cysteine. Electrochim. Acta 56(7), 2934-2940.

Ravaine, S., Lafuente, C., Mingotaud, C., 1998. Electrochemistry of Langmuir-Blodgett films based on Prussian blue. Langmuir 14(22), 6347-6349.

Ravi Shankaran, D., Sriman Narayanan, S., 2002. Amperometric Sensor for Glutathione Based on a Mechanically Immobilized Cobalt Hexacyanoferrate Modified Electrode. Bull. Chem. Soc. Jpn. 75(3), 501-505.

Reddy, S.J., Dostal, A., Scholz, F., 1996. Solid state electrochemical studies of mixed nickel-iron hexacyanoferrates with the help of abrasive stripping voltammetry. J. Electroanal. Chem. 403(1–2), 209-212.

Reynolds, E.J., 1887. LXIII.-The composition of Prussian blue and Turnbull's blue. Journal of the Chemical Society, Transactions 51(0), 644-646.

Ricci, F., Palleschi, G., 2005. Sensor and biosensor preparation, optimisation and applications of Prussian Blue modified electrodes. Biosens Bioelectron 21(3), 389-407.

Robin, M.B., Day, P., 1968. Mixed Valence Chemistry-A Survey and Classification. In: Emeléus, H.J., Sharpe, A.G. (Eds.), Advances in Inorganic Chemistry and Radiochemistry, pp. 247-422. Academic Press.

Rogez, G., Parsons, S., Paulsen, C., Villar, V., Mallah, T., 2001. A Prussian Blue Nanomolecule: Crystal Structure and Low-Temperature Magnetism. Inorg. Chem. 40(16), 3836-3837.

Roka, A., Varga, I., Inzelt, G., 2006. Electrodeposition and dissolution of yttrium-hexacyanoferrate layers. Electrochim. Acta 51(28), 6243-6250.

Safavi, A., Kazemi, S.H., Kazemi, H., 2011. Electrochemically deposited hybrid nickel–cobalt hexacyanoferrate nanostructures for electrochemical supercapacitors. Electrochim. Acta 56(25), 9191-9196.

Salazar, P., Martín, M., O'Neill, R., Roche, R., González-Mora, J., 2012. Surfactant-promoted Prussian Blue-modified carbon electrodes: Enhancement of electro-deposition step, stabilization, electrochemical properties and application to lactate microbiosensors for the neurosciences. Colloids Surf. B. Biointerfaces 92, 180-189.

Salazar, P., Martín, M., Roche, R., O'Neill, R.D., González-Mora, J.L., 2010. Prussian Blue-modified microelectrodes for selective transduction in enzyme-based amperometric microbiosensors for in vivo neurochemical monitoring. Electrochim. Acta 55(22), 6476-6484.

Salimi, A., Abdi, K., 2004. Enhancement of the analytical properties and catalytic activity of a nickel hexacyanoferrate modified carbon ceramic electrode prepared by two-step sol–gel technique: application to amperometric detection of hydrazine and hydroxyl amine. Talanta 63(2), 475-483.

Samain, L., Grandjean, F., Long, G.J., Martinetto, P., Bordet, P., Sanyova, J., Strivay, D., 2013. Synthesis and fading of eighteenth-century Prussian blue pigments: a combined study by spectroscopic and diffractive techniques using laboratory and synchrotron radiation sources. J Synchrotron Radiat 20(Pt 3), 460-473.

Sato, O., Iyoda, T., Fujishima, A., Hashimoto, K., 1996. Photoinduced Magnetization of a Cobalt-Iron Cyanide. Science 272(5262), 704-705.

Sato, O., Kawakami, T., Kimura, M., Hishiya, S., Kubo, S., Einaga, Y., 2004. Electric-Field-Induced Conductance Switching in FeCo Prussian Blue Analogues. J. Am. Chem. Soc. 126(41), 13176-13177.

Sattarahmady, N., Heli, H., 2011. An electrocatalytic transducer for l-cysteine detection based on cobalt hexacyanoferrate nanoparticles with a core–shell structure. Anal. Biochem. 409(1), 74-80.

Scharf, U., Grabner, E.W., 1996. Electrocatalytic oxidation of hydrazine at a Prussian Blue-modified glassy carbon electrode. Electrochim. Acta 41(2), 233-239.

Schwudke, D., Stößer, R., Scholz, F., 2000. Solid-state electrochemical, X-ray and spectroscopic characterization of substitutional solid solutions of iron–copper hexacyanoferrates. Electrochem. Commun. 2(5), 301-306.

Shan Lin, M., Feng Tseng, T., 1998. Chromium(III) hexacyanoferrate(II)-based chemical sensor for the cathodic determination of hydrogen peroxide. Analyst 123(1), 159-163.

Shankaran, D.R., Narayanan, S.S., 1999. Characterization and application of an electrode modified by mechanically immobilized copper hexacyanoferrate. Fresenius J. Anal. Chem. 364(8), 686-689.

Shaojun, D., Fengbin, L., 1986. Researches on chemically modified electrodes. J Electroanal Chem Interfacial Electrochem 210(1), 31-44.

Shatruk, M., Dragulescu-Andrasi, A., Chambers, K.E., Stoian, S.A., Bominaar, E.L., Achim, C., Dunbar, K.R., 2007. Properties of Prussian blue materials manifested in molecular complexes: observation of cyanide linkage isomerism and spin-crossover behavior in pentanuclear cyanide clusters. J. Am. Chem. Soc. 129(19), 6104-6116.

Sheng, Q.-L., Yu, H., Zheng, J.-B., 2007a. Solid state electrochemical of the erbium hexacyanoferrate-modified carbon ceramic electrode and its electrocatalytic oxidation of l-cysteine. J. Solid State Electrochem. 12(9), 1077-1084.

Sheng, Q., Yu, H., Zheng, J., 2007b. Sol–gel derived terbium hexacyanoferrate modified carbon ceramic electrode: Electrochemical behavior and its electrocatalytical oxidation of ascorbic acid. J. Electroanal. Chem. 606(1), 39-46.

Shi, L., Wu, T., He, P., Li, D., Sun, C., Li, J., 2005. Amperometric Sensor for Hydroxylamine Based on Hybrid Nickel-Cobalt Hexacyanoferrate Modified Electrode. Electroanalysis 17(23), 2190-2194.

Shiba, F., 2010. Preparation of monodisperse Prussian blue nanoparticles via reduction process with citric acid. Colloids Surf. Physicochem. Eng. Aspects 366(1–3), 178-182.

Shiba, F., Fujishiro, R., Kojima, T., Okawa, Y., 2012. Preparation of Monodisperse Cobalt(II) Hexacyanoferrate(III) Nanoparticles Using Cobalt Ions Released from a Citrate Complex. The Journal of Physical Chemistry C 116(5), 3394-3399.

Shigeo, H., Hisashi, T., Tohru, K., Madoka, T., Mami, Y., Akihito, G., Hiroaki, U., Masato, K., Masaomi, S., 2007. Electrochromic Thin Film of Prussian Blue Nanoparticles Fabricated using Wet Process. Japanese Journal of Applied Physics 46(10L), L945.

Shokouhimehr, M., Soehnlen, E.S., Khitrin, A., Basu, S., Huang, S.D., 2010. Biocompatible Prussian blue nanoparticles: Preparation, stability, cytotoxicity, and potential use as an MRI contrast agent. Inorg. Chem. Commun. 13(1), 58-61.

Sinha, S., Humphrey, B.D., Fu, E., Bocarsly, A.B., 1984. The coordination chemistry of chemically derivatized nickel surfaces generation of an electrochromic interface. J Electroanal Chem Interfacial Electrochem 162(1), 351-357.

Siperko, L.M., Kuwana, T., 1983. Electrochemical and Spectroscopic Studies of Metal Hexacyanometalate Films: I . Cupric Hexacyanoferrate. J. Electrochem. Soc. 130(2), 396-402.

Sone, Y., Kishimoto, A., Kudo, T., Ikeda, K., 1996. Reversible electrochromic performance of Prussian blue coated with proton conductive Ta2O5 · nH2O film. Solid State Ionics 83(1–2), 135-143.

Song, Y., Qu, K., Zhao, C., Ren, J., Qu, X., 2010a. Graphene oxide: intrinsic peroxidase catalytic activity and its application to glucose detection. Adv. Mater. 22(19), 2206-2210.

Song, Y., Wang, X., Zhao, C., Qu, K., Ren, J., Qu, X., 2010b. Label-Free Colorimetric Detection of Single Nucleotide Polymorphism by Using Single-Walled Carbon Nanotube Intrinsic Peroxidase-Like Activity. Chemistry–A European Journal 16(12), 3617-3621.

Sono, M., Roach, M.P., Coulter, E.D., Dawson, J.H., 1996. Heme-containing oxygenases. Chem. Rev. 96(7), 2841-2888.

Sun, H.-L., Shi, H., Zhao, F., Qi, L., Gao, S., 2005. Shape-dependent magnetic properties of low-dimensional nanoscale Prussian blue (PB) analogue SmFe (CN) 6· 4H2O. Chem. Commun.(34), 4339-4341.

Sun, X., Dong, S., Wang, E., 2004. One-step synthesis and characterization of polyelectrolyte-protected gold nanoparticles through a thermal process. Polymer 45(7), 2181-2184.

Sun, X., Dong, S., Wang, E., 2006. One-step polyelectrolyte-based route to well-dispersed gold nanoparticles: synthesis and insight. Mater. Chem. Phys. 96(1), 29-33.

Szaciłowski, K., Macyk, W., Stochel, G., 2006. Synthesis, structure and photoelectrochemical properties of the TiO 2–Prussian blue nanocomposite. J. Mater. Chem. 16(47), 4603-4611.

Tan, X.-C., Tian, Y.-X., Cai, P.-X., Zou, X.-Y., 2005. Glucose biosensor based on glucose oxidase immobilized in sol–gel chitosan/silica hybrid composite film on Prussian blue modified glass carbon electrode. Anal. Bioanal. Chem. 381(2), 500-507.

Tennakone, K., Kumarasinghe, A., Sirimanne, P., 1994. Photocurrent enhancement in a cadmium sulphide anode coated with Prussian blue. Thin Solid Films 238(1), 101-103.

Thomsen, K.N., Baldwin, R.P., 1989. Amperometric detection of nonelectroactive cations in flow systems at a cupric hexacyanoferrate electrode. Anal. Chem. 61(23), 2594-2598.

Tokarev, A., Agulhon, P., Long, J., Quignard, F., Robitzer, M., Ferreira, R.A.S., Carlos, L.D., Larionova, J., Guerin, C., Guari, Y., 2012. Synthesis and study of Prussian blue type nanoparticles in an alginate matrix. J. Mater. Chem. 22(38), 20232-20242.

Tokoro, H., Hashimoto, K., Ohkoshi, S.-i., 2007. Photo-induced charge-transfer phase transition of rubidium manganese hexacyanoferrate in ferromagnetic and paramagnetic states. J. Magn. Magn. Mater. 310(2, Part 2), 1422-1428.

Tokoro, H., Matsuda, T., Nuida, T., Moritomo, Y., Ohoyama, K., Dangui, E.D.L., Boukheddaden, K., Ohkoshi, S.-i., 2008. Visible-Light-Induced Reversible Photomagnetism in Rubidium Manganese Hexacyanoferrate. Chem. Mater. 20(2), 423-428.

Tokoro, H., Ohkoshi, S.-i., Matsuda, T., Hashimoto, K., 2004. A Large Thermal Hysteresis Loop Produced by a Charge-Transfer Phase Transition in a Rubidium Manganese Hexacyanoferrate. Inorg. Chem. 43(17), 5231-5236.

Tsiafoulis, C.G., Trikalitis, P.N., Prodromidis, M.I., 2005. Synthesis, characterization and performance of vanadium hexacyanoferrate as electrocatalyst of H 2 O 2. Electrochem. Commun. 7(12), 1398-1404.

Uemura, T., Kitagawa, S., 2003. Prussian Blue Nanoparticles Protected by Poly(vinylpyrrolidone). J. Am. Chem. Soc. 125(26), 7814-7815.

Umar, A., Rahman, M.M., Kim, S.H., Hahn, Y.-B., 2008. Zinc oxide nanonail based chemical sensor for hydrazine detection. Chem. Commun.(2), 166-168.

Upadhyay, D., Gomathi, H., Rao, G.P., 1991. Photoelectrochemical properties of prussian blue-modified glassy carbon. J Electroanal Chem Interfacial Electrochem 301(1-2), 199-205.

Vaucher, S., Fielden, J., Li, M., Dujardin, E., Mann, S., 2002. Molecule-Based Magnetic Nanoparticles: Synthesis of Cobalt Hexacyanoferrate, Cobalt Pentacyanonitrosylferrate, and Chromium Hexacyanochromate Coordination Polymers in Water-in-Oil Microemulsions. Nano Lett. 2(3), 225-229.

Vaucher, S., Li, M., Mann, S., 2000. Synthesis of Prussian Blue Nanoparticles and Nanocrystal Superlattices in Reverse Microemulsions. Angew. Chem. Int. Ed. 39(10), 1793-1796.

Verdaguer, M., Bleuzen, A., Marvaud, V., Vaissermann, J., Seuleiman, M., Desplanches, C., Scuiller, A., Train, C., Garde, R., Gelly, G., 1999a. Molecules to build solids: high T C molecule-based magnets by design and recent revival of cyano complexes chemistry. Coord. Chem. Rev. 190, 1023-1047.

Verdaguer, M., Bleuzen, A., Train, C., Garde, R., de Biani, F.F., Desplanches, C., 1999b. Room-temperature molecule-based magnets. Philosophical Transactions of the Royal Society of London A: Mathematical, Physical and Engineering Sciences 357(1762), 2959-2976.

Vidal, J.-C., Espuelas, J., Garcia-Ruiz, E., Castillo, J.-R., 2004. Amperometric cholesterol biosensors based on the electropolymerization of pyrrole and the electrocatalytic effect of Prussian-Blue layers helped with self-assembled monolayers. Talanta 64(3), 655-664.

Vittal, R., Jayalakshmi, M., Gomathi, H., Rao, G.P., 1999. Surfactant promoted enhancement in electrochemical and electrochromic properties of films of Prussian Blue and its analogs. J. Electrochem. Soc. 146(2), 786-793.

Vittal, R., Kim, K.-J., Gomathi, H., Yegnaraman, V., 2008. CTAB-promoted prussian blue-modified electrode and its cation transport characteristics for K+, Na+, Li+, and NH4+ ions. The Journal of Physical Chemistry B 112(4), 1149-1156.

Wan, Y., Qi, P., Zhang, D., Wu, J., Wang, Y., 2012. Manganese oxide nanowire-mediated enzyme-linked immunosorbent assay. Biosens. Bioelectron. 33(1), 69-74.

Wang, C., Chen, S., Xiang, Y., Li, W., Zhong, X., Che, X., Li, J., 2011. Glucose biosensor based on the highly efficient immobilization of glucose oxidase on Prussian blue-gold nanocomposite films. J. Mol. Catal. B: Enzym. 69(1), 1-7.

Wang, C., Zhang, L., Guo, Z., Xu, J., Wang, H., Shi, H., Zhai, K., Zhuo, X., 2010. A New Amperometric Hydrazine Sensor Based on Prussian Blue/Single-walled Carbon Nanotube Nanocomposites. Electroanalysis 22(16), 1867-1872.

Wang, L., Lu, Y., Liu, J., Xu, M., Cheng, J., Zhang, D., Goodenough, J.B., 2013a. A Superior Low-Cost Cathode for a Na-Ion Battery. Angew. Chem. Int. Ed. 52(7), 1964-1967.

Wang, L., Tricard, S., Cao, L., Liang, Y., Zhao, J., Fang, J., Shen, W., 2015. Prussian blue/1-butyl-3-methylimidazolium tetrafluoroborate–Graphite felt electrodes for efficient electrocatalytic determination of nitrite. Sensors and Actuators B: Chemical 214, 70-75.

Wang, L., Tricard, S., Yue, P., Zhao, J., Fang, J., Shen, W., 2016a. Polypyrrole and graphene quantum dots@ Prussian Blue hybrid film on graphite felt electrodes: Application for amperometric determination of l-cysteine. Biosens. Bioelectron. 77, 1112-1118.

Wang, L., Ye, Y., Lu, X., Wu, Y., Sun, L., Tan, H., Xu, F., Song, Y., 2013b. Prussian blue nanocubes on nitrobenzene-functionalized reduced graphene oxide and its application for H2O2 biosensing. Electrochim. Acta 114, 223-232.

Wang, P., Jing, X., Zhang, W., Zhu, G., Renewable manganous hexacyanoferrate-modified graphite organosilicate composite electrode and its electrocatalytic oxidation of L-cysteine. J. Solid State Electrochem. 5(6), 369-374.

Wang, Q., Yang, Z., Zhang, X., Xiao, X., Chang, C.K., Xu, B., 2007a. A Supramolecular-Hydrogel-Encapsulated Hemin as an Artificial Enzyme to Mimic Peroxidase. Angew. Chem. Int. Ed. 46(23), 4285-4289.

Wang, Q., Zhang, L., Qiu, L., Sun, J., Shen, J., 2007b. Fabrication and Electrochemical Investigation of Layer-by-Layer Deposited Titanium Phosphate/Prussian Blue Composite Films. Langmuir 23(11), 6084-6090.

WANG, S.-f., JIANG, M., ZHOU, X.-y., 1992. The Electrocatalytic Oxidation of Ascorbic Acid on Nickel Hexacyanoferrate Film Modified Electrode [J]. Chemical Research In Chinese Universities 3, 012.

Wang, S.-J., Chen, C.-S., Chen, L.-C., 2016b. Prussian blue nanoparticles as nanocargoes for delivering DNA drugs to cancer cells. Science and Technology of Advanced Materials.

Wang, T., Fu, Y., Chai, L., Chao, L., Bu, L., Meng, Y., Chen, C., Ma, M., Xie, Q., Yao, S., 2014. Filling Carbon Nanotubes with Prussian Blue Nanoparticles of High Peroxidase-Like Catalytic Activity for Colorimetric Chemo-and Biosensing. Chemistry–A European Journal 20(9), 2623-2630.

Wang, W.-N., Widiyastuti, W., Ogi, T., Lenggoro, I.W., Okuyama, K., 2007c. Correlations between Crystallite/Particle Size and Photoluminescence Properties of Submicrometer Phosphors. Chem. Mater. 19(7), 1723-1730.

Wang, W., Jiang, X., Chen, K., 2012. Iron phosphate microflowers as peroxidase mimic and superoxide dismutase mimic for biocatalysis and biosensing. Chem. Commun. 48(58), 7289-7291.

Wang, X., Gu, H., Yin, F., Tu, Y., 2009. A glucose biosensor based on Prussian blue/chitosan hybrid film. Biosens. Bioelectron. 24(5), 1527-1530.

Wang, Y., Zhong, H., Hu, L., Yan, N., Hu, H., Chen, Q., 2013c. Manganese hexacyanoferrate/MnO2 composite nanostructures as a cathode material for supercapacitors. Journal of Materials Chemistry A 1(7), 2621-2630.

Wang, Y., Zhu, J., Zhu, R., Zhu, Z., Lai, Z., Chen, Z., 2003. Chitosan/Prussian blue-based biosensors. Meas. Sci. Technol. 14(6), 831.

Ware, M., 2008. Prussian Blue: Artists' Pigment and Chemists' Sponge. J. Chem. Educ. 85(5), 612.

Wei, H., Wang, E., 2013. Nanomaterials with enzyme-like characteristics (nanozymes): next-generation artificial enzymes. Chem. Soc. Rev. 42(14), 6060-6093.

Weinstein, J.S., Varallyay, C.G., Dosa, E., Gahramanov, S., Hamilton, B., Rooney, W.D., Muldoon, L.L., Neuwelt, E.A., 2010. Superparamagnetic iron oxide nanoparticles: diagnostic magnetic resonance imaging and potential therapeutic applications in neurooncology and central nervous system inflammatory pathologies, a review. Journal of Cerebral Blood Flow and Metabolism: Official Journal of the International Society of Cerebral Blood Flow and Metabolism 30(1), 15-35.

Wen, S., Zheng, F., Shen, M., Shi, X., 2013. Synthesis of polyethyleneimine-stabilized gold nanoparticles for colorimetric sensing of heparin. Colloids Surf. Physicochem. Eng. Aspects 419, 80-86.

Wessells, C.D., Huggins, R.A., Cui, Y., 2011a. Copper hexacyanoferrate battery electrodes with long cycle life and high power. Nature communications 2, 550.

Wessells, C.D., Huggins, R.A., Cui, Y., 2011b. Copper hexacyanoferrate battery electrodes with long cycle life and high power. Nat Commun 2, 550.

Wessells, C.D., Peddada, S.V., Huggins, R.A., Cui, Y., 2011c. Nickel Hexacyanoferrate Nanoparticle Electrodes For Aqueous Sodium and Potassium Ion Batteries. Nano Lett. 11(12), 5421-5425.

Wilde, R.E., Ghosh, S.N., Marshall, B.J., 1970. Prussian blues. Inorg. Chem. 9(11), 2512-2516.

Wu, P., Cai, C., 2005. The Solid State Electrochemistry of Dysprosium(III) Hexacyanoferrate(II). Electroanalysis 17(17), 1583-1588.

Wu, X., Cao, M., Hu, C., He, X., 2006. Sonochemical Synthesis of Prussian Blue Nanocubes from a Single-Source Precursor. Crystal Growth & Design 6(1), 26-28.

Wu, Y., Yang, H., Shin, H.-J., 2013. Encapsulation and crystallization of Prussian blue nanoparticles by cowpea chlorotic mottle virus capsids. Biotechnol. Lett 36(3), 515-521.

Wulff, G., Sarhan, A., 1972. Use of polymers with enzyme-analogous structures for resolution of racemates. Angewandte Chemie-International Edition, pp. 341-&. WILEY-V CH VERLAG GMBH MUHLENSTRASSE 33-34, D-13187 BERLIN, GERMANY.

Xian, Y., Hu, Y., Liu, F., Xian, Y., Feng, L., Jin, L., 2007. Template synthesis of highly ordered Prussian blue array and its application to the glucose biosensing. Biosens. Bioelectron. 22(12), 2827-2833.

Xue, M.-H., Xu, Q., Zhou, M., Zhu, J.-J., 2006. In situ immobilization of glucose oxidase in chitosan–gold nanoparticle hybrid film on Prussian Blue modified electrode for high-sensitivity glucose detection. Electrochem. Commun. 8(9), 1468-1474.

Yamada, M., Ohnishi, N., Watanabe, M., Hino, Y., 2009. Prussian blue nanoparticles protected by the water-soluble [small pi]-conjugated polymer PEDOT-S: synthesis and multiple-color pH-sensing with a redox reaction. Chem. Commun.(46), 7203-7205.

Yamada, S., Kuwabara, K., Koumoto, K., 1997. Electrochemical redox behavior of nickel-iron cyanide film deposited onto indium tin oxide substrate. Thin Solid Films 292(1), 227-231.

Yang, H., Lu, B., Guo, L., Qi, B., 2011. Cerium hexacyanoferrate/ordered mesoporous carbon electrode and its application in electrochemical determination of hydrous hydrazine. J. Electroanal. Chem. 650(2), 171-175.

Yang, J.-H., Myoung, N., Hong, H.-G., 2012. Facile and controllable synthesis of Prussian blue on chitosan-functionalized graphene nanosheets for the electrochemical detection of hydrogen peroxide. Electrochim. Acta 81, 37-43.

Yao, H., Li, N., Xu, S., Xu, J.-Z., Zhu, J.-J., Chen, H.-Y., 2005. Electrochemical study of a new methylene blue/silicon oxide nanocomposition mediator and its application for stable biosensor of hydrogen peroxide. Biosens. Bioelectron. 21(2), 372-377.

Yin, J., Cao, H., Lu, Y., 2012. Self-assembly into magnetic Co 3 O 4 complex nanostructures as peroxidase. J. Mater. Chem. 22(2), 527-534.

Yin, W.X., Li, Z.P., Zhu, J.K., Qin, H.Y., 2008. Effects of NaOH addition on performance of the direct hydrazine fuel cell. J. Power Sources 182(2), 520-523.

You, Y., Wu, X.-L., Yin, Y.-X., Guo, Y.-G., 2014. High-quality Prussian blue crystals as superior cathode materials for room-temperature sodium-ion batteries. Energy & Environmental Science 7(5), 1643-1647.

Yu, H., Jian, X., Jin, J., Wang, F., Wang, Y., Qi, G.-c., 2013. Preparation of hybrid cobalt–iron hexacyanoferrate nanoparticles modified multi-walled carbon nanotubes composite electrode and its application. J. Electroanal. Chem. 700, 47-53.

Yu, H., Sheng, Q.L., Zheng, J.B., 2007a. Preparation, electrochemical behavior and performance of gallium hexacyanoferrate as electrocatalyst of H2O2. Electrochim. Acta 52(13), 4403-4410.

Yu, H., Sheng, Q.L., Zheng, J.B., 2007b. Preparation, electrochemical behavior and performance of gallium hexacyanoferrate as electrocatalyst of H 2 O 2. Electrochim. Acta 52(13), 4403-4410.

Zakharchuk, N., Naumov, N., Stösser, R., Schröder, U., Scholz, F., Mehner, H., 1999. Solid state electrochemistry, X-ray powder diffraction, magnetic susceptibility, electron spin resonance, Mössbauer and diffuse reflectance spectroscopy of mixed iron (III)-cadmium (II) hexacyanoferrates. J. Solid State Electrochem. 3(5), 264-276.

Zamora, B., Roque, J., Balmaseda, J., Reguera, E., 2010. Methane Storage in Prussian Blue Analogues and Related Porous Solids: Nature of the Involved Adsorption Forces. Z. Anorg. Allg. Chem. 636(15), 2574-2578.

Zamponi, S., Berrettoni, M., Kulesza, P.J., Miecznikowski, K., Malik, M.A., Makowski, O., Marassi, R., 2003. Influence of experimental conditions on electrochemical behavior of Prussian blue type nickel hexacyanoferrate film. Electrochim. Acta 48(28), 4261-4269.

Zen, J.-M., Kumar, A.S., Chen, H.-W., 2001. Electrochemical behavior of stable cinder/prussian blue analogue and its mediated nitrite oxidation. Electroanalysis 13(14), 1171.

Zeng, J., Wei, W., Liu, X., Wang, Y., Luo, G., 2008. A simple method to fabricate a Prussian Blue nanoparticles/carbon nanotubes/poly (1, 2-diaminobenzene) based glucose biosensor. Microchimica Acta 160(1-2), 261-267.

Zhai, J., Zhai, Y., Wang, L., Dong, S., 2008. Rapid Synthesis of Polyethylenimine-Protected Prussian Blue Nanocubes through a Thermal Process. Inorg. Chem. 47(16), 7071-7073.

Zhang, D., Wang, K., Sun, D., Xia, X., Chen, H.-Y., 2003. Ultrathin layers of densely packed Prussian blue nanoclusters prepared from a ferricyanide solution. Chem. Mater. 15(22), 4163-4165.

Zhang, J., Li, J., Yang, F., Zhang, B., Yang, X., 2009. Preparation of Prussian blue@ Pt nanoparticles/carbon nanotubes composite material for efficient determination of H 2 O 2. Sensors and Actuators B: Chemical 143(1), 373-380.

Zhang, L., Zhang, A., Du, D., Lin, Y., 2012a. Biosensor based on Prussian blue nanocubes/reduced graphene oxide nanocomposite for detection of organophosphorus pesticides. Nanoscale 4(15), 4674-4679.

Zhang, N., Wang, G., Gu, A., Feng, Y., Fang, B., 2010a. Fabrication of prussian blue/multi-walled carbon nanotubes modified electrode for electrochemical sensing of hydroxylamine. Microchimica Acta 168(1-2), 129-134.

Zhang, W., Ma, D., Du, J., 2014. Prussian blue nanoparticles as peroxidase mimetics for sensitive colorimetric detection of hydrogen peroxide and glucose. Talanta 120, 362-367.

Zhang, W., Zhang, Y., Chen, Y., Li, S., Gu, N., Hu, S., Sun, Y., Chen, X., Li, Q., 2013. Prussian Blue Modified Ferritin as Peroxidase Mimetics and Its Applications in Biological Detection. J Nanosci Nanotechnol 13(1), 60-67.

Zhang, X.-Q., Gong, S.-W., Zhang, Y., Yang, T., Wang, C.-Y., Gu, N., 2010b. Prussian blue modified iron oxide magnetic nanoparticles and their high peroxidase-like activity. J. Mater. Chem. 20(24), 5110-5116.

Zhang, X., Xu, H., Dong, Z., Wang, Y., Liu, J., Shen, J., 2004. Highly efficient dendrimer-based mimic of glutathione peroxidase. J. Am. Chem. Soc. 126(34), 10556-10557.

Zhang, X., Zhang, J., Zhou, D., Wang, G., 2012b. Electrodeposition method synthesise gold nanoparticles–Prussian blue–graphene nanocomposite and its application in electrochemical sensor for H₂O₂. Micro & Nano Letters, pp. 60-63. Institution of Engineering and Technology.

Zhang, Y., Gao, X., Chen, H., Chen, Z., Lin, X., 2011a. A Strategy for Constructing Ordered Multilayer Composite Films Based on Alternate Electrodeposition and Self-Assembly. J. Electrochem. Soc. 159(2), J17-J22.

Zhang, Y., Sun, X., Zhu, L., Shen, H., Jia, N., 2011b. Electrochemical sensing based on graphene oxide/Prussian blue hybrid film modified electrode. Electrochim. Acta 56(3), 1239-1245.

Zhang, Y., Tian, J., Liu, S., Wang, L., Qin, X., Lu, W., Chang, G., Luo, Y., Asiri, A.M., Al-Youbi, A.O., 2012c. Novel application of CoFe layered double hydroxide nanoplates for colorimetric detection of H 2 O 2 and glucose. Analyst 137(6), 1325-1328.

Zhao, F., Wang, Y., Xu, X., Liu, Y., Song, R., Lu, G., Li, Y., 2014. Cobalt Hexacyanoferrate Nanoparticles as a High-Rate and Ultra-Stable Supercapacitor Electrode Material. ACS Applied Materials & Interfaces 6(14), 11007-11012.

Zhao, F., Zhang, J., Hou, X., Abe, T., Kaneko, M., 1998. Quenching of photoluminescence from copolymer pendant Ru(bpy)32+complexes by colloidal Prussian Blue. J. Chem. Soc., Faraday Trans. 94(2), 277-281.

Zheng, X.-J., Kuang, Q., Xu, T., Jiang, Z.-Y., Zhang, S.-H., Xie, Z.-X., Huang, R.-B., Zheng, L.-S., 2007. Growth of Prussian Blue Microcubes under a Hydrothermal Condition: Possible Nonclassical Crystallization by a Mesoscale Self-Assembly. The Journal of Physical Chemistry C 111(12), 4499-4502.

Zhiqiang, G., Xingyao, Z., Guangqing, W., Peibiao, L., Zaofan, Z., 1991. Potassium ion-selective electrode based on a cobalt (II)-hexacyanoferrate film-modified electrode. Anal. Chim. Acta 244, 39-48.

Zhou, D.-M., Ju, H.-X., Chen, H.-Y., 1996. Catalytic oxidation of dopamine at a microdisk platinum electrode modified by electrodeposition of nickel hexacyanoferrate and Nafion®. J. Electroanal. Chem. 408(1–2), 219-223.

Zhou, L., Wu, S., Xu, H., Zhao, Q., Zhang, Z., Yao, Y., 2014. Preparation of poly(N-acetylaniline)-Prussian blue hybrid composite film and its application to hydrogen peroxide sensing. Analytical Methods 6(19), 8003-8010.

Zhou, P., Xue, D., Luo, H., Chen, X., 2002. Fabrication, structure, and magnetic properties of highly ordered Prussian blue nanowire arrays. Nano Lett. 2(8), 845-847.

Zloczewska, A., Celebanska, A., Szot, K., Tomaszewska, D., Opallo, M., Jönsson-Niedziolka, M., 2014. Self-powered biosensor for ascorbic acid with a Prussian blue electrochromic display. Biosens. Bioelectron. 54, 455-461.

Zou, Y., Sun, L.-X., Xu, F., 2007. Biosensor based on polyaniline–Prussian Blue/multi-walled carbon nanotubes hybrid composites. Biosens. Bioelectron. 22(11), 2669-2674.

List of Publications

1. Pandey, P.C., **Pandey, D.,** Singh, R., 2012. Extraction and Purification of Purple Membrane for Photochromic Thin Film Development: Application in Photoelectrochemical Investigation. Appl. Biochem. Biotechnol. 168(4), 936-946.
2. Pandey, P.C., Prakash, A., Pandey, A.K., **Pandey, D.,** 2014. 3-Aminopropyltrimethoxysilane and 3-Glycidoxypropyltrimethoxysilane Mediated Synthesis of Graphene and its Nanocomposite: Potential Bioanalytical Appliactions. Journal of Analytical & Bioanalytical Techniques 2015. (DOI No- http://dx.doi.org/10.4172/2155-9872.S7-012)
3. Pandey, P.C., **Panday, D.**, Pandey, G., 2014. 3-Aminopropyltrimethoxysilane and organic electron donors mediated synthesis of functional amphiphilic gold nanoparticles and their bioanalytical applications. RSC Adv 4(105), 60563-60572.
4. Pandey, P.C., **Panday, D**., 2016. Tetrahydrofuran and hydrogen peroxide mediated conversion of potassium hexacyanoferrate into Prussian blue nanoparticles: Application to hydrogen peroxide sensing. Electrochim. Acta 190, 758-765.
5. Pandey, P.C., **Panday, D**., 2016. Novel synthesis of nickel-iron hexacyanoferrate nanoparticles and its application in electrochemical sensing. J. Electroanal. Chem. 763, 63-70.
6. Pandey, P.C., **Panday, D**., 2016. Polyethylenimine mediated Synthesis of Prussian blue nanoparticles and cooperative self assembly of gold nanoparticles on Polycationic surface. (Communicated to Journal of Electrochemical Society) (ISSN No: 1945-7111)
7. Pandey, P.C., **Panday, D**., Pandey, A.K., 2016. Polyethylenimine mediated synthesis of copper-Iron and nickel-iron hexacyanoferrate nanoparticles and their electroanalytical applications. (Communicated and revised uploaded to Journal of Electroanalytical Chemistry). (ISSN No: 1572-6657)